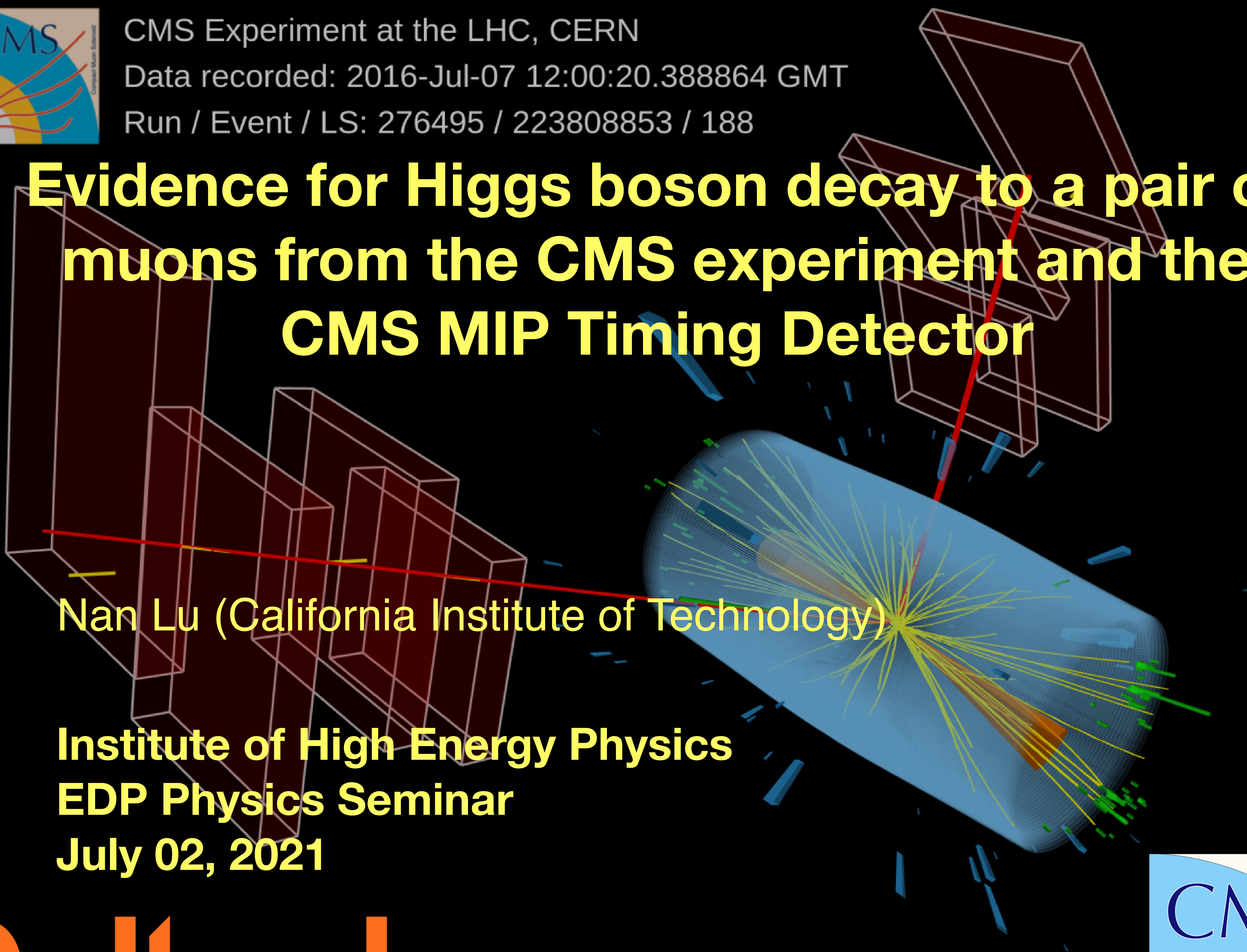

Evidence for Higgs boson decay to a pair of muons from the CMS experiment and the CMS MIP Timing Detector

Nan Lu (California Institute of Technology)

Institute of High Energy Physics
EDP Physics Seminar
July 02, 2021

Caltech

The Standard Model and the Higgs Boson

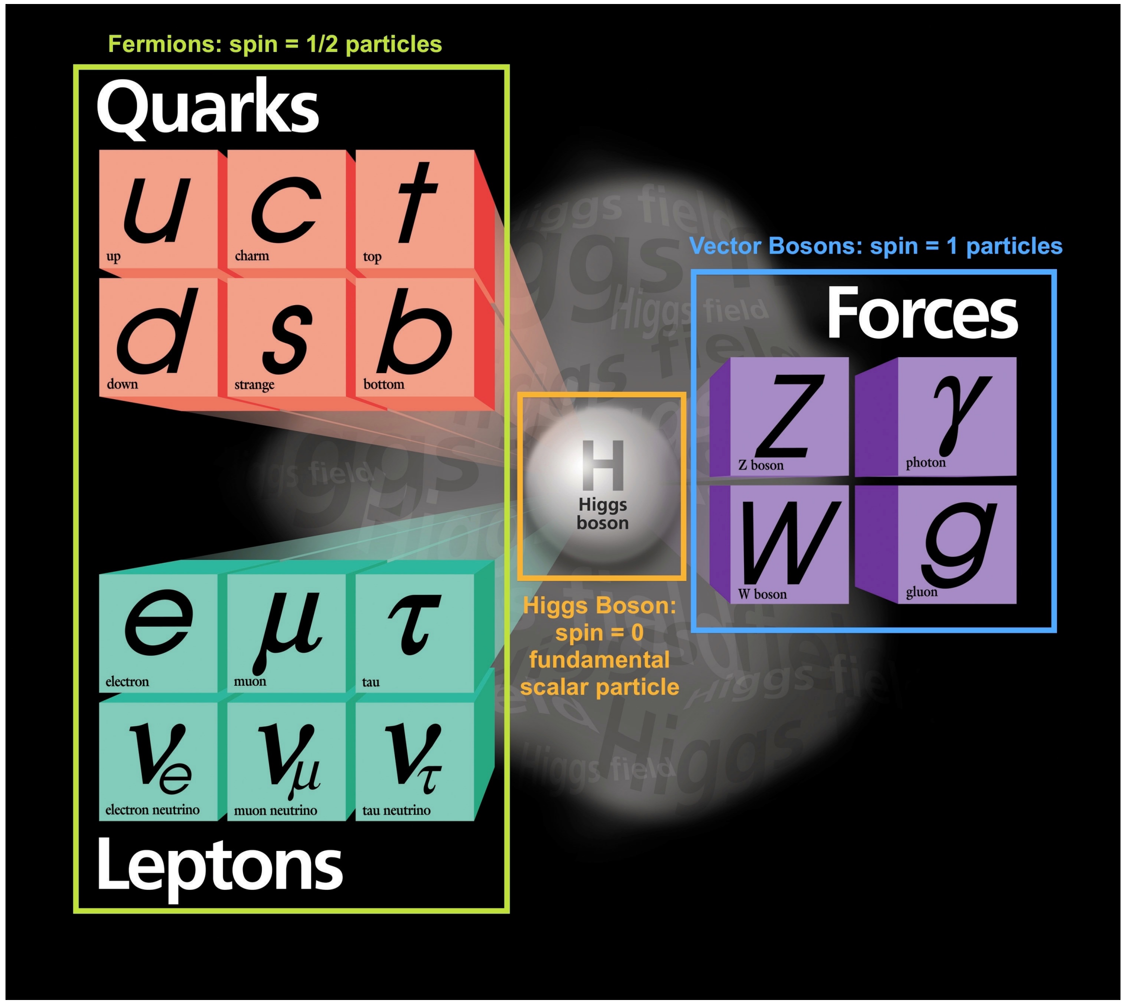

- The fundamental building blocks of matter and their interactions are summarized in theory – Standard Model of Particle Physics
- A unique spin-0 elementary particle Higgs boson - arising from Brout-Englert-Higgs (BEH) mechanism
- Higgs Boson Discovery: an achievement of humanity

Higgs Boson Coupling Measurements

- Higgs boson couplings to W and Z boson (Run 1), 3rd generation fermions t, b, τ (Run 1+2) established
- H→μμ: current most sensitive channel to probe Higgs boson coupling to 2nd-generation fermion at LHC
  - first part today: H→μμ search using full Run 2 data from CMS (JHEP 01 (2021) 148)

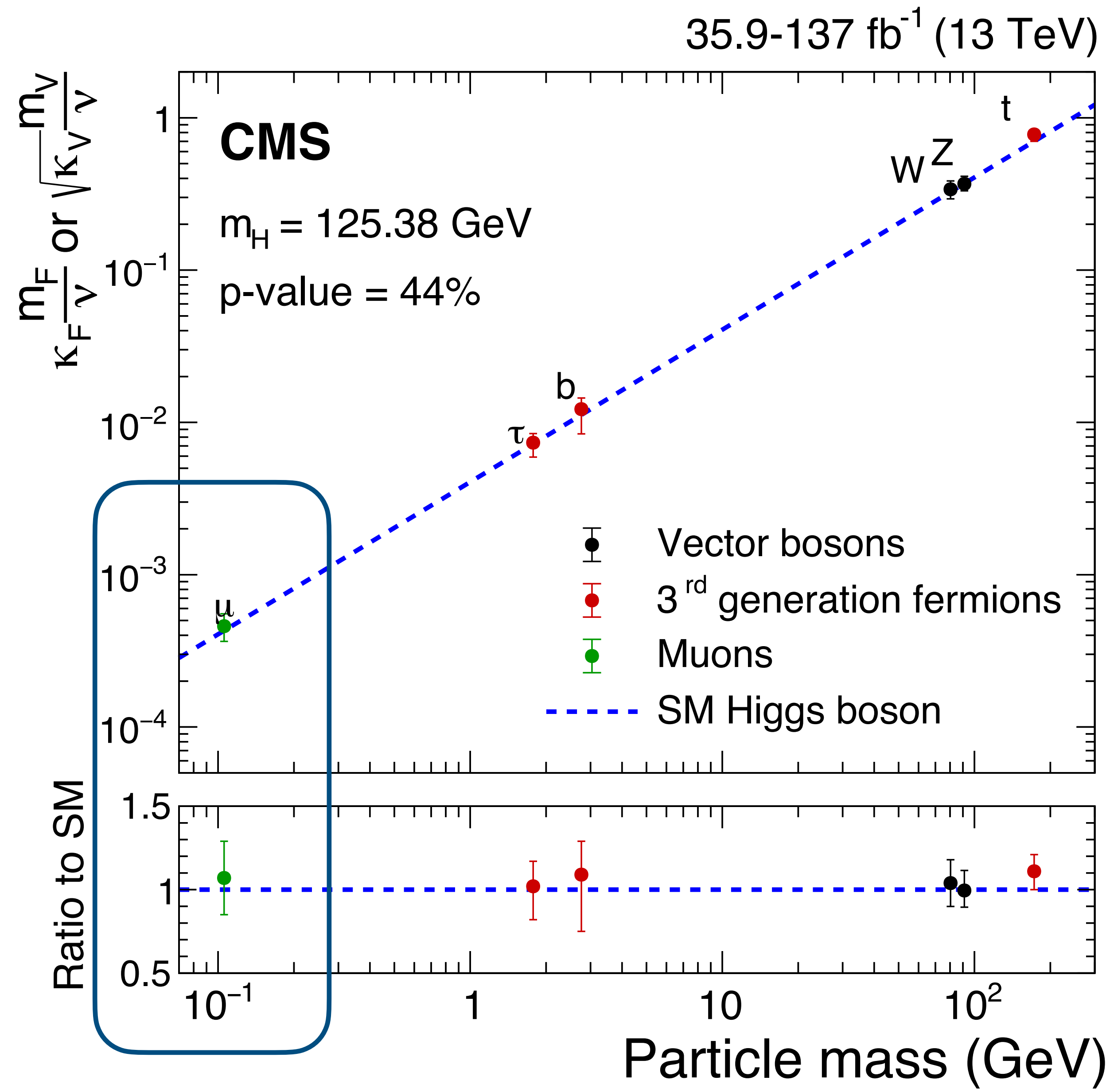

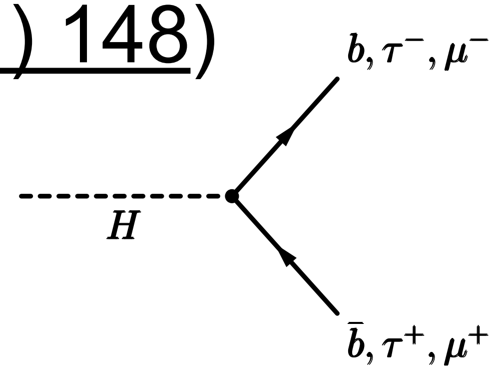

$\kappa_\mu = 1.07^{+0.22}_{-0.22}$ at 68% CL

Run 2 Data-taking

- Excellent operation of the LHC and performance of the CMS detector in Run 2
- A large dataset recorded in Run 2 with high efficiency:
    - 137 fb^{-1} of 13 TeV pp collision data collected by CMS after data quality requirements

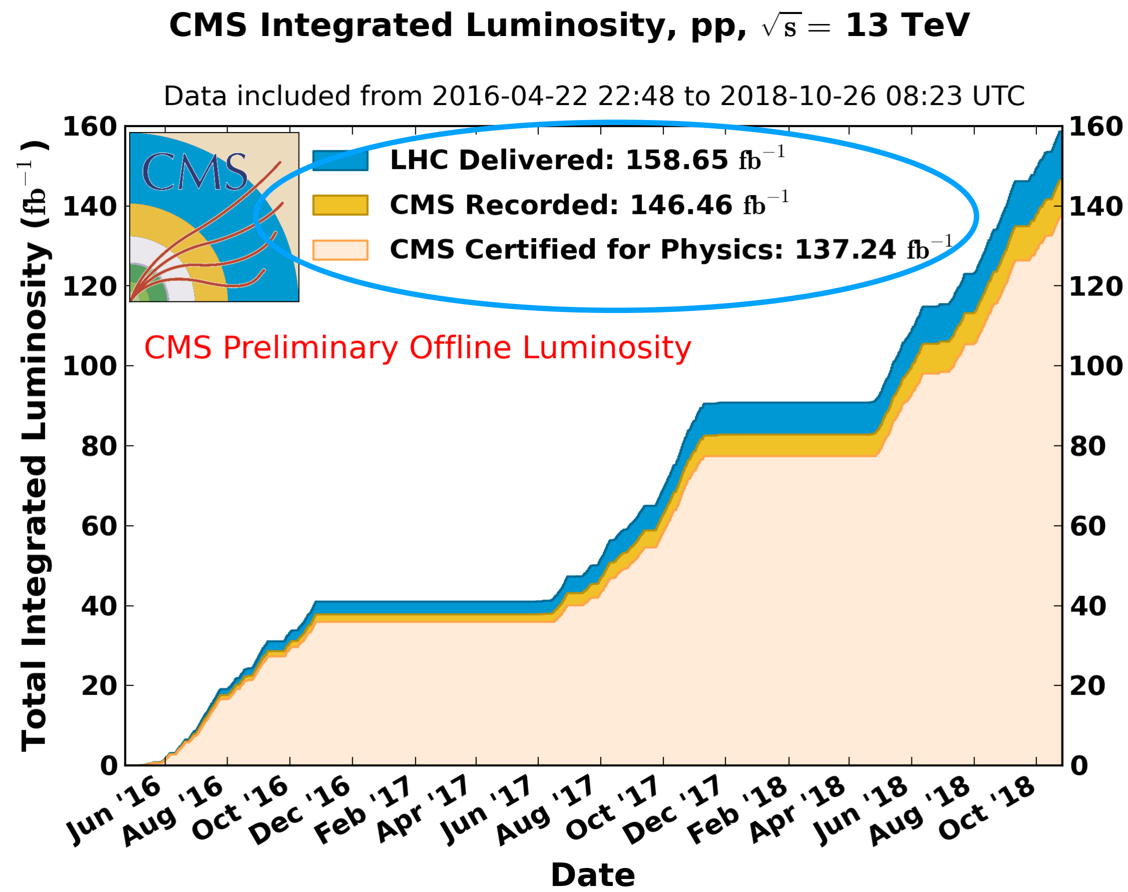

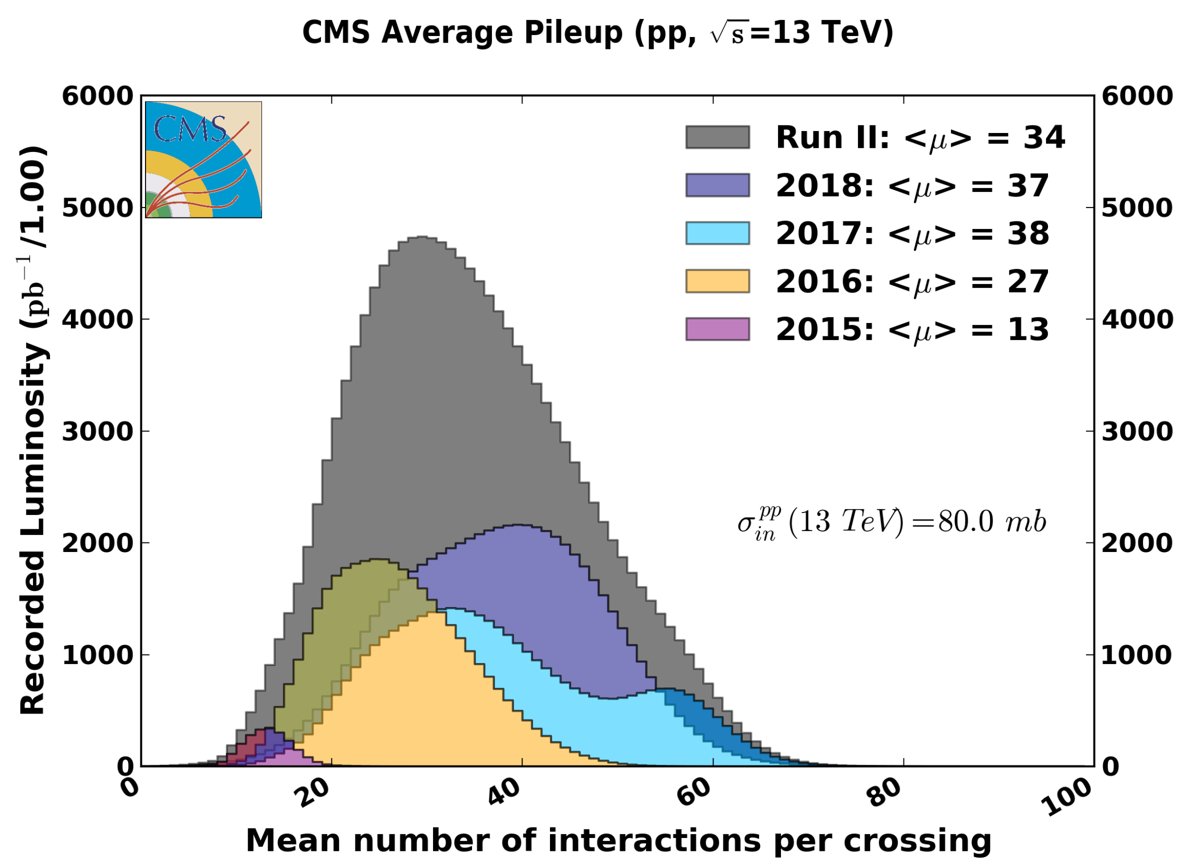

How Many H→μμ Events Produced in Run 2 ?

Gluon-fusion ggF 48.5 pb

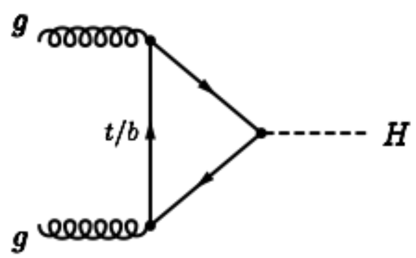

Vector boson fusion (VBF) 3.78 pb

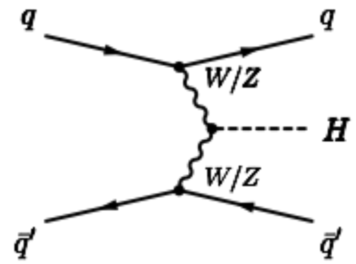

VH 2.25 pb

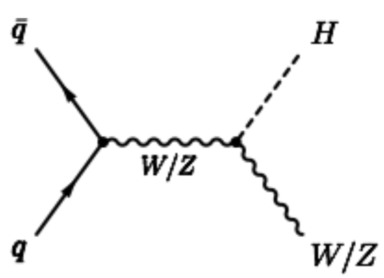

ttH 0.51 pb

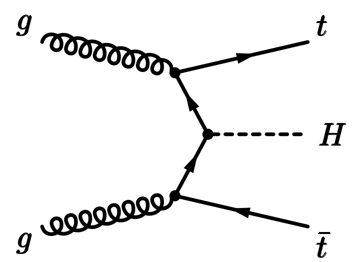

About 1624 H→μμ events produced with 137 fb^{-1} at 13 TeV

production modes	ggF	VBF	WH	ZH	ttH
H→μμ events produced in Run 2 at 13 TeV (137 fb^{-1})	1431	112	40	26	15

Small Branching Ratio BR(H→μμ): 0.02%

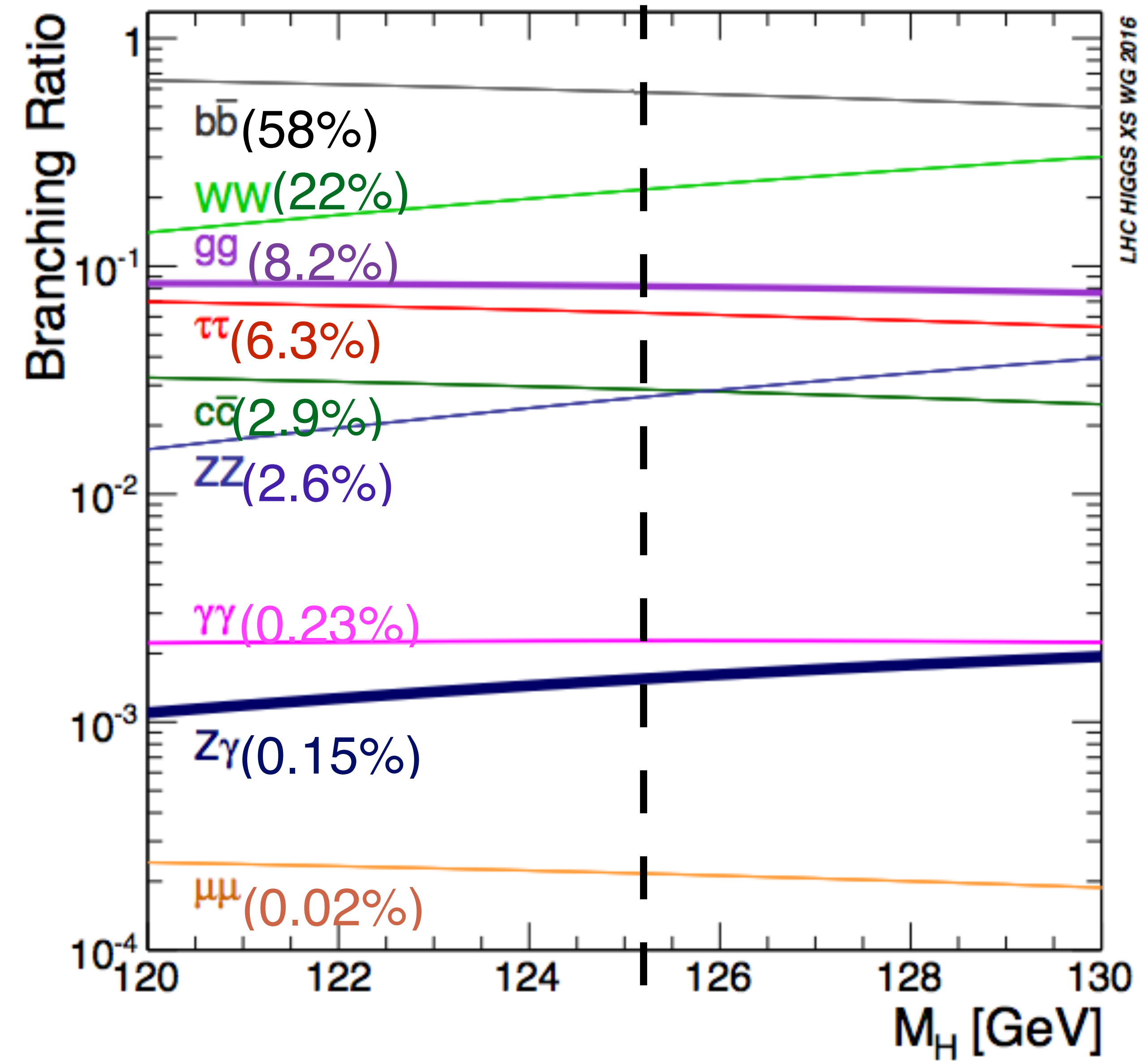

Excellent Muon Reconstruction Performance in Run 2

- |η|< 2.4 within geometrical acceptance of muon detectors
- high efficiency for reconstruction and identification > 96%, isolation > 95%
- good dimuon mass resolution: 1~2% for Z→μμ events

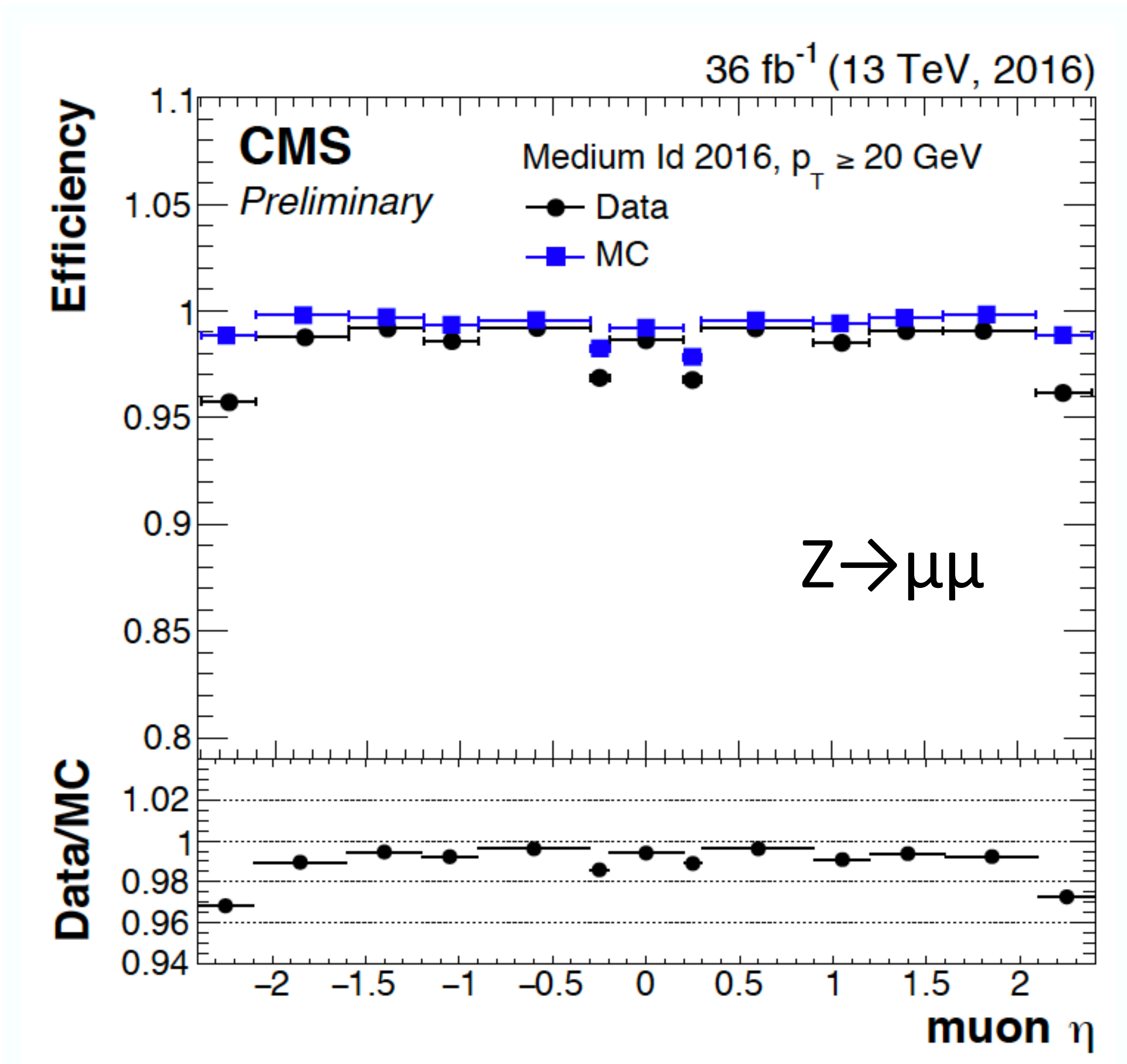

DP2017_007

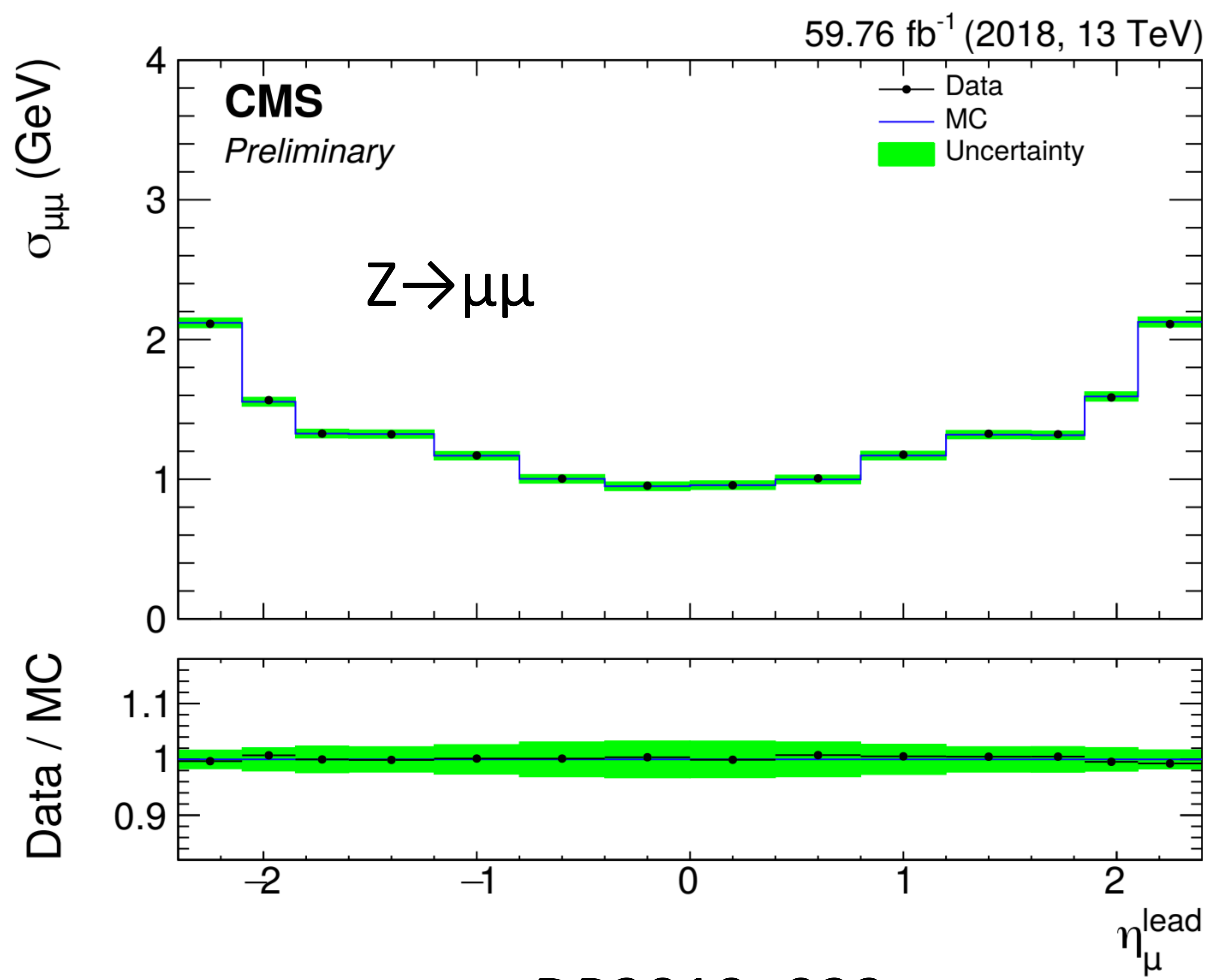

DP2019_022

H→μμ Event Selection

- Event selection: expect 954 signal events selected in $110 < m_{\mu\mu} < 150$ GeV, efficiency 59%:
  - pass single muon high level trigger
  - require two isolated opposite charged muons: leading muon pT > 26 (2016, 2018) / 29 (2017), sub-leading muon pT > 20 GeV
- H→μμ narrow signal on top of smoothly falling background in $m_{\mu\mu}$:
  - narrow signal peak: $\sigma(m_{\mu\mu}) \sim 1.4$ GeV
  - large background: S/B ~ 1/500

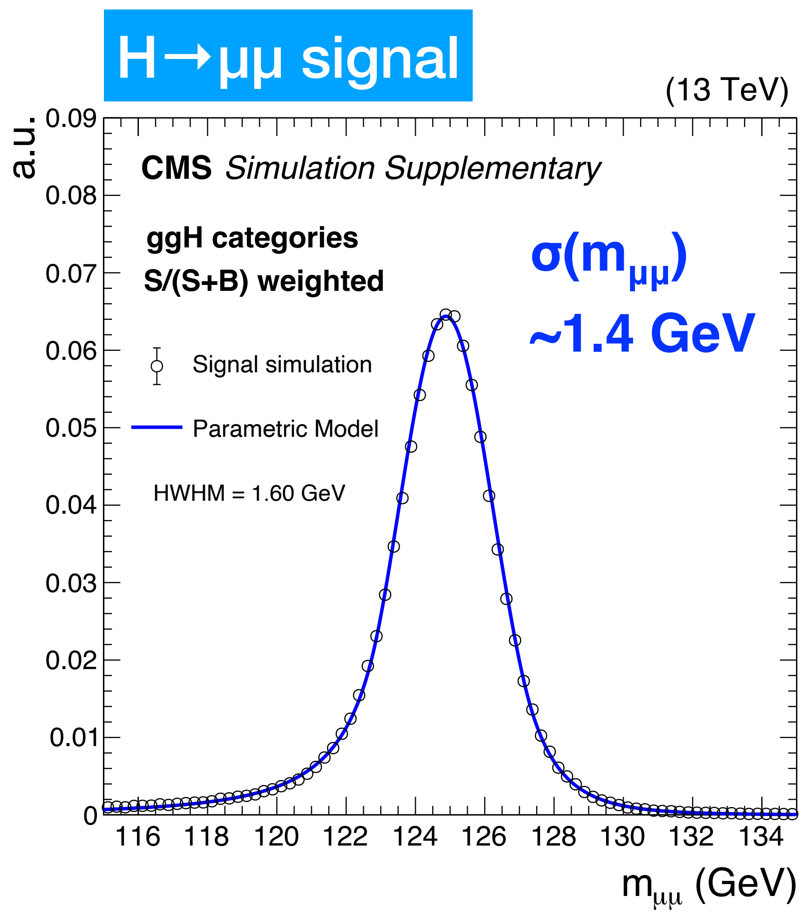

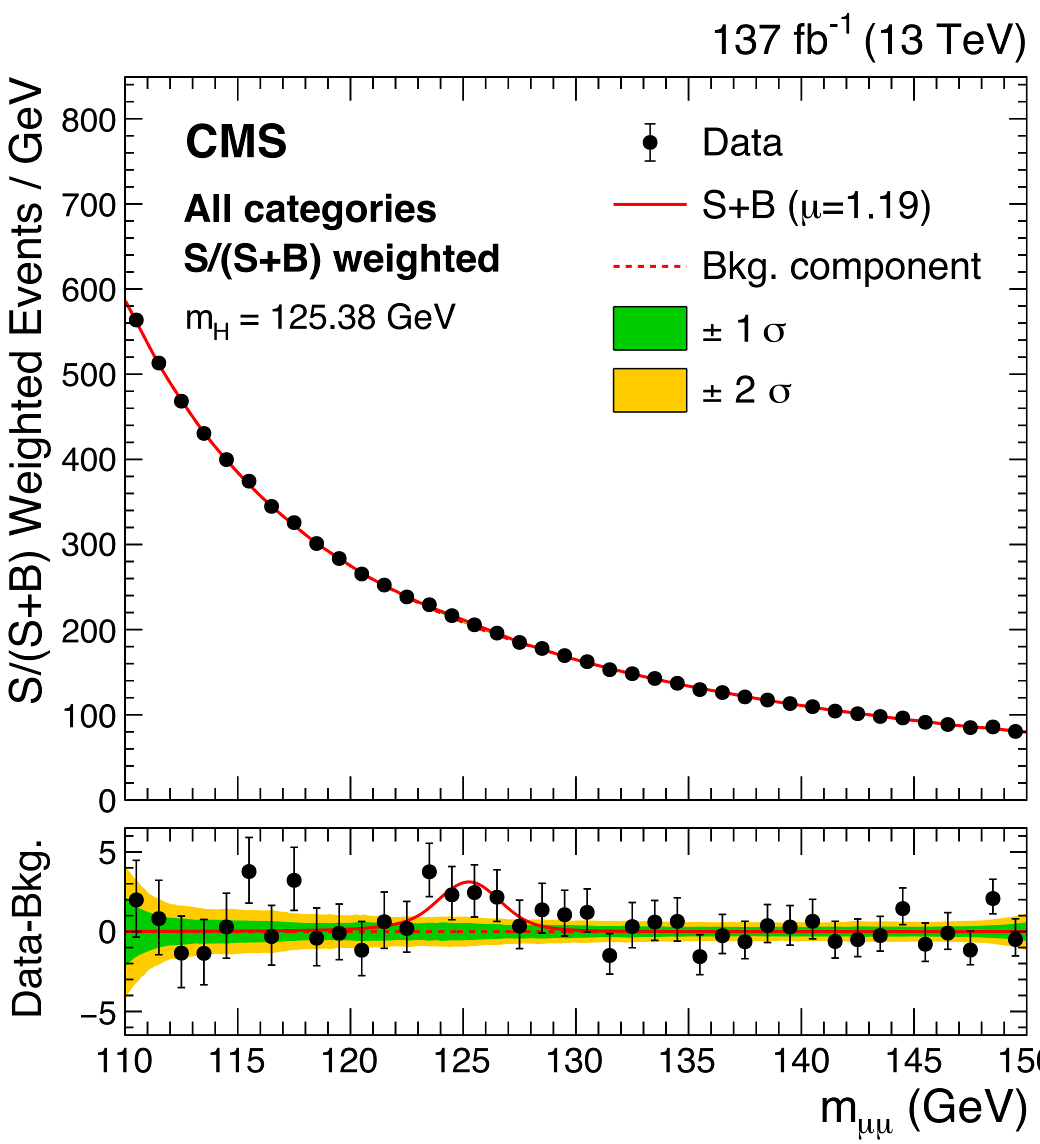

H→μμ: Exclusive Categories: ggF, VBF, VH and ttH

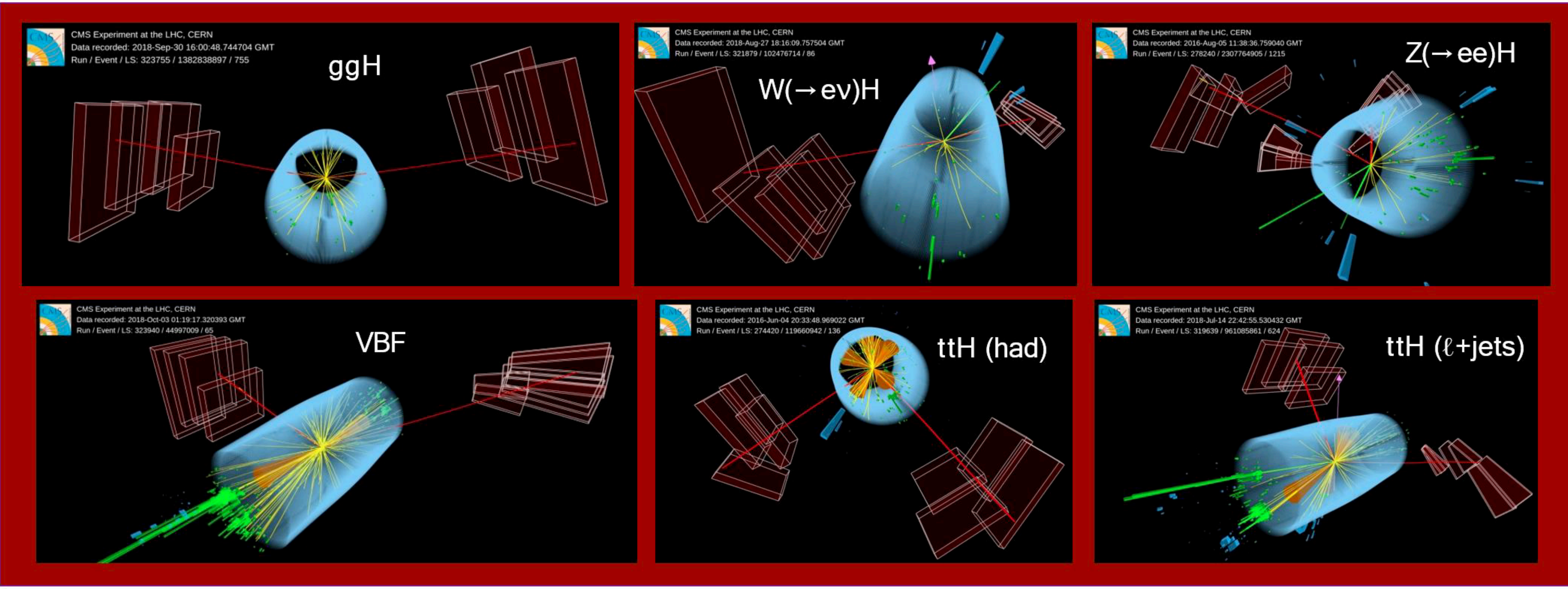

$H\to\mu\mu$: Exclusive Categories: ggF, VBF, VH and ttH

After event selection

$110 < m_{\mu\mu} < 150$ GeV

$N_{\text{b-tag medium}} > 0$ or $N_{\text{b-tag loose}} > 1$

ttH channel

additional lepton e or μ

VH-leptonic channel

new channels dedicated to ttH and VH

pT_{j1}>35 GeV, pT_{j2} >25 GeV

m_{jj}>400 GeV, $|\Delta\eta_{jj}|$>2.5

VBF channel

new strategy

the rest of events

ggH channel

significantly improved strategy

ggF Channel: Overview

ggF channel includes all events not selected by VBF, ttH and VH channels

- largest signal yield
  - about 890 signals
- BDT to separate signal from background
  - BDT uncorrelated with $m_{\mu\mu}$ to allow using the mass fit method
- Five ggF categories defined:
  - aim to optimize overall best ggF channel significance

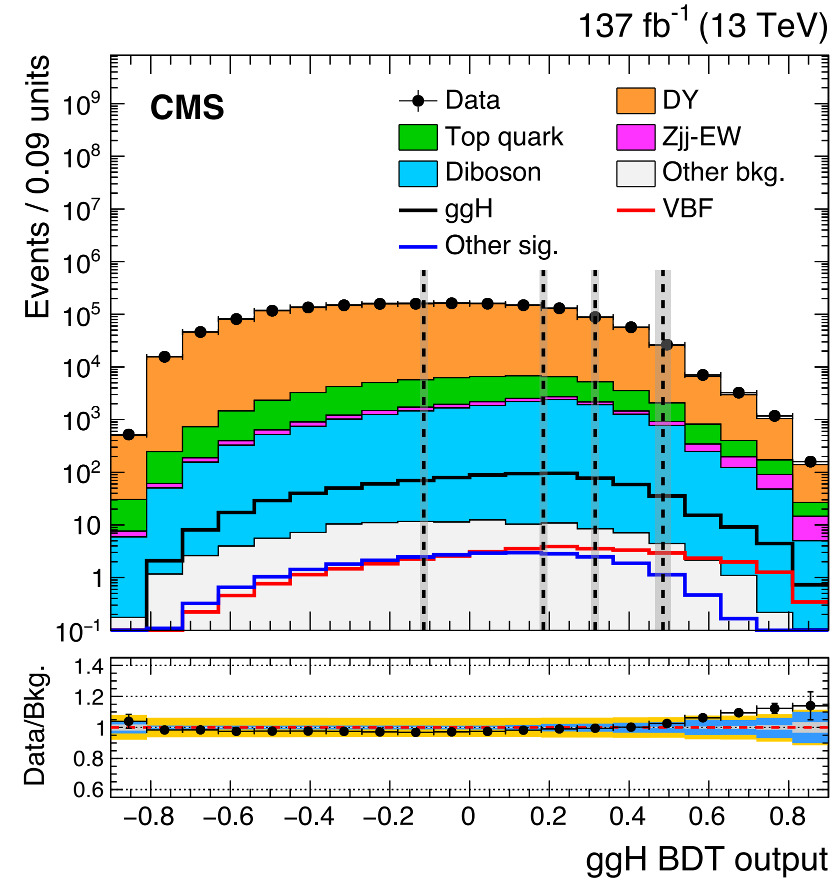

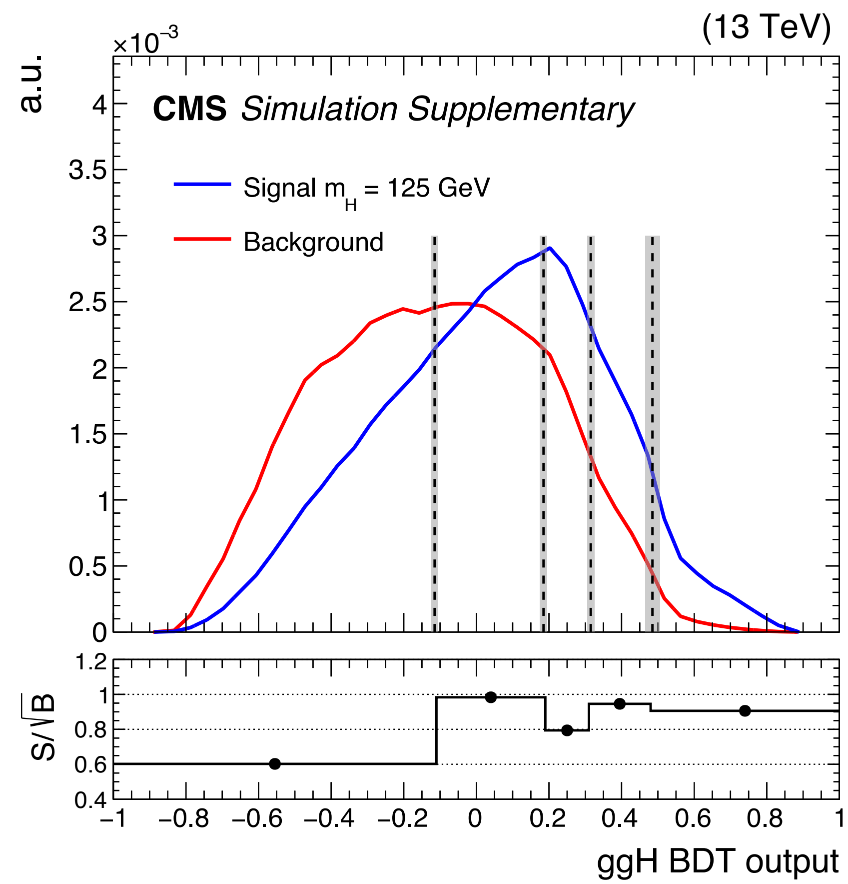

ggF Channel: BDT

- training variables: muon and jet kinematic information, N_{jets}
- signal MC weighted ~ $m_{\mu\mu}/\sigma_{\mu\mu}$: prioritize high-resolution signal events

BDT Training variables

(di)muon:

- $pT_{\mu\mu}$
- $\text{rapidity}_{\mu\mu}$
- $\cos(\theta_{CS})$, ϕ_{CS} computed in dimuon Collins-Soper rest frame
- $pT_{\mu 1}/m_{\mu\mu}$, $pT_{\mu 2}/m_{\mu\mu}$
- $\eta(\mu 1)$
- $\eta(\mu 2)$

muon and jet:

- pT_{j1}, pT_{j2}
- η_{j1}
- N_{jets}
- $\Delta\eta_{jj}$, m_{jj}, $\Delta\phi_{jj}$
- Zeppenfeld variable

$$z^* = \frac{y_{\mu\mu} - (y_{j_1} + y_{j_2})/2}{|y_{j_1} - y_{j_2}|}$$

- min-$\Delta\phi(\mu\mu,(j1,j2))$
- min-$\Delta\eta(\mu\mu,(j1,j2))$

Signal modeling: double-sided Crystal Ball function

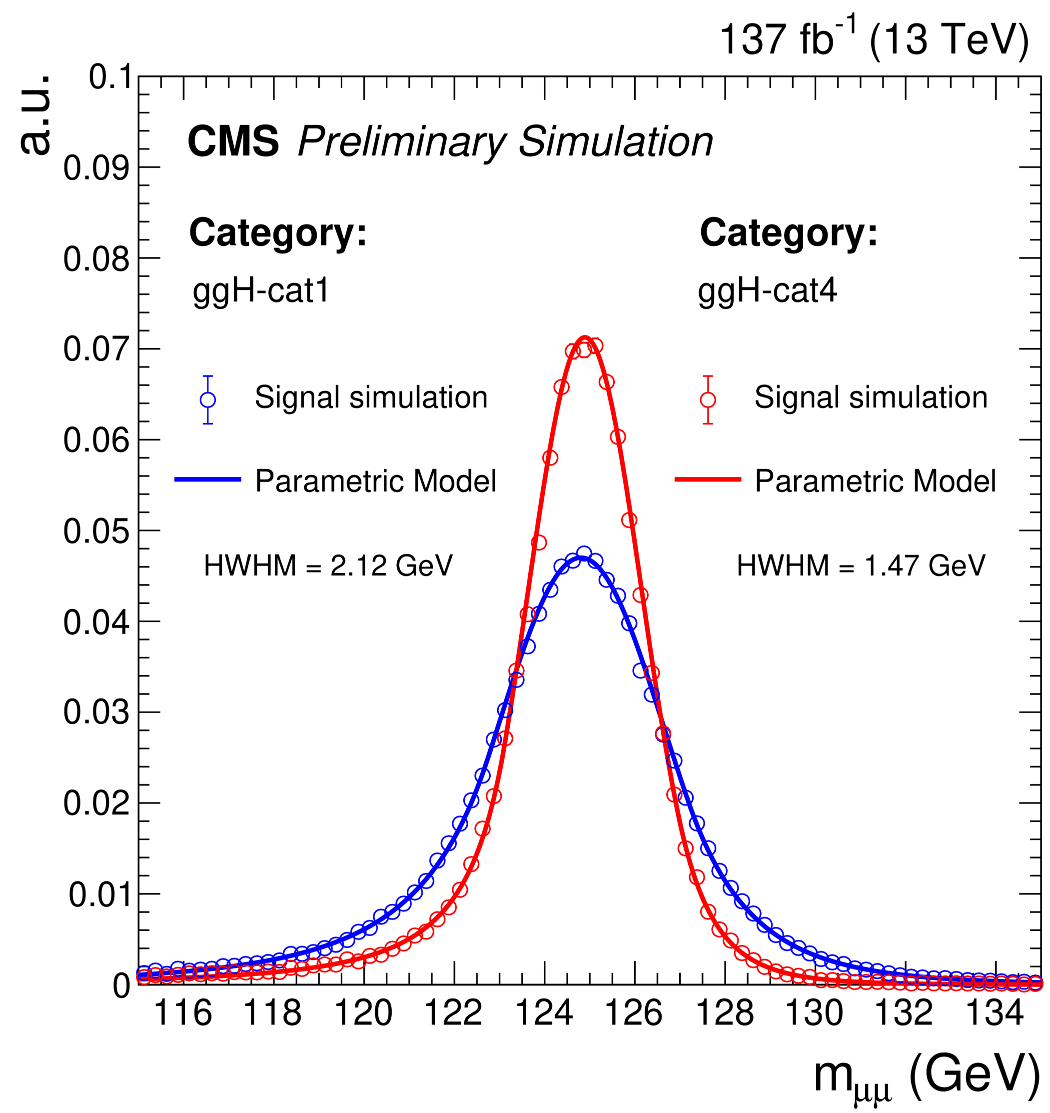

ggF Channel: Result

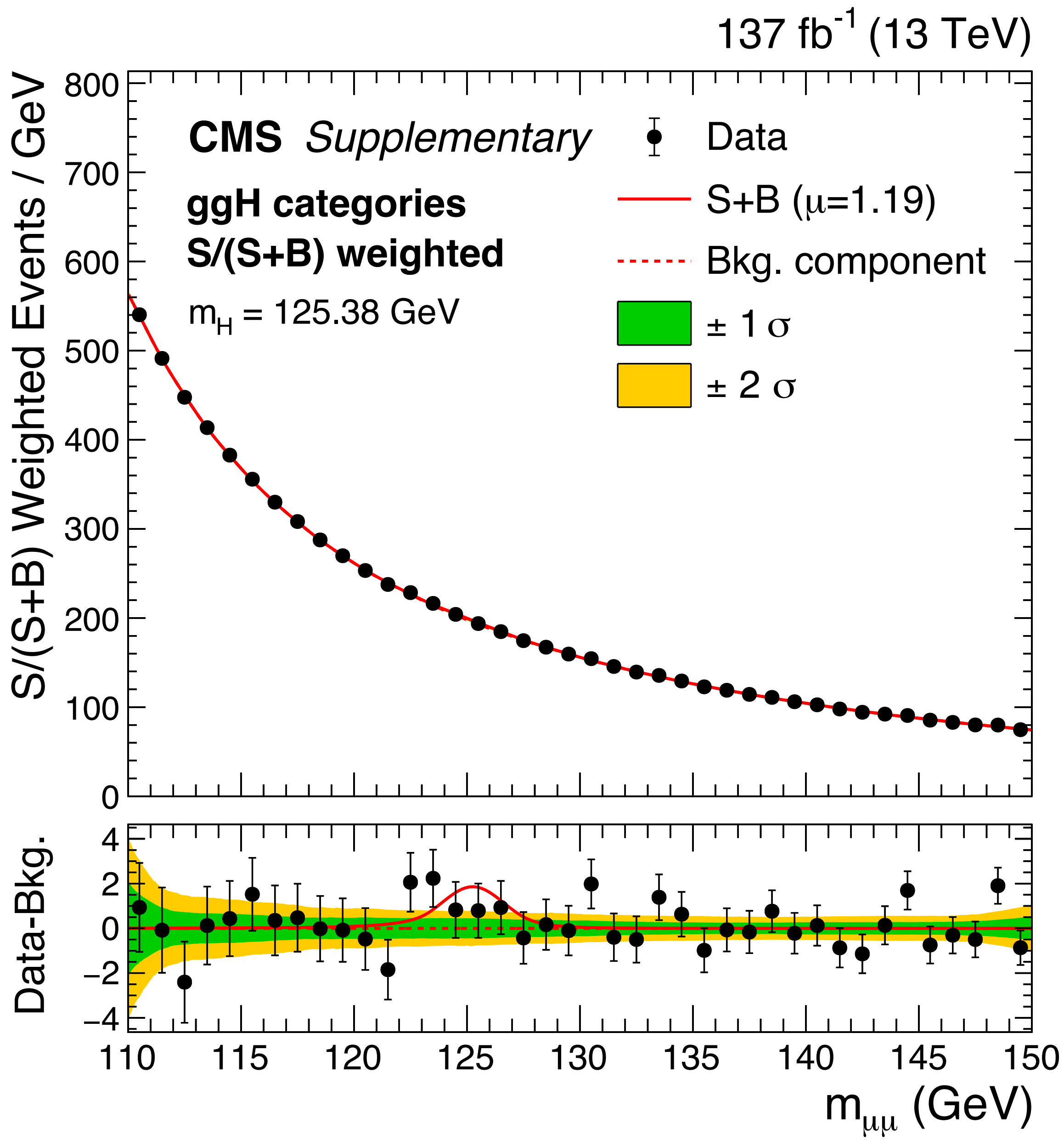

Observed (expected) significance: 0.99σ (1.56σ) @m_H = 125.38 GeV

Event category	Total signal	ggH (%)	VBF (%)	Other (%)	HWHM (GeV)	Bkg. @HWHM	Data @HWHM	S/(S+B) (%) @HWHM	$S/\sqrt{B}$ @HWHM
ggH-cat1	268	93.7	2.9	3.4	2.12	86 360	86 632	0.20	0.60
ggH-cat2	312	93.5	3.4	3.1	1.75	46 350	46 393	0.46	0.98
ggH-cat3	131	93.2	4.0	2.8	1.60	12 660	12 738	0.70	0.80
ggH-cat4	126	91.5	5.5	3.0	1.47	8260	8377	1.03	0.96
ggH-cat5	53.8	83.5	14.3	2.2	1.50	1680	1711	2.16	0.91

VBF Channel: Overview

- Small signal event yield in VBF channel: ~48 signal events expected
- New analysis strategy based on Monte Carlo (MC) simulation

VBF Higgs signal

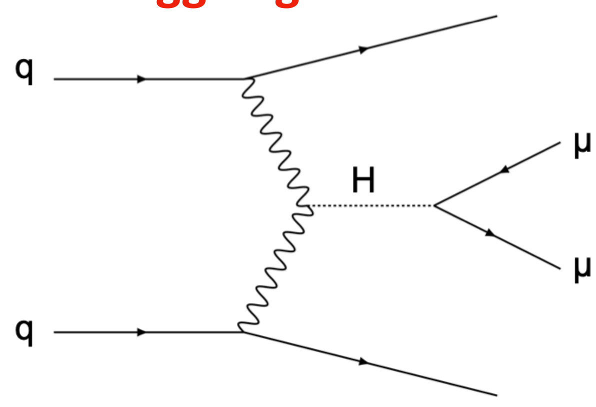

main background: electroweak production of two jets in association with a Z boson

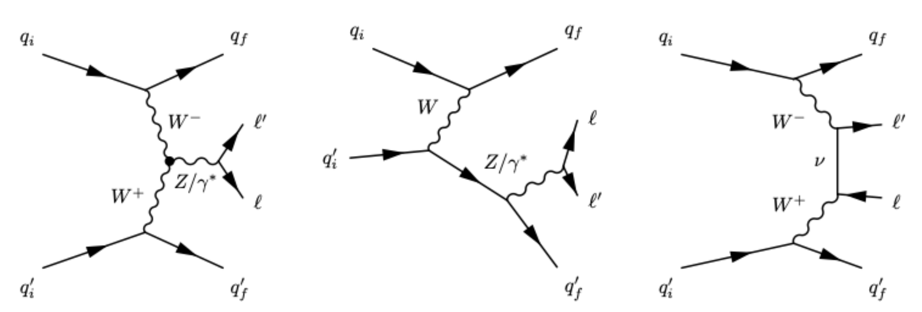

main background: Drell–Yan production with two jets

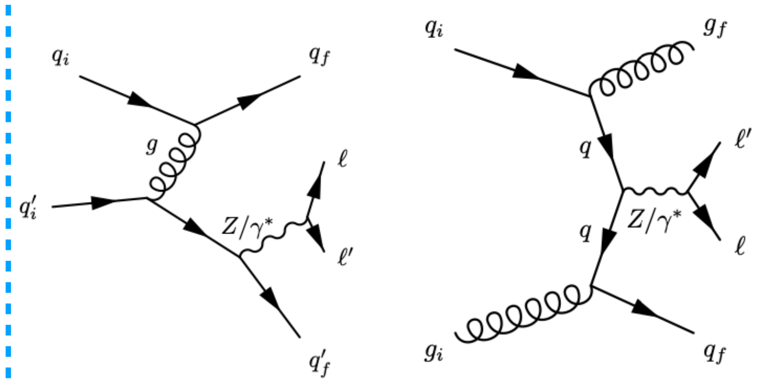

- Deep neural network (DNN) output score used as final discriminant
  - 20% improvement compared to mass fit method
  - DNN trained on kinematic information of the two muons and VBF signature (24 variables in total, including $m_{\mu\mu}$)
  - Analysis strategy similar to the CMS study on electroweak Z+2jets production:
    - *JHEP 10 (2013) 101 (7 TeV), Eur. Phys. J. C 75 (2015) 66 (8 TeV observation), Eur. Phys. J. C 78 (2018) 589 (13 TeV measurement)*

VBF Channel: Analysis Strategy

Simultaneously fit in 6 VBF categories in total (signal and sideband regions in each year 2016, 17 and 18)

Full Run 2

signal region

115 < $m_{\mu\mu}$ < 135 GeV

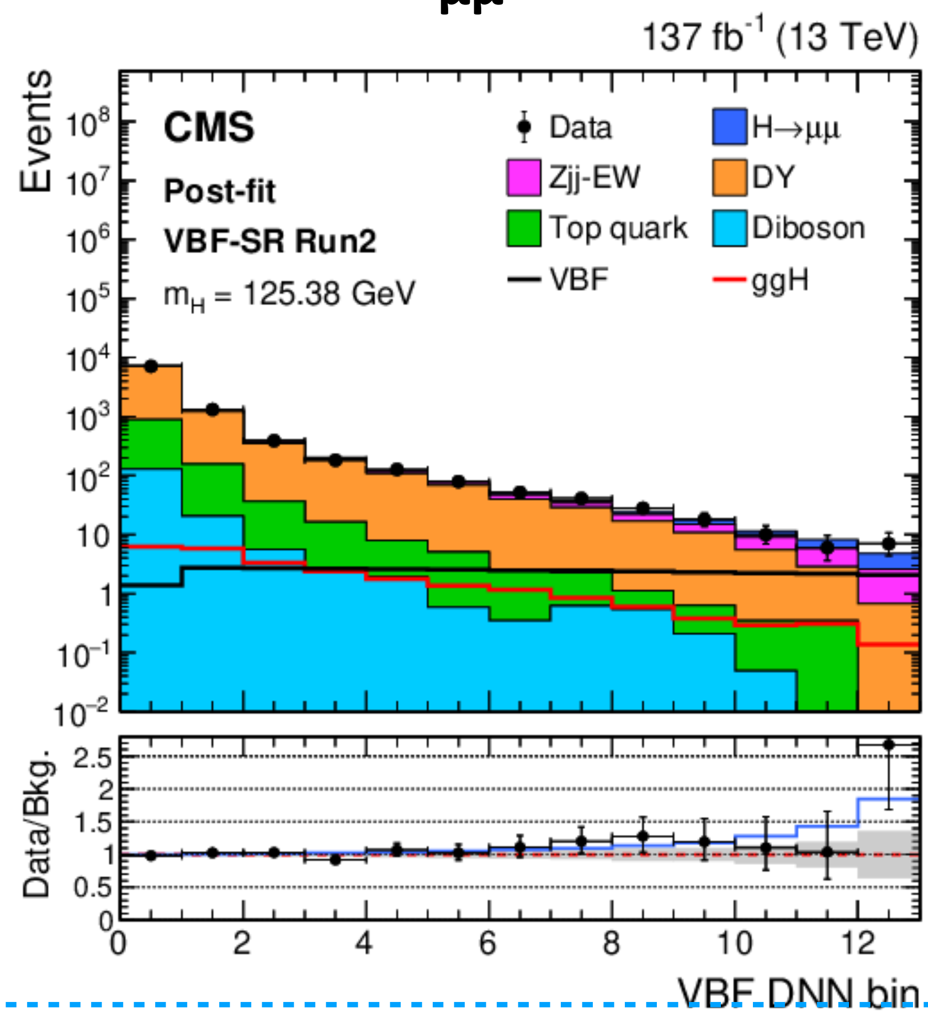

Full Run 2

sideband region: constraint background

110 < $m_{\mu\mu}$ < 115 GeV or 135 < $m_{\mu\mu}$ < 150 GeV

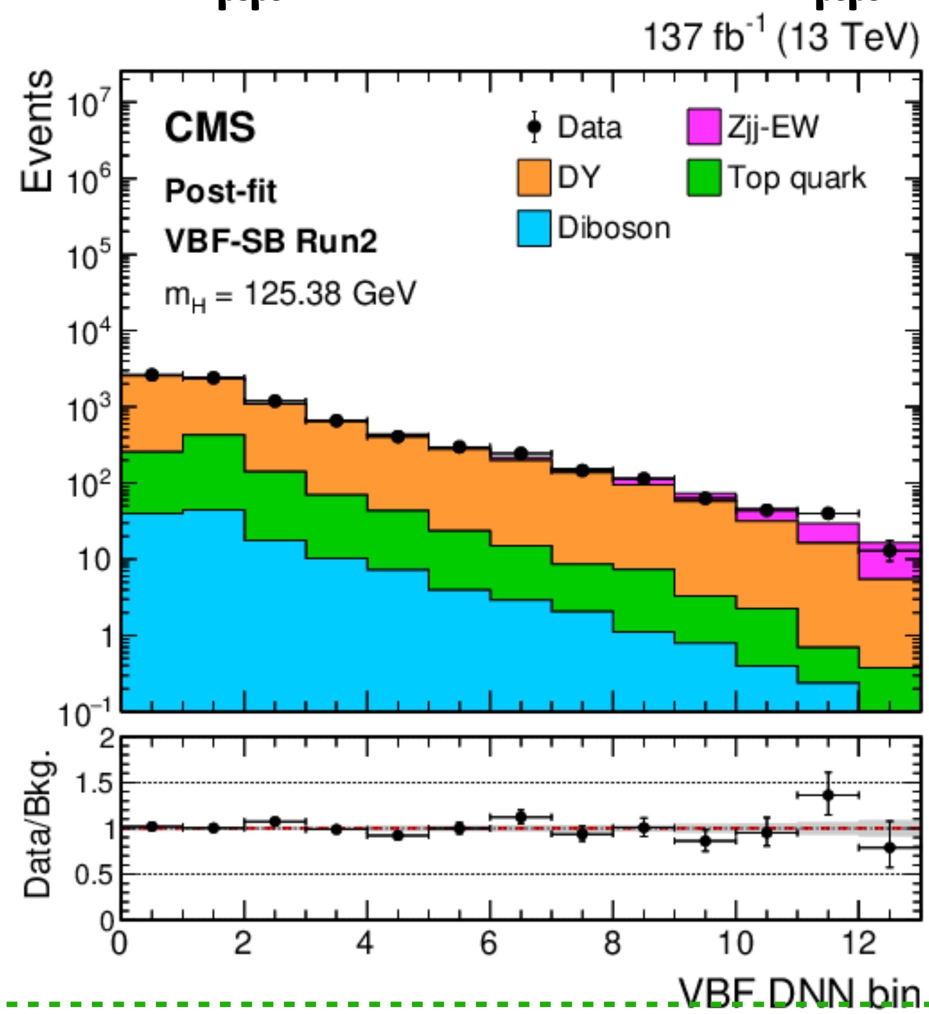

VBF Channel: Result

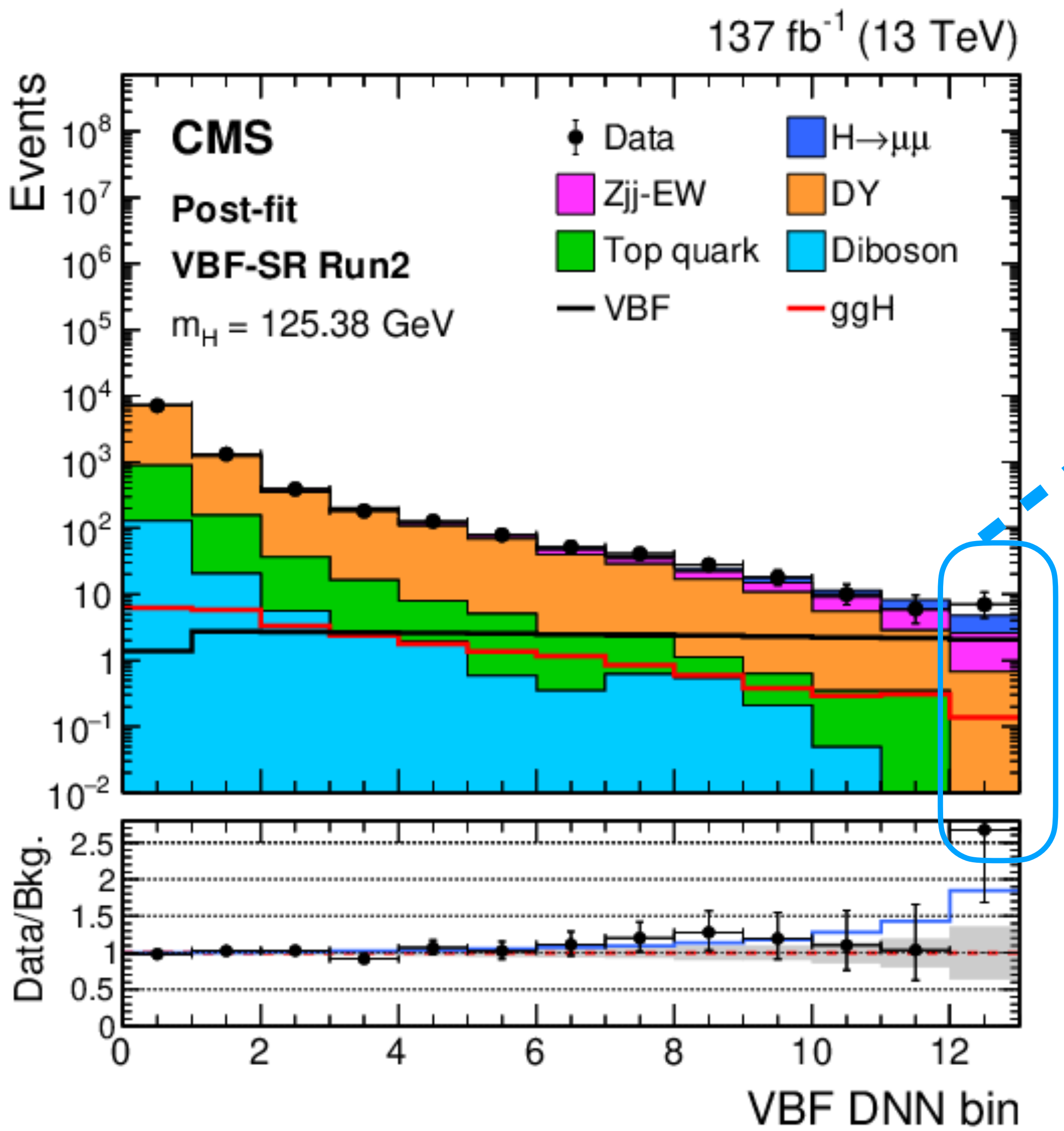

- **Achieve good signal purity in high DNN bins**
  - **last DNN bin signal purity 42%**
  - main background: electroweak Z+2jets, DY+2jets
- 20% improvement in sensitivity compared to $m_{\mu\mu}$ mass fit method
- Observed (expected) significance: 2.40σ (1.77σ), m_H = 125.38 GeV

DNN bin	Total signal	VBF (%)	ggH (%)	Bkg. ± ΔB	Data	S/(S+B) (%)	$S/\sqrt{B}$
1–3	19.5	30	70	8890 ± 67	8815	0.22	0.21
4–6	11.6	57	43	394 ± 8	388	2.86	0.58
7–9	8.43	73	27	103 ± 4	121	7.56	0.83
10	2.30	85	15	15.1 ± 1.4	18	13.2	0.59
11	2.15	88	12	9.1 ± 1.2	10	19.1	0.71
12	2.10	87	13	5.8 ± 1.1	6	26.6	0.87
13	1.87	94	6	2.6 ± 0.9	7	41.8	1.16

First Evidence of H→μμ

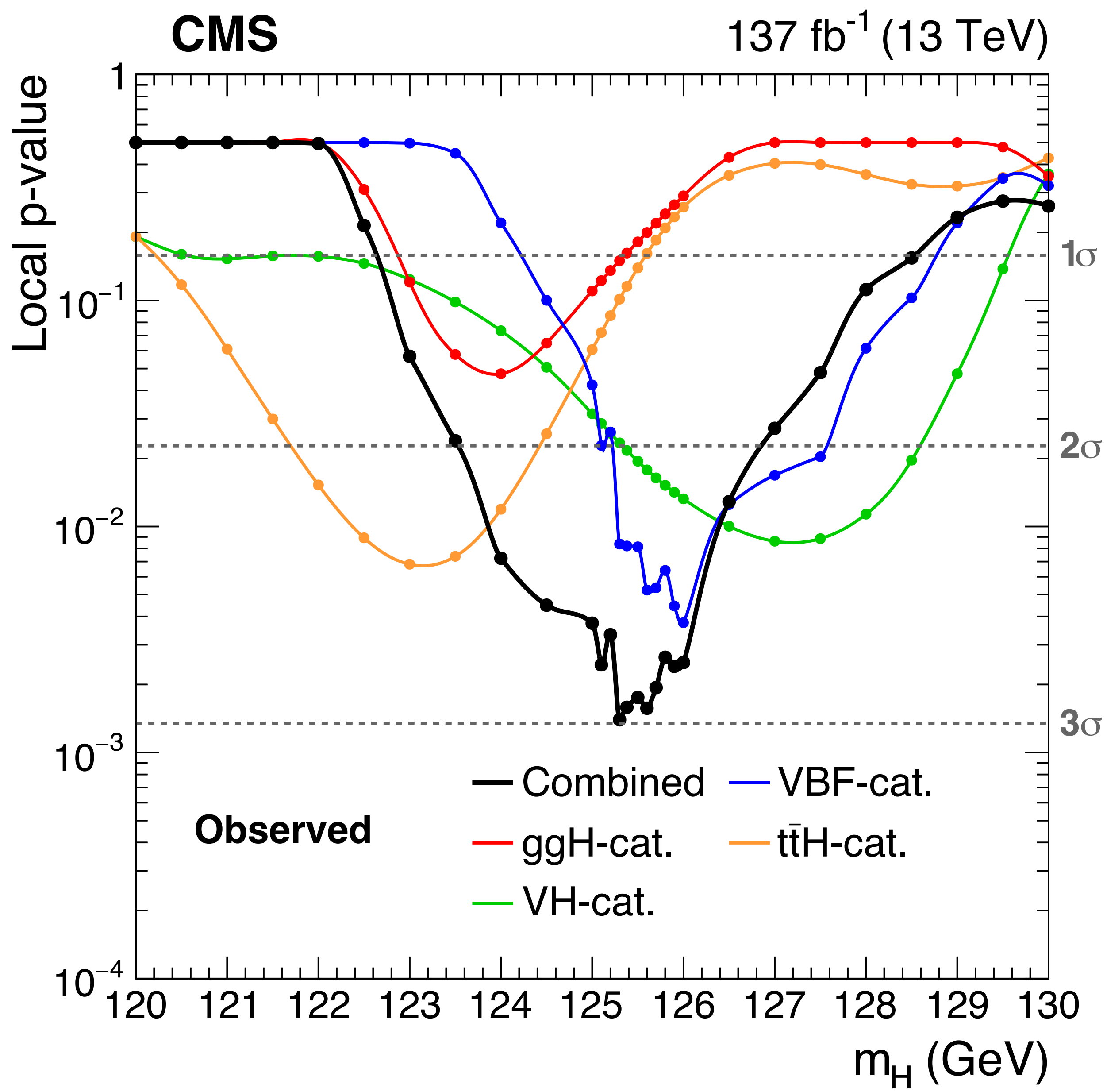

@m_H = 125.38 GeV:

- Run 2: observed (expected) signal significance **3.0σ (2.5σ)**

First Evidence of H→μμ !

Higgs Boson Coupling to Muon

- Precision of κ_μ improved from 89% to 21% in two years.
- 35% improvement in analysis strategy

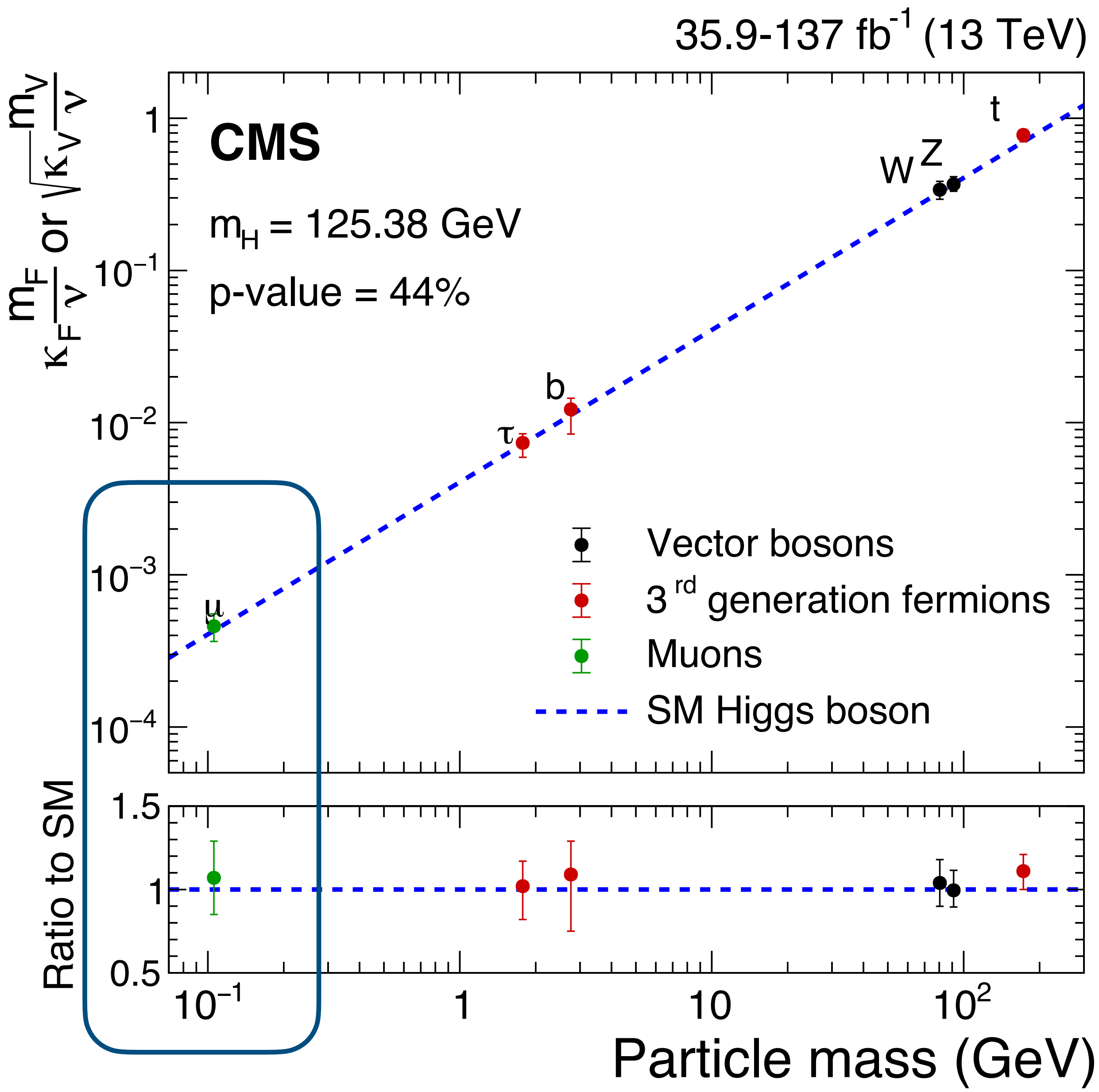

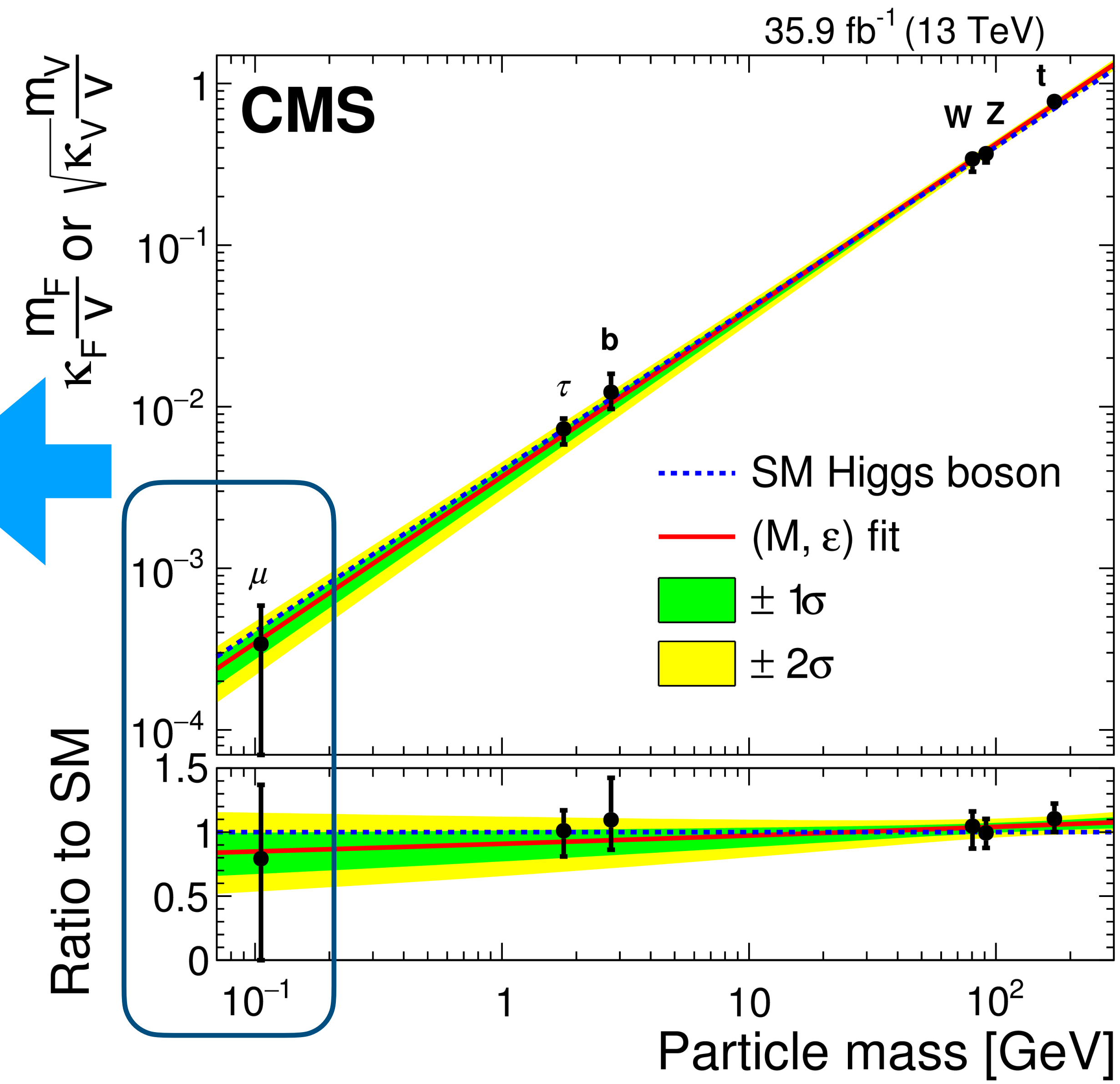

EPJC 79 (2019) 421

$\kappa_\mu = 1.07^{+0.22}_{-0.22}$ at 68% CL

$\kappa_\mu = 0.79^{+0.58}_{-0.79}$ at 68% CL

Great Discovery Potential at the LHC

We are in early stage of the LHC research program, 5% of total data taken so far

https://project-hl-lhc-industry.web.cern.ch/content/project-schedule

HL-LHC Prospect of Higgs Coupling to Muon

- Projection at HL-LHC combining ATLAS and CMS: 4.3% precision
- Complementary with proposed future e^+e^- collider Higgs factories

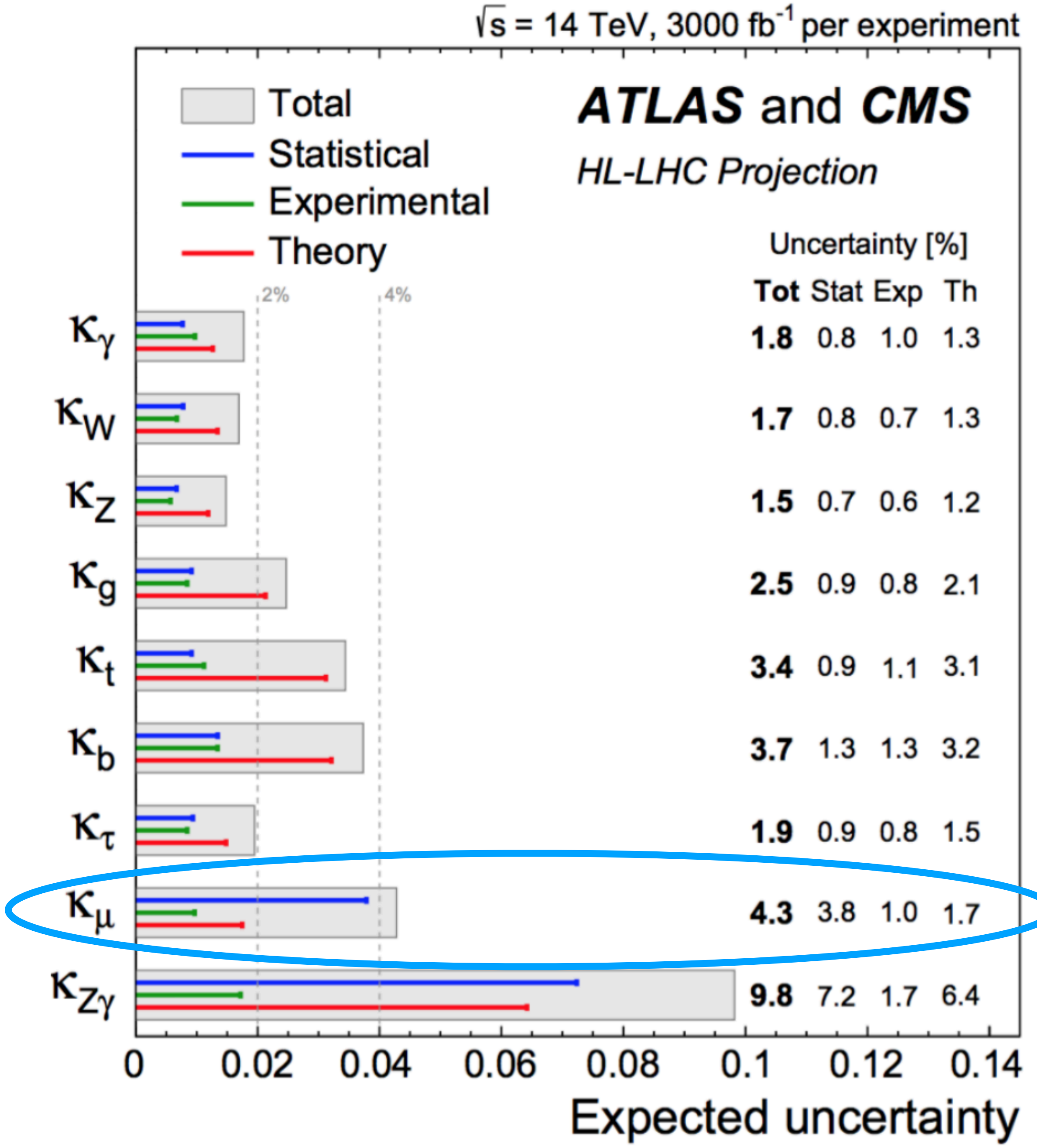

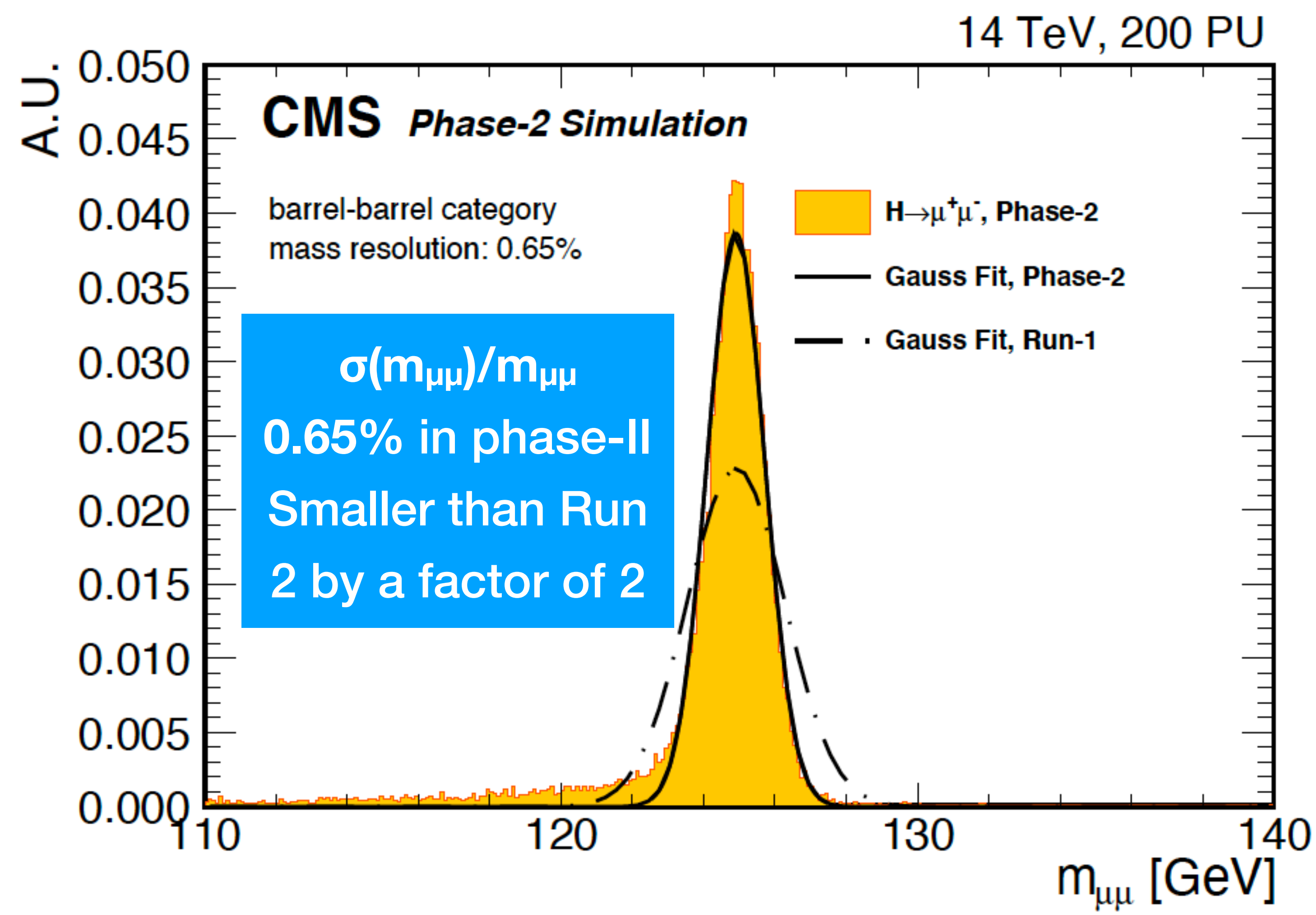

arxiv:1902.00134

Pileup Challenge at the HL-LHC

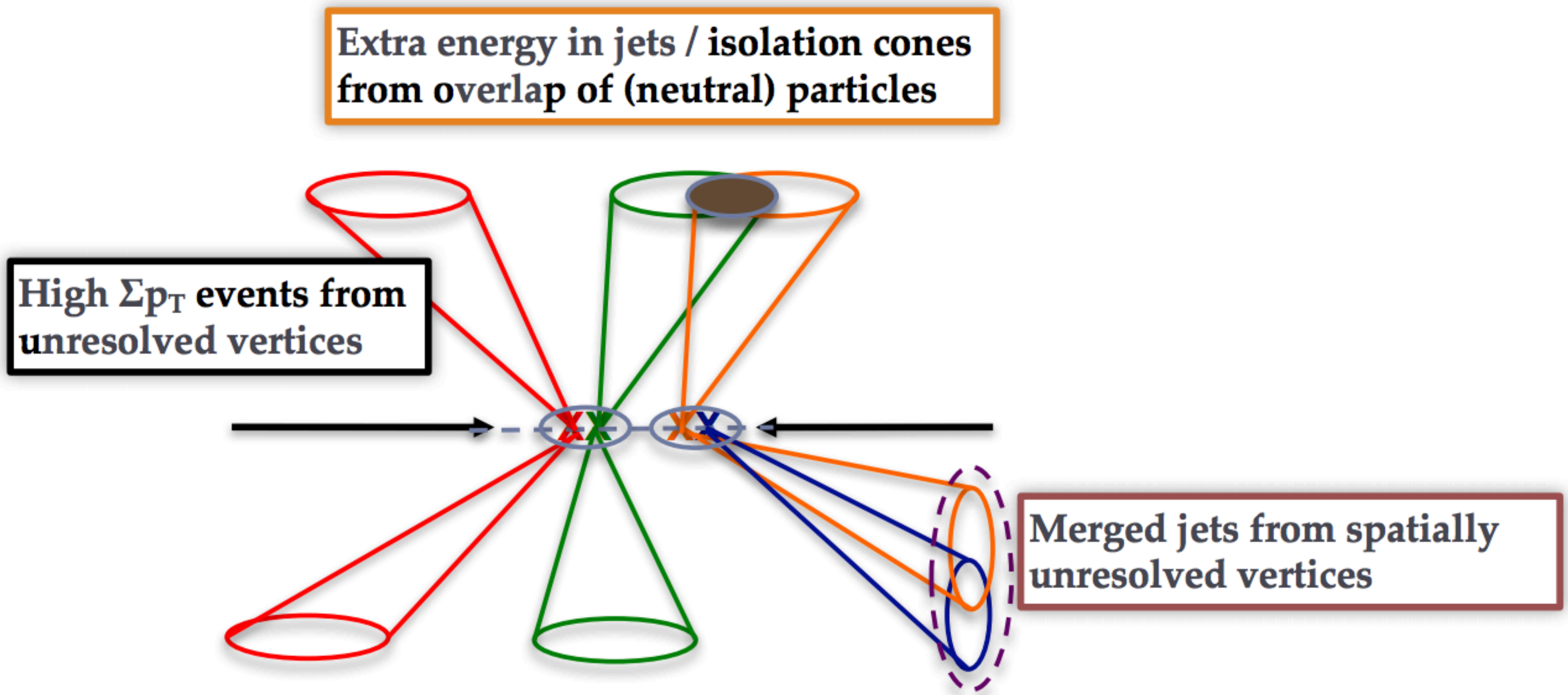

140-200 collisions per bunch crossing at HL-LHC

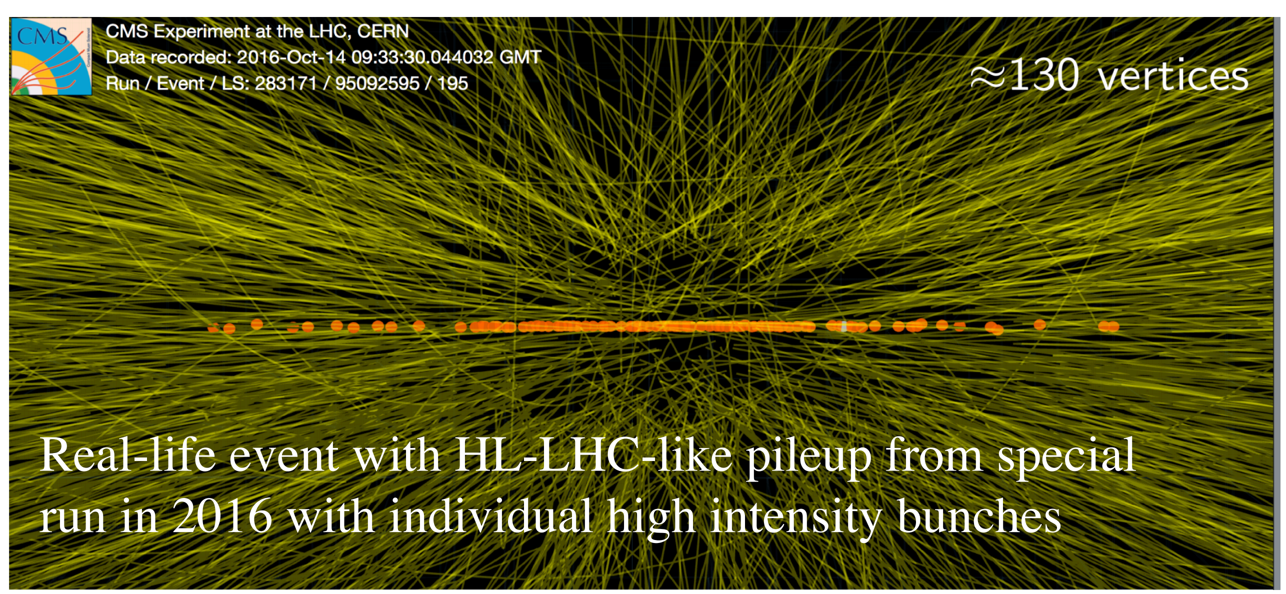

CMS MIP Timing Detector: New Precision Timing Dimension Measurement

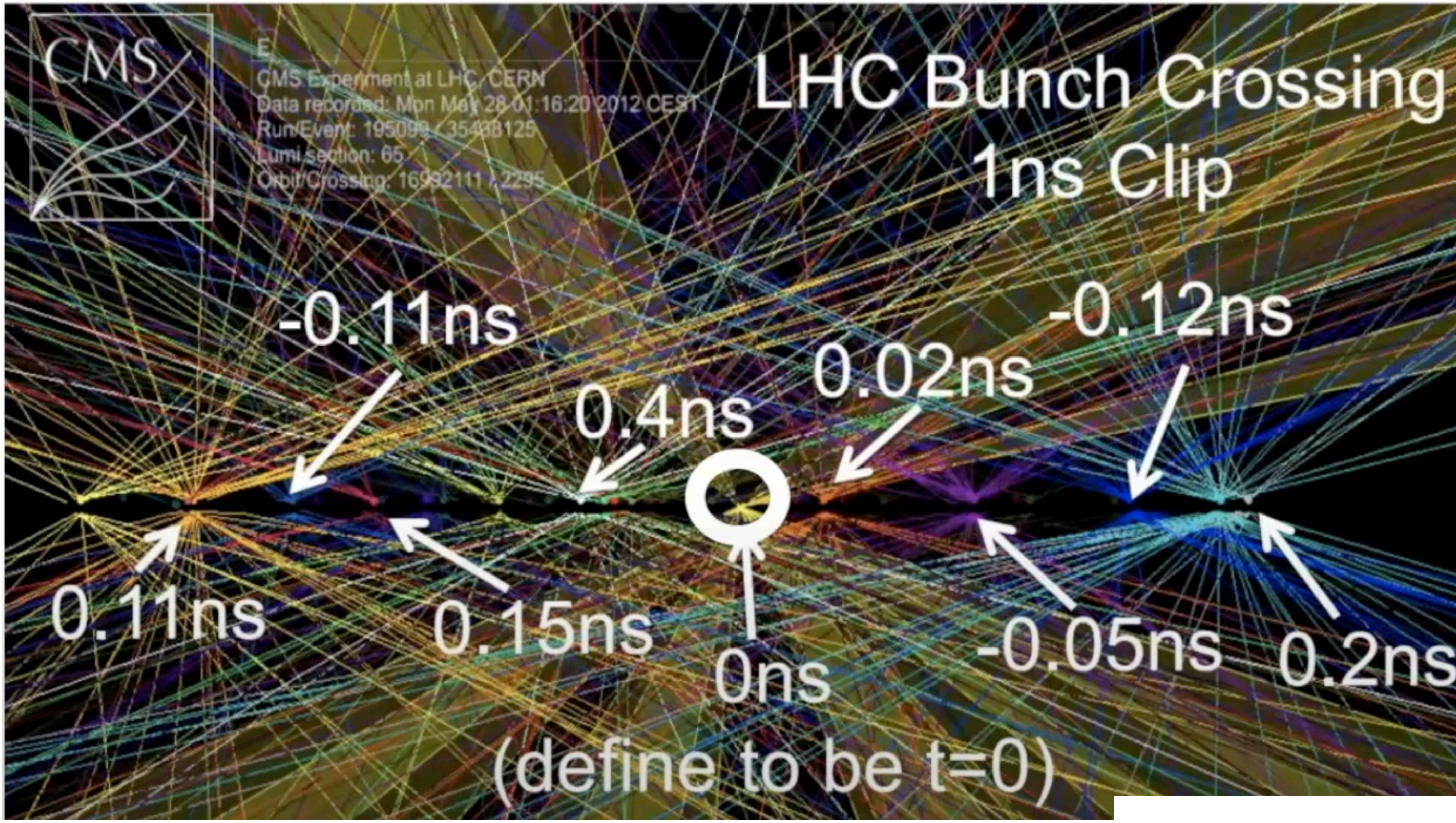

beam spot has a spread of about 180-200 ps: precision timing of 30-40 ps to mitigate the high pileup challenge

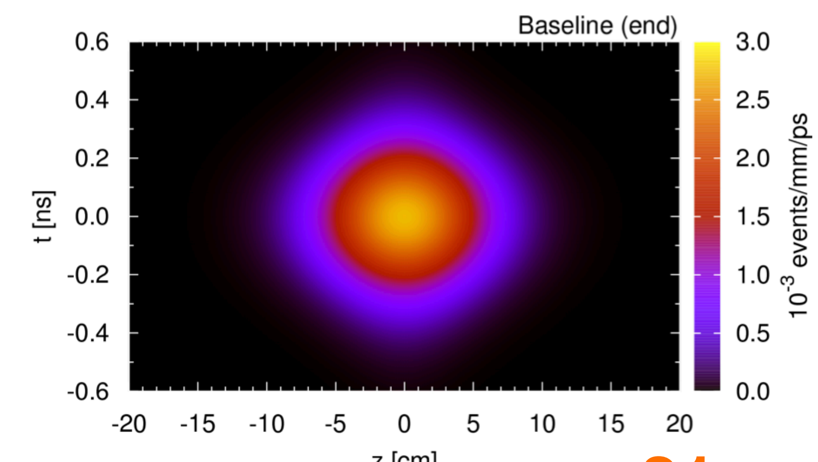

CMS MIP Timing Detector Overview

- Completely new capability to CMS: measure precisely (30-40 ps) the production time of MIPs

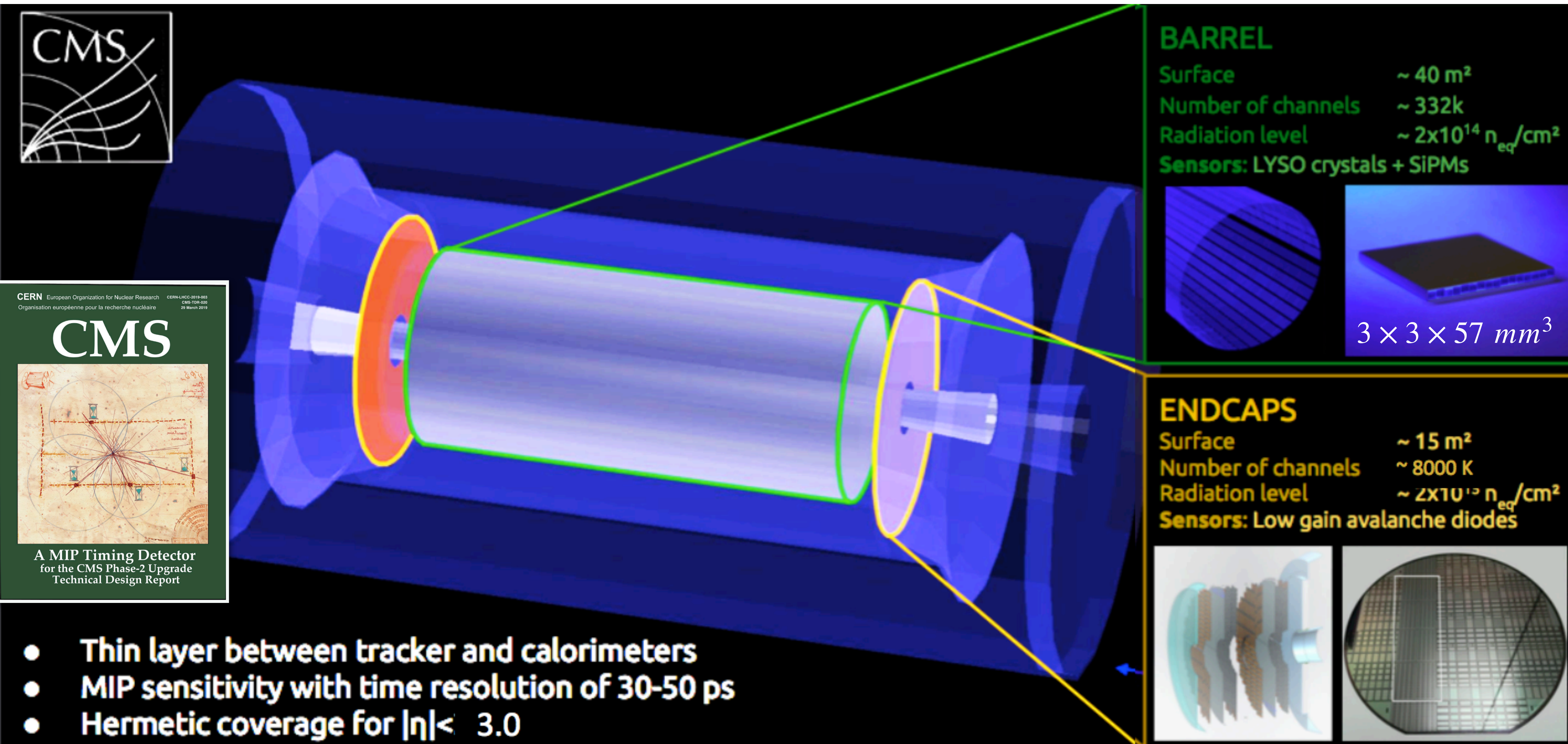

CMS-TDR-020 March 2019

MTD Physics Potential: Enhance Physics Object Reconstruction

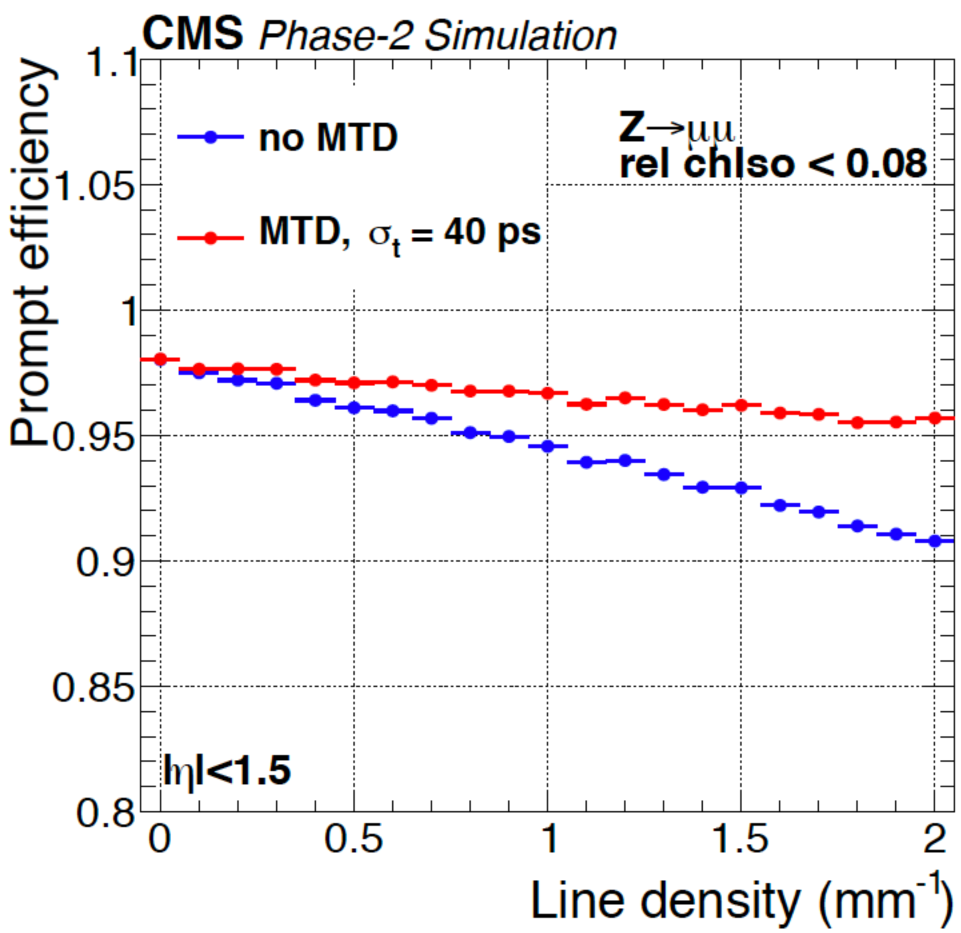

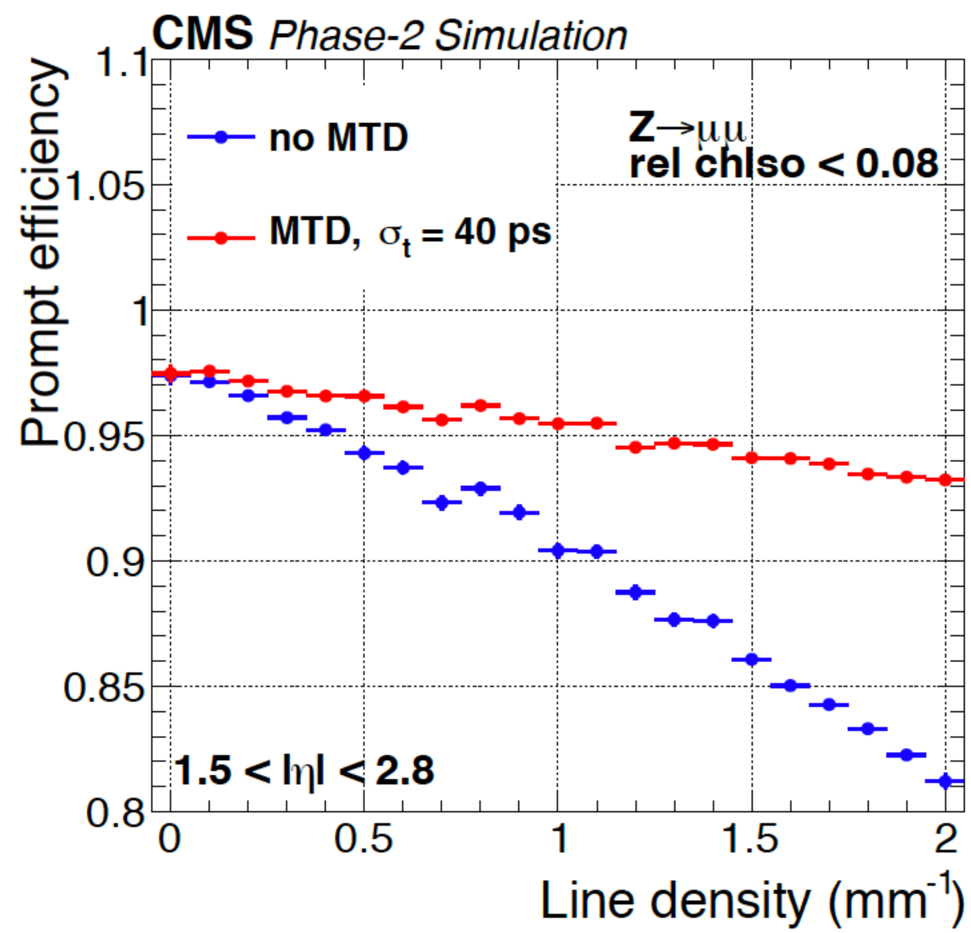

MTD guards against adverse pileup effect on muon reconstruction at HL-LHC

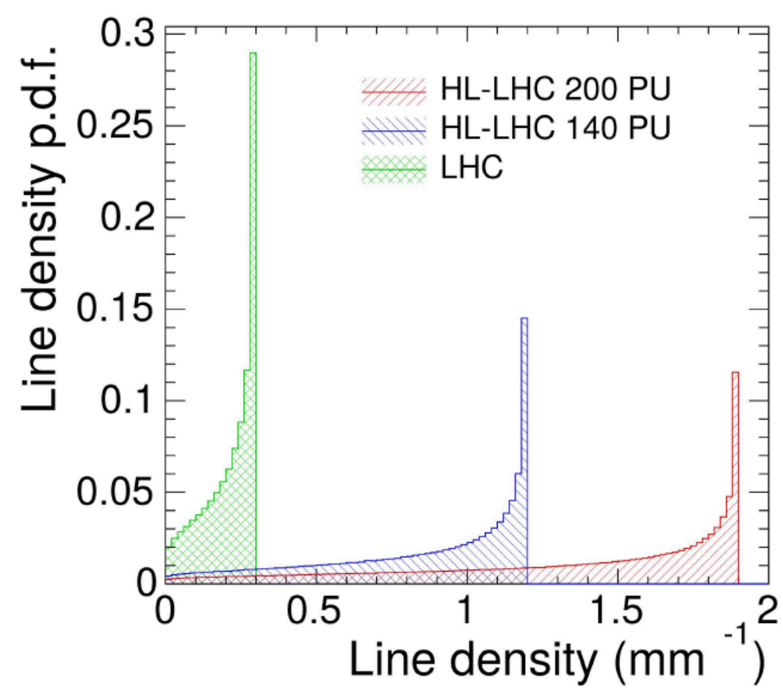

MTD Physics Potential: Expand Physics Reach at HL-LHC

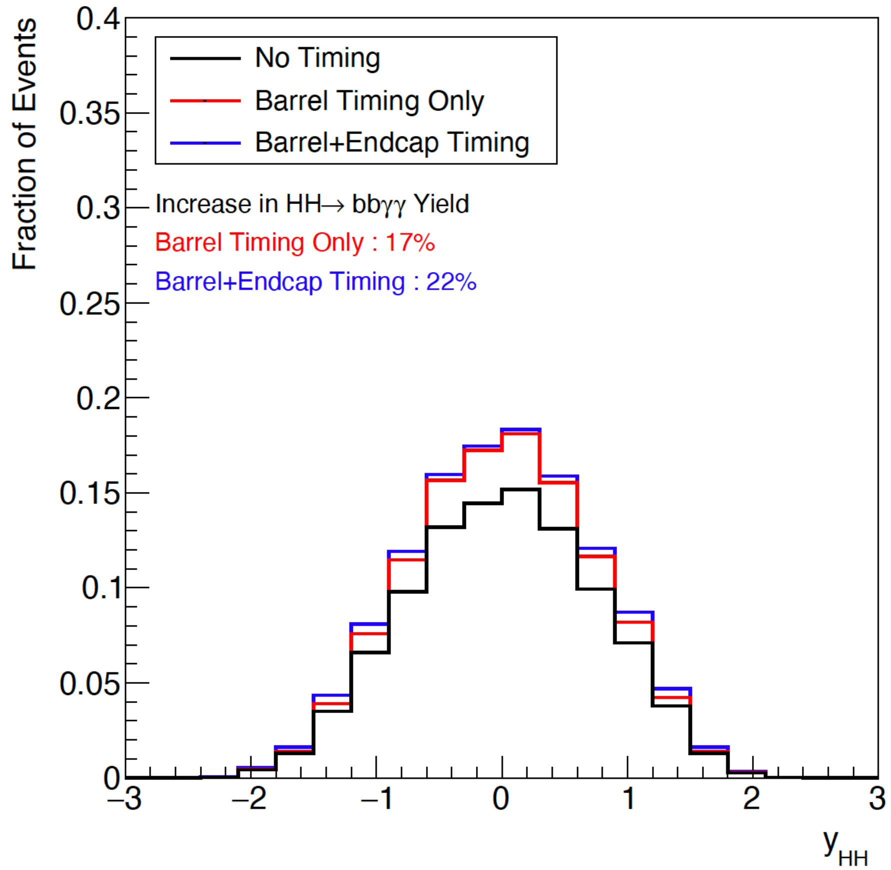

	Expected significance	
Di-Higgs decay	No MTD	MTD
bbbb	0.88	0.94
$bb\tau\tau$	1.3	1.48
$bb\gamma\gamma$	1.7	1.83
bbWW	0.53	0.58
bbZZ	0.38	0.42
Combined	2.4	2.63

- Reduction of pile-up enhances quality of particle reconstruction
    - 10 - 20% gain in di-Higgs significance
- Particle ID for low p_T hadrons, new reach for Heavy Ion Physics:
    - π/K separation up to 2 GeV, p/K separation up to 5 GeV
- Mass reconstruction of the long-lived particles

Test beam campaigns to characterize detector performance

Many test beam campaigns:

- Fermilab (FTBF)
- CERN North-Area (SPS)

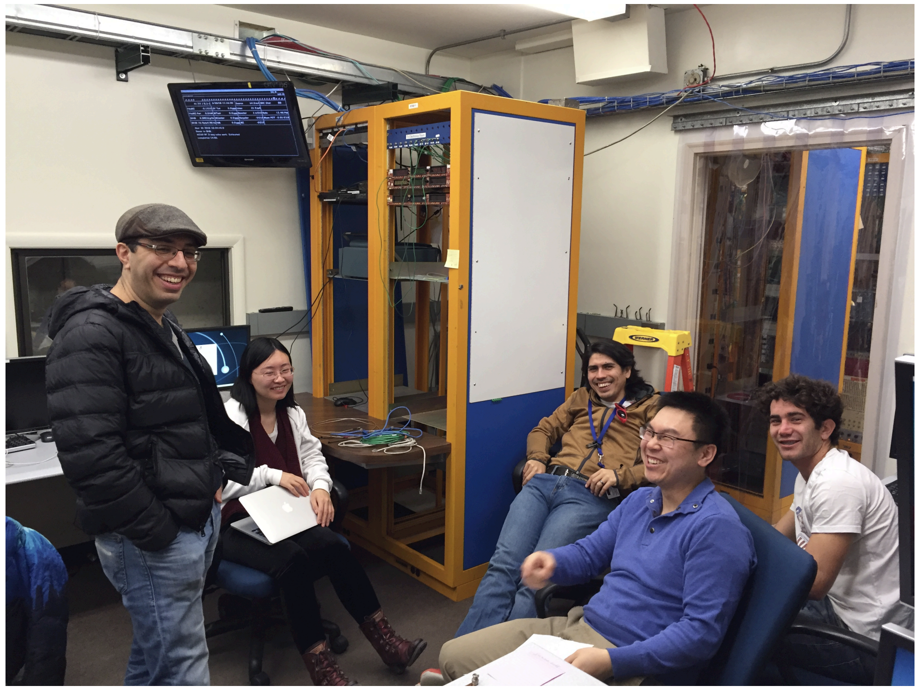

MTD test beam setup

- Time resolution measured against reference timing detector (Photek 240 micro-channel plate, time resolution ~15 ps)
- Tracking of charged particles by precision telescope, 0.2 mm position resolution

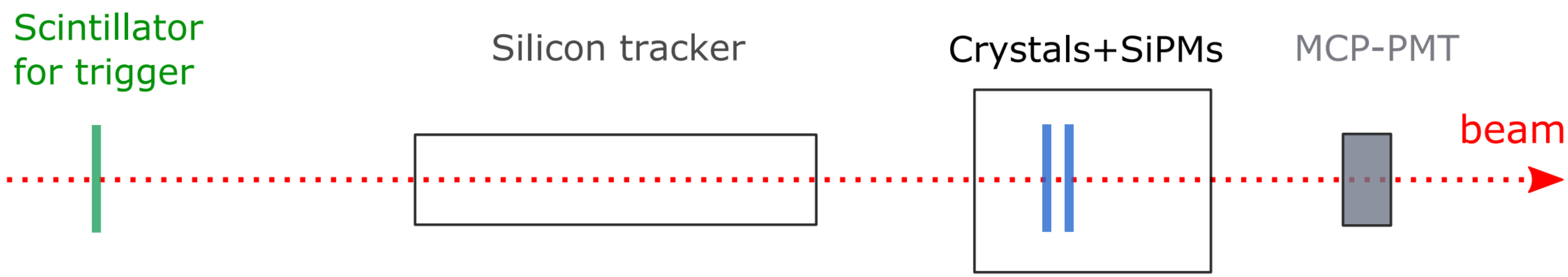

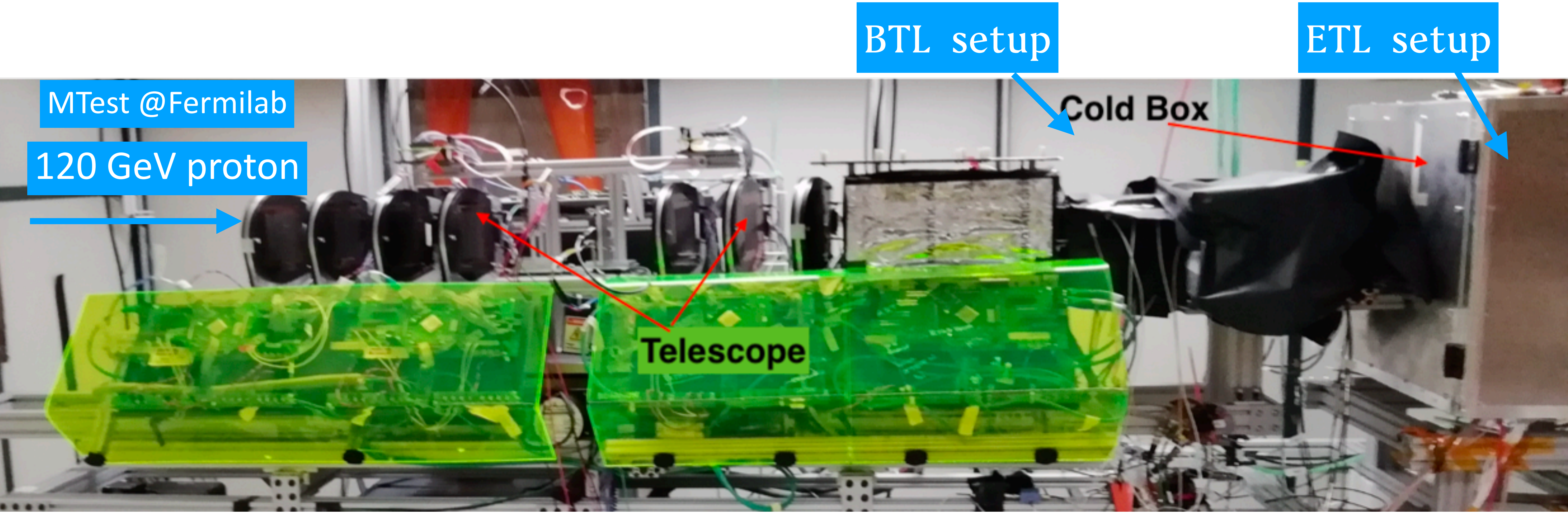

BTL: crystal based precision timing

BTL sensor: Lutetium-yttrium orthosilicate crystals activated with cerium (LYSO:Ce) as scintillator readout by Silicon Photomultipliers

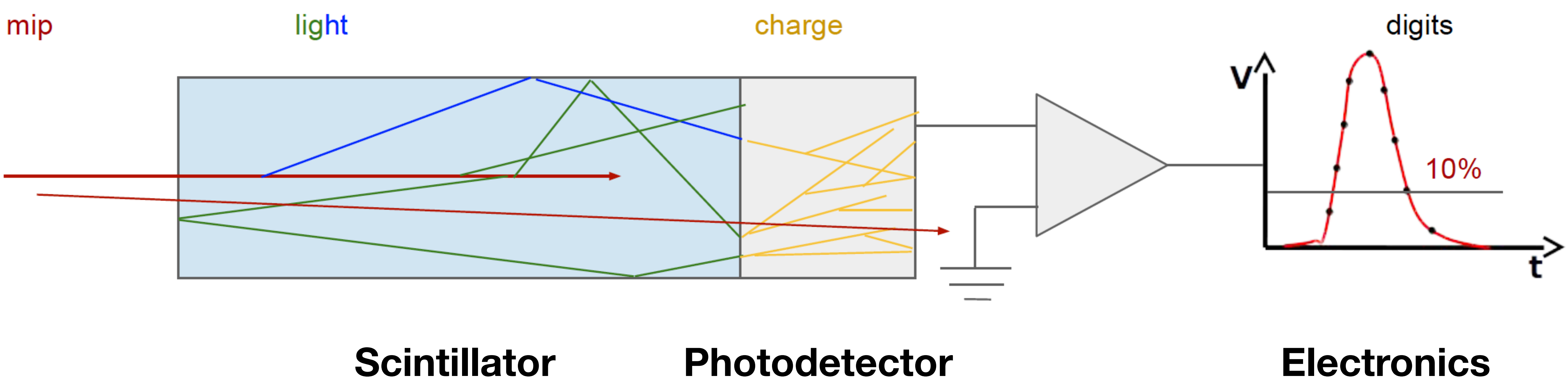

Digram credit: Marco Lucchini

BTL Sensor design optimization - crystal tiles

Design in MTD Technical Proposal
Nov 2017 LHCC-P-009

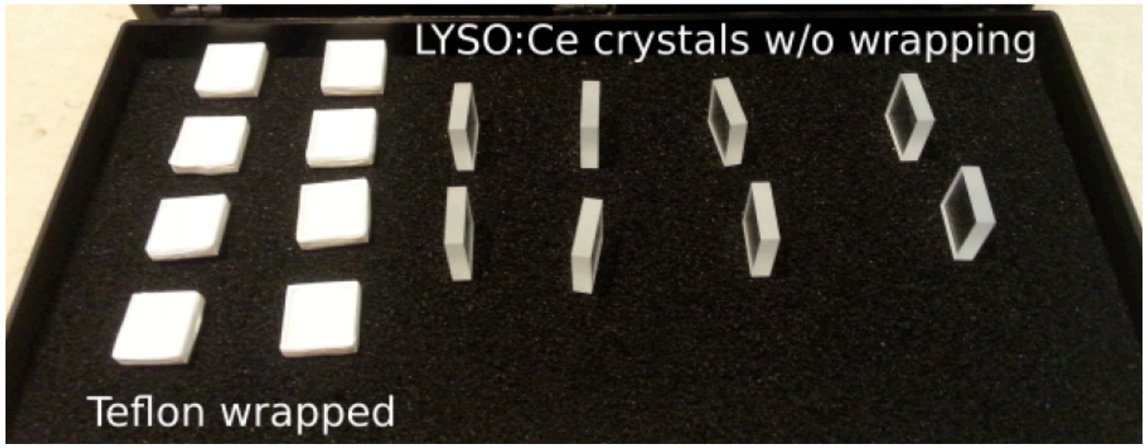

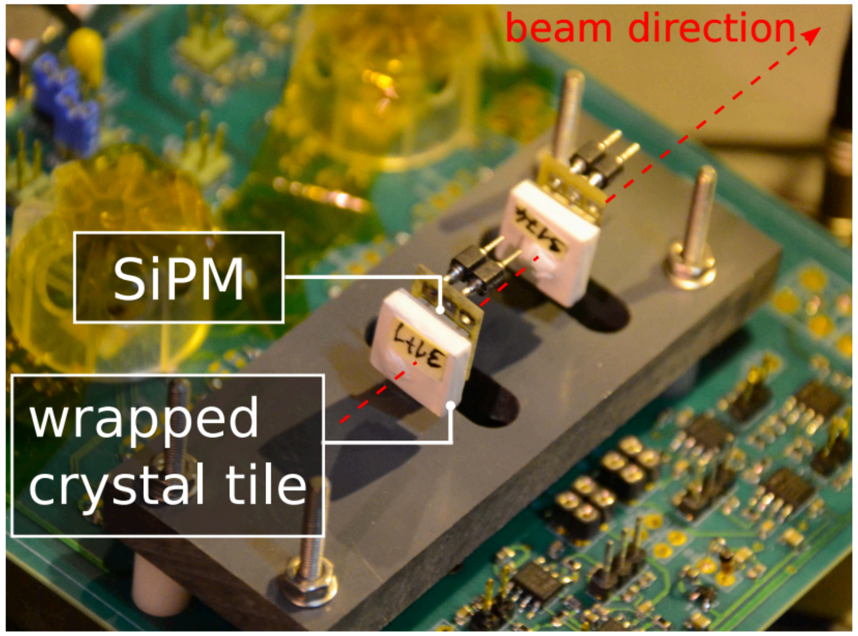

test beam measurement of 11 × 11 × 3 mm³ LYSO tile with 5 × 5 mm² SiPM

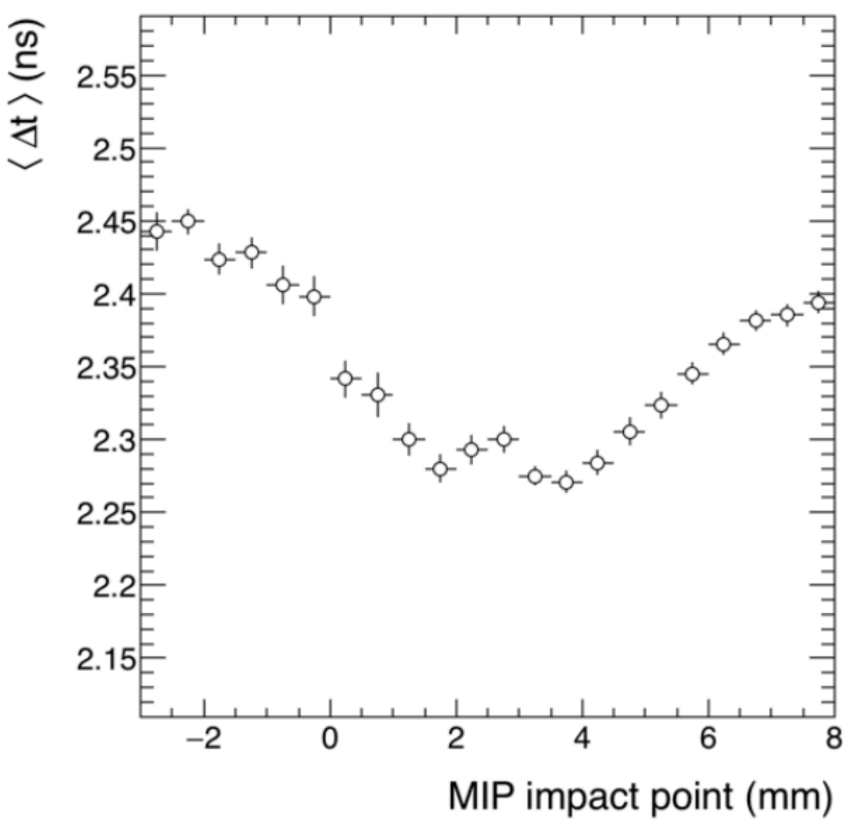

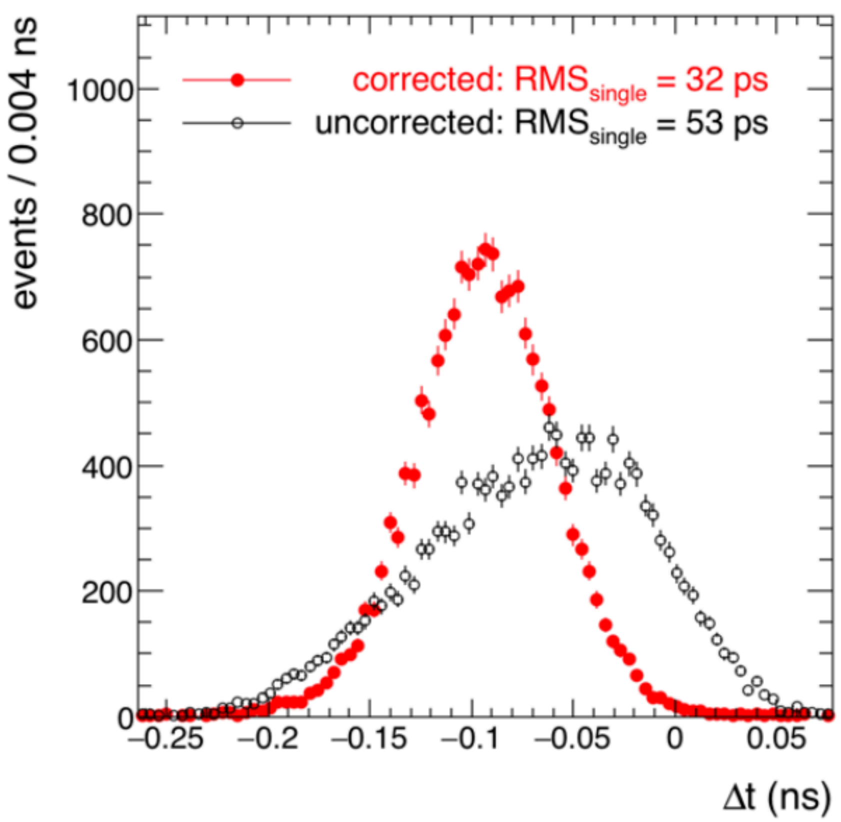

Sensor Design Pptimization - Crystal bars

Baseline design since CMS-TDR-020 March 2019

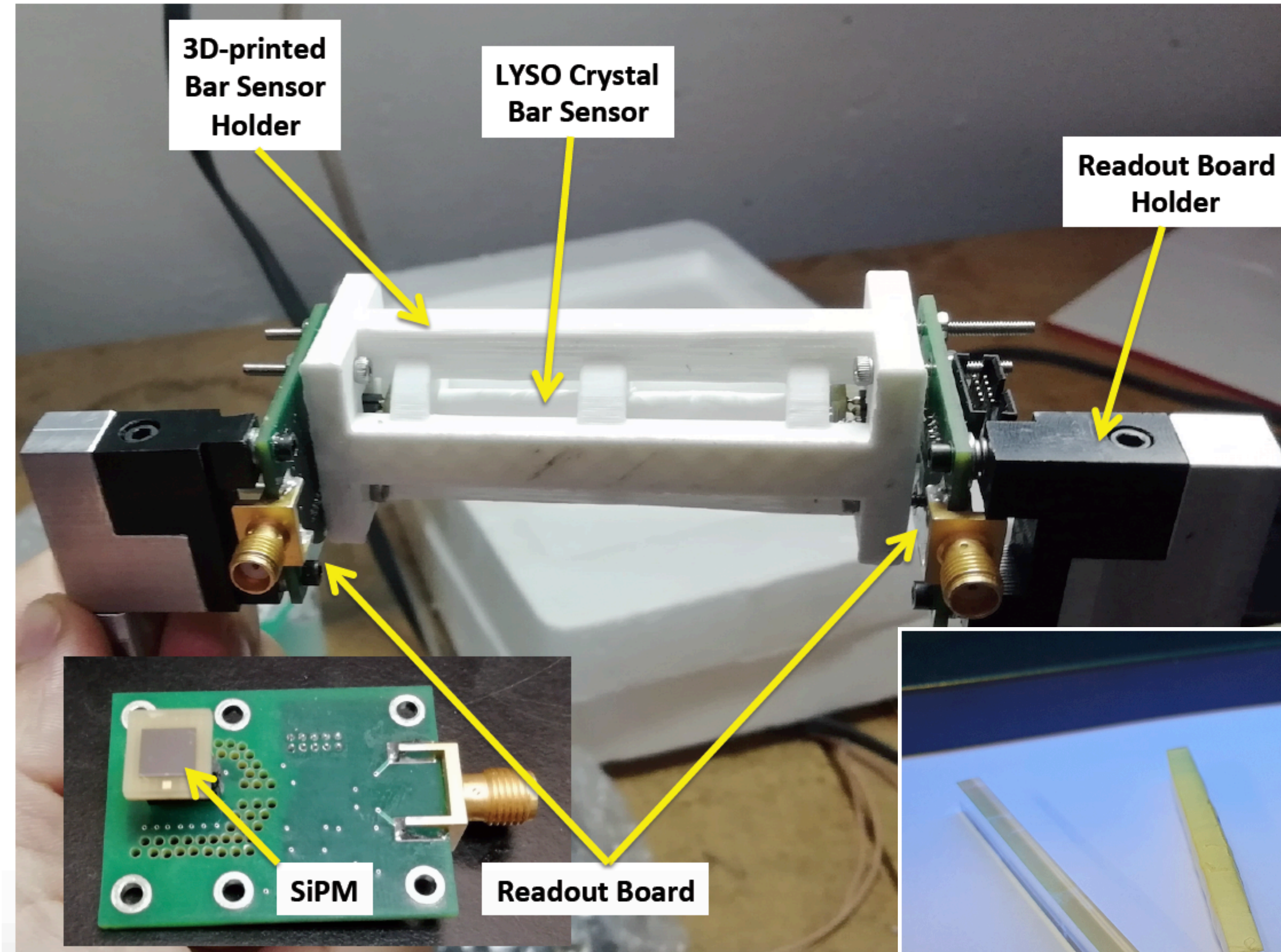

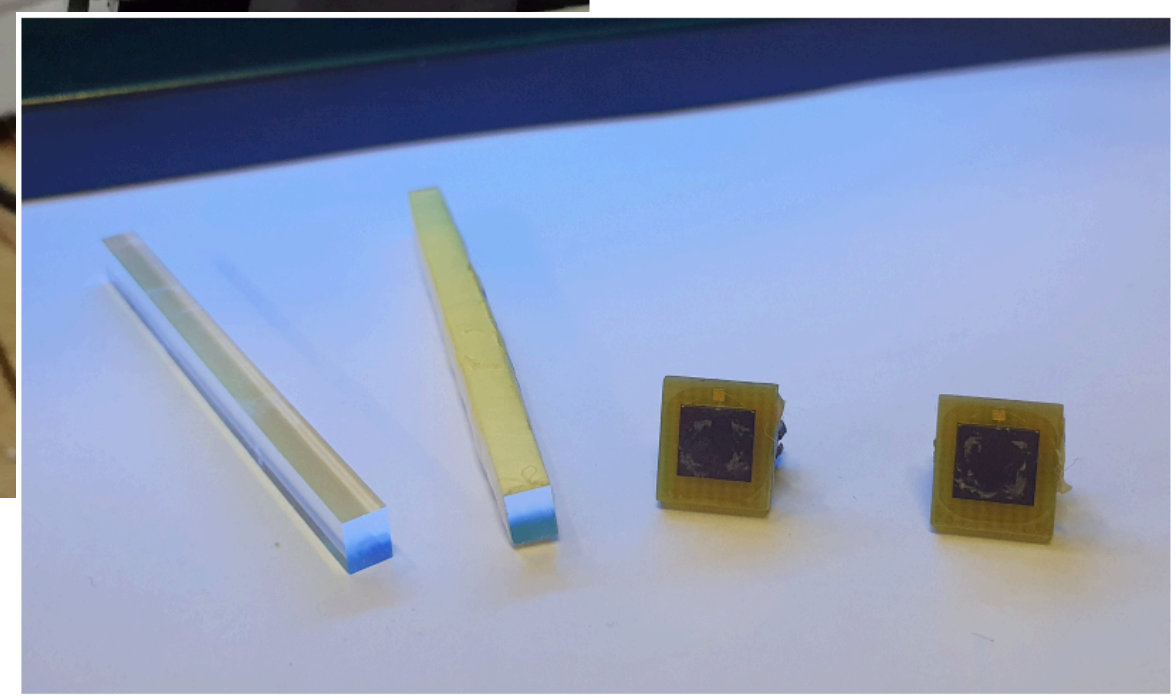

BTL sensor performance in test beam

- Timestamp of a MIP traversing BTL: $t_{Ave} = (t_{left} + t_{right})/2$
- Achieved ~25 ps time resolution per sensor before irradiation
- Uniform time response and resolution across sensor area

BTL first test beam paper accepted by JINST arxiv: 2104.07786

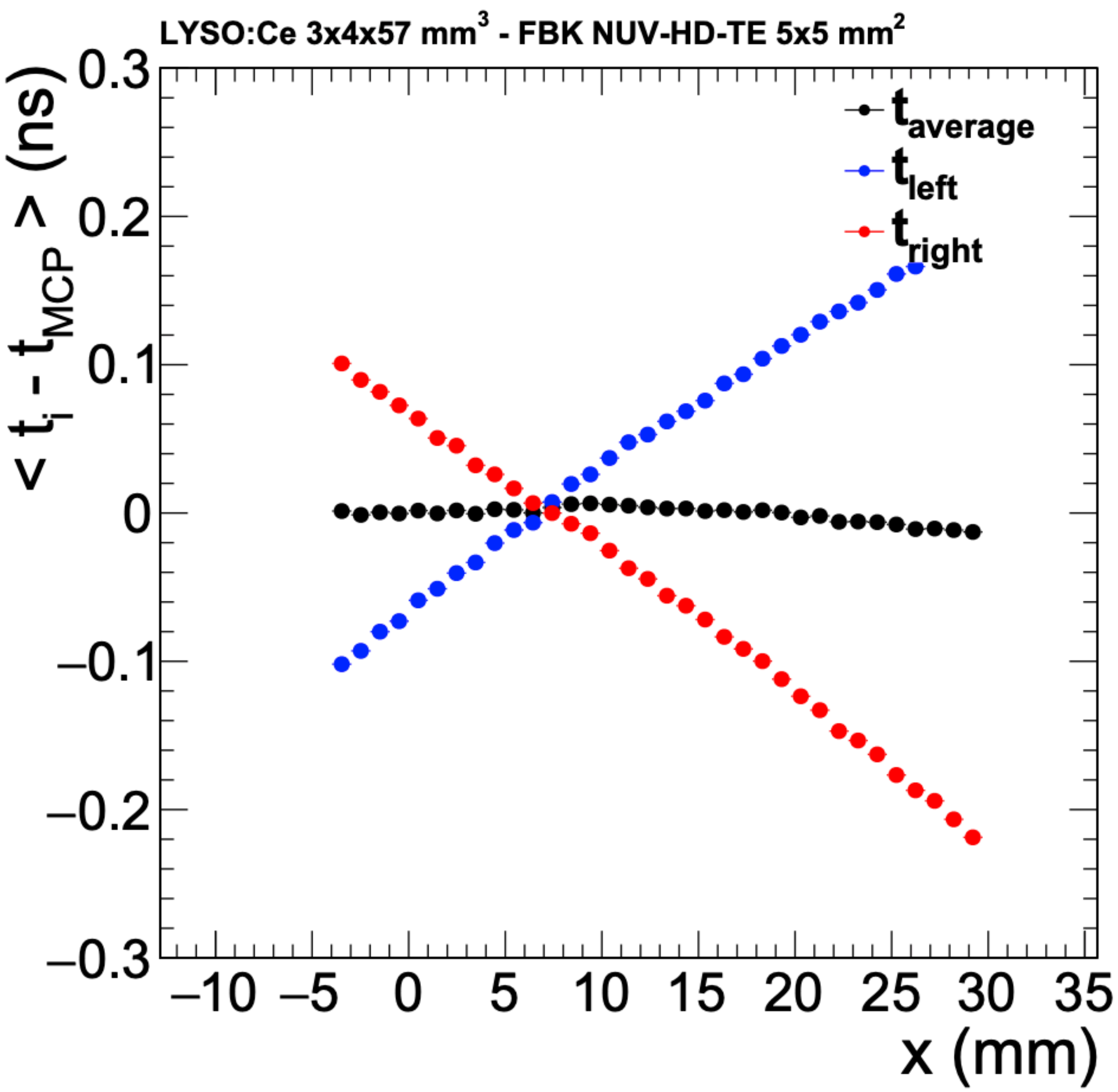

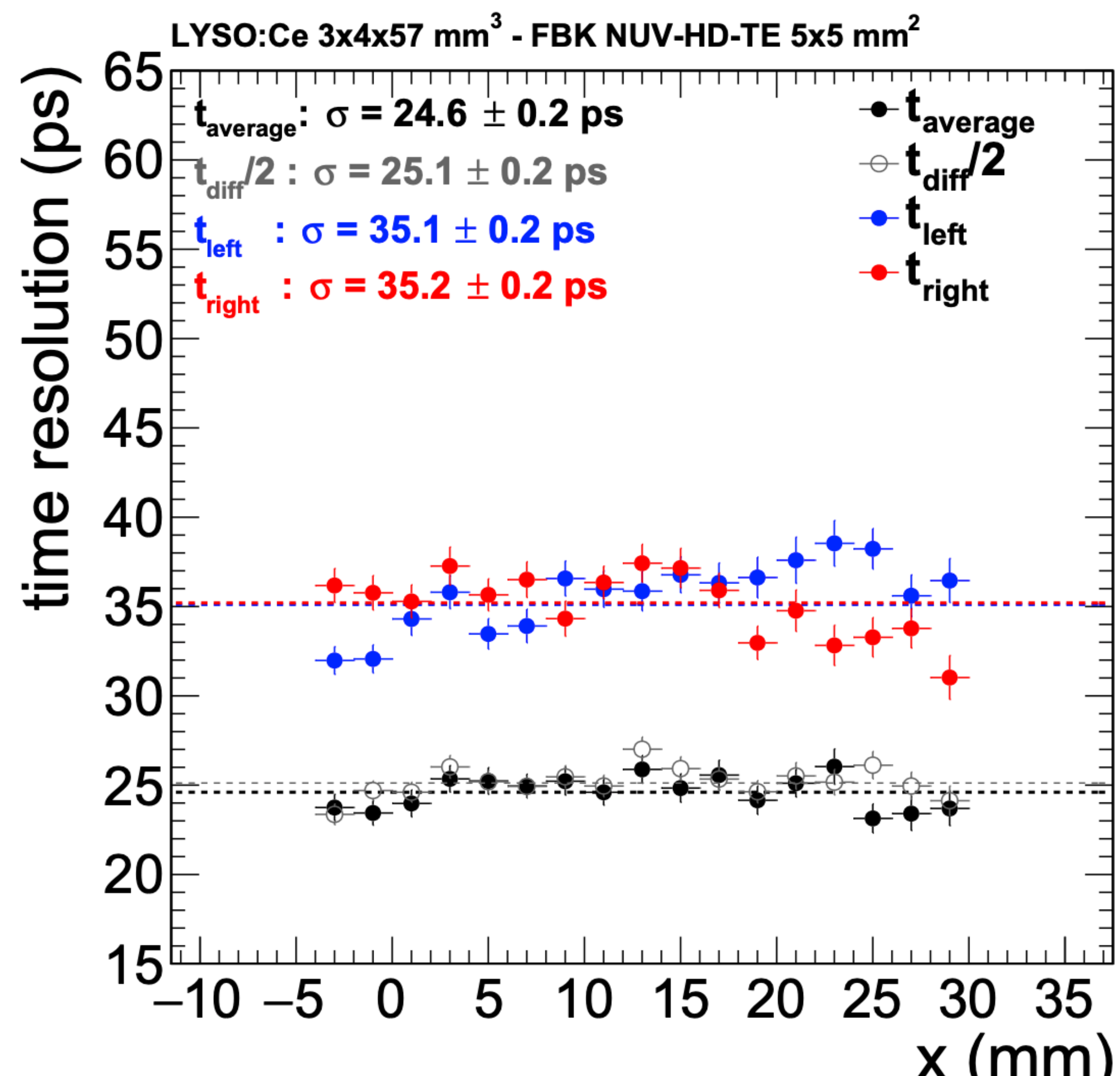

$3 \times 4 \times 57$ mm³ LYSO:Ce bar coupled to FBK SiPMs

Dose rate and neutron flux at HL-LHC

Dose rate and neutron flux expected at HL-LHC induce photo-current and readout noise in BTL sensor

Need to measure the impact experimentally

CMS MTD	η	n_{eq} (cm^{-2})	n_{eq} Flux ($cm^{-2}s^{-1}$)	Protons (cm^{-2})	p Flux ($cm^{-2}s^{-1}$)	Dose (Mrad)	Dose rate (rad/h)
Barrel	0.00	2.48E+14	2.75E+06	2.2E+13	2.4E+05	2.7	108
Barrel	1.15	2.70E+14	3.00E+06	2.4E+13	2.6E+05	3.8	150
Barrel	**1.45**	**2.85E+14**	**3.17E+06**	**2.5E+13**	**2.8E+05**	**4.8**	**192**
Endcap	1.60	2.3E+14	2.50E+06	2.0E+13	2.2E+05	2.9	114
Endcap	2.00	4.5E+14	5.00E+06	3.9E+13	4.4E+05	7.5	300
Endcap	2.50	1.1E+15	1.25E+07	9.9E+13	1.1E+06	25.5	1020
Endcap	**3.00**	**2.4E+15**	**2.67E+07**	**2.1E+14**	**2.3E+06**	**67.5**	**2700**

Experimental setup at Caltech

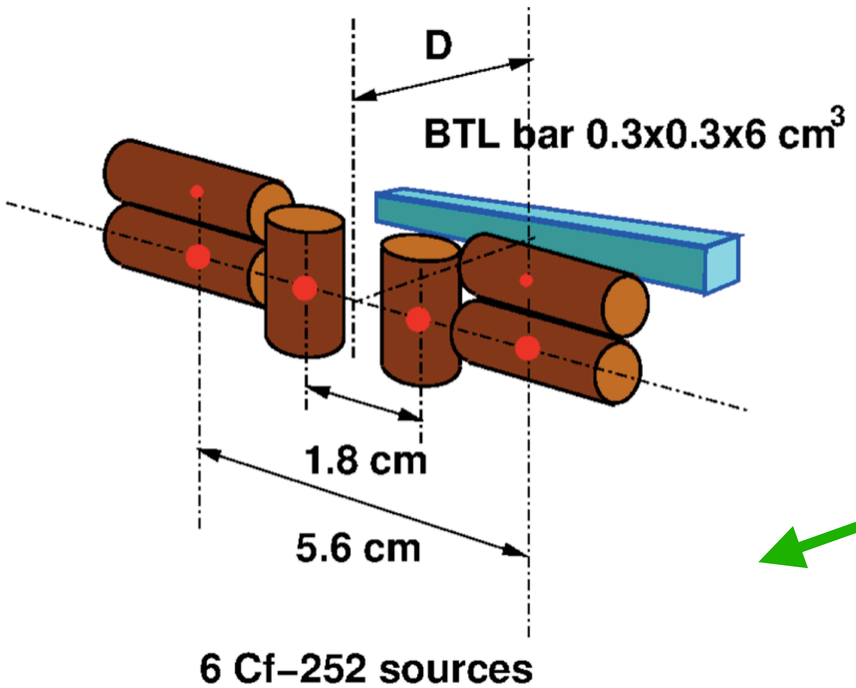

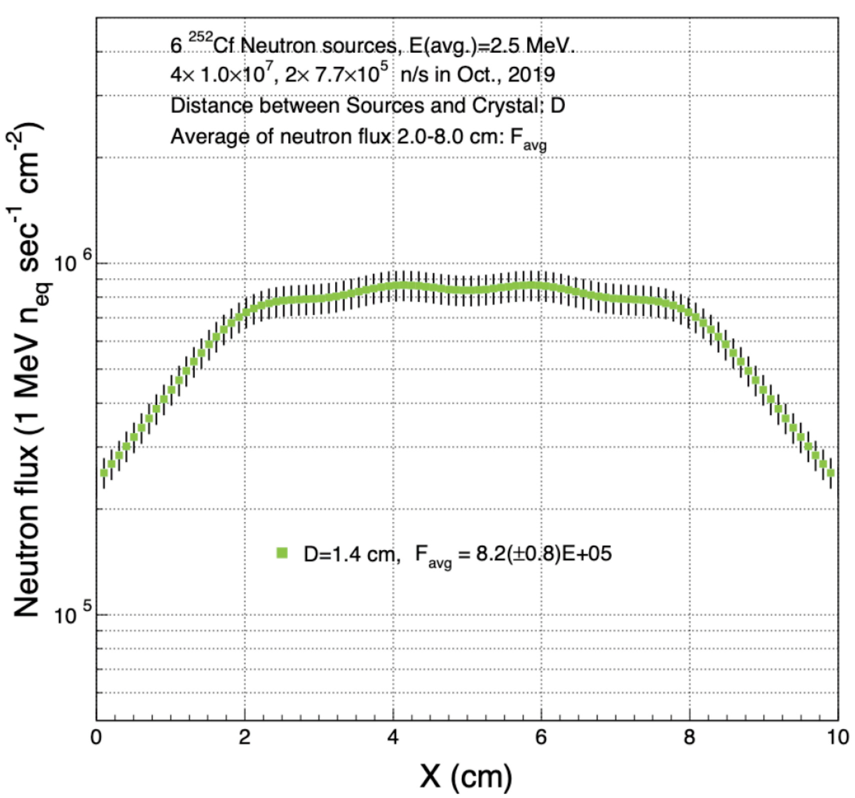

Collaborating with Caltech HEP Crystal Lab

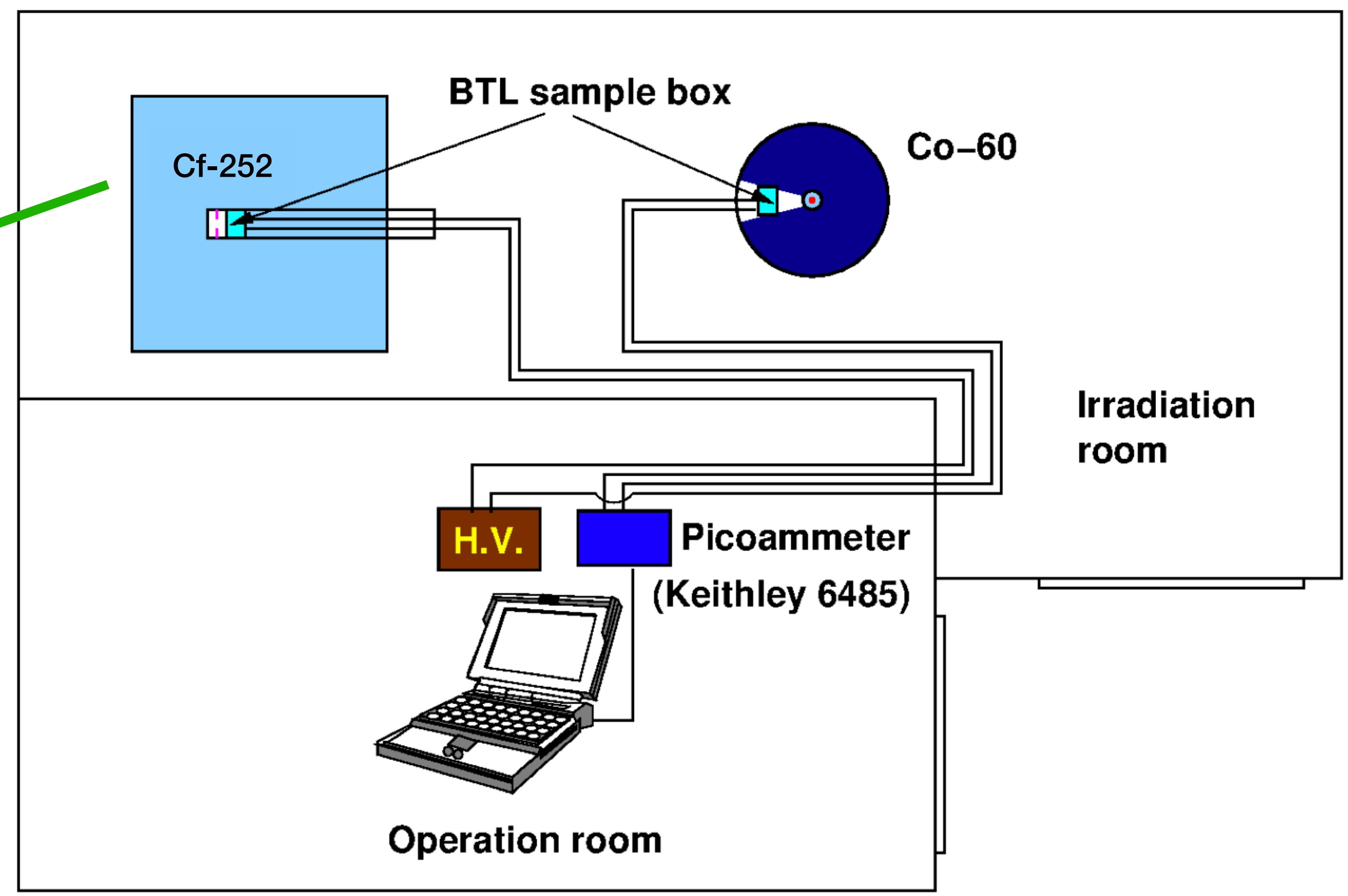

Dose rate and neutron flux induced readout noise

- **Negligible readout noise** induced by gamma-ray (192 rad/h) and neutron flux (3.17×10^6 [$1\ MeV\ n_{eq}\ cm^{-2}s^{-1}$]) at @BTL |η|=1.45 expected at HL-LHC

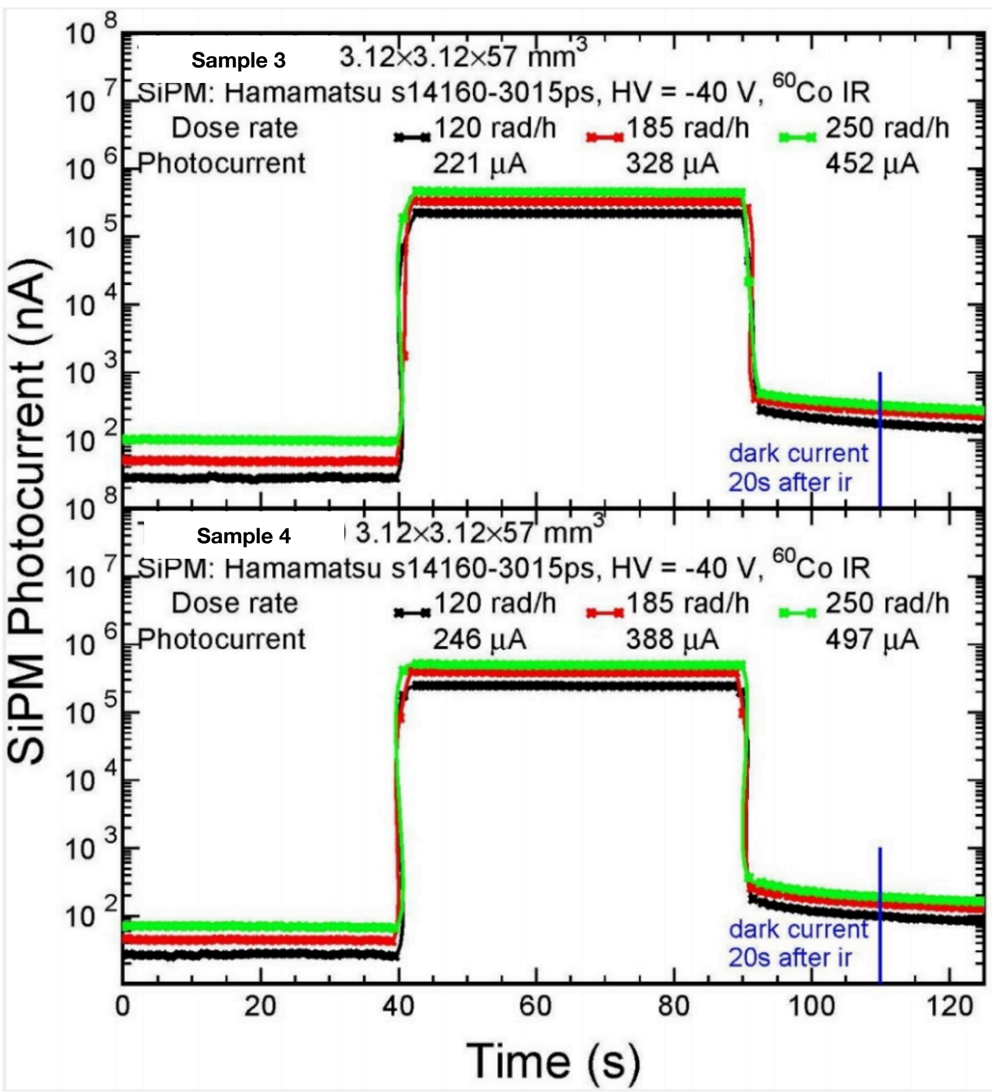

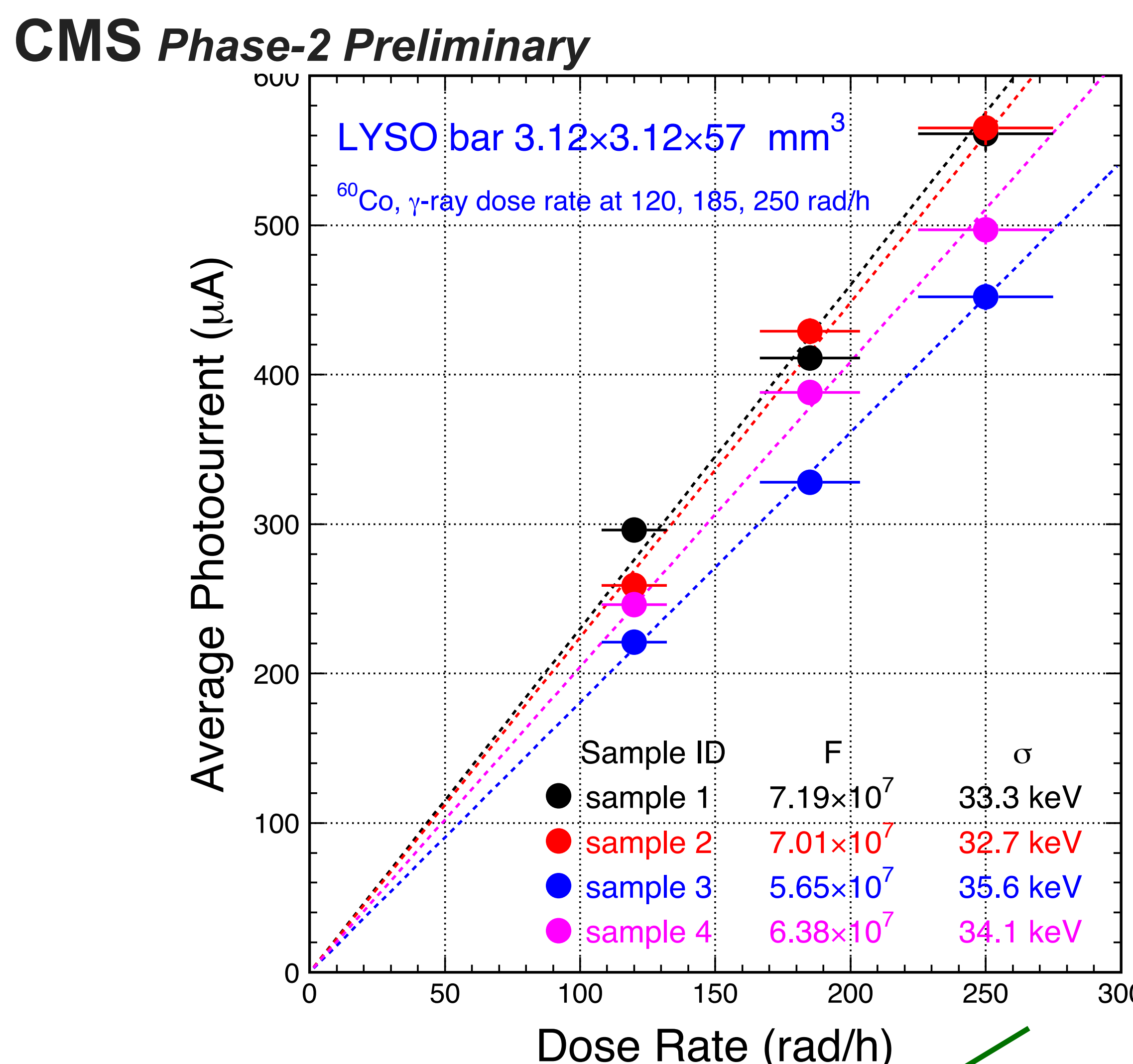

Negligible compared to MIP signal of 4.2 MeV

From BTL Single Bar to Module

Motivation of the BTL module design:

- Minimize distance between the SiPM's and ASICs for best possible signal integrity
- Encapsulate variability of the dimensions of the module components
- Simplify tray assembly

BTL module prototypes (2021)

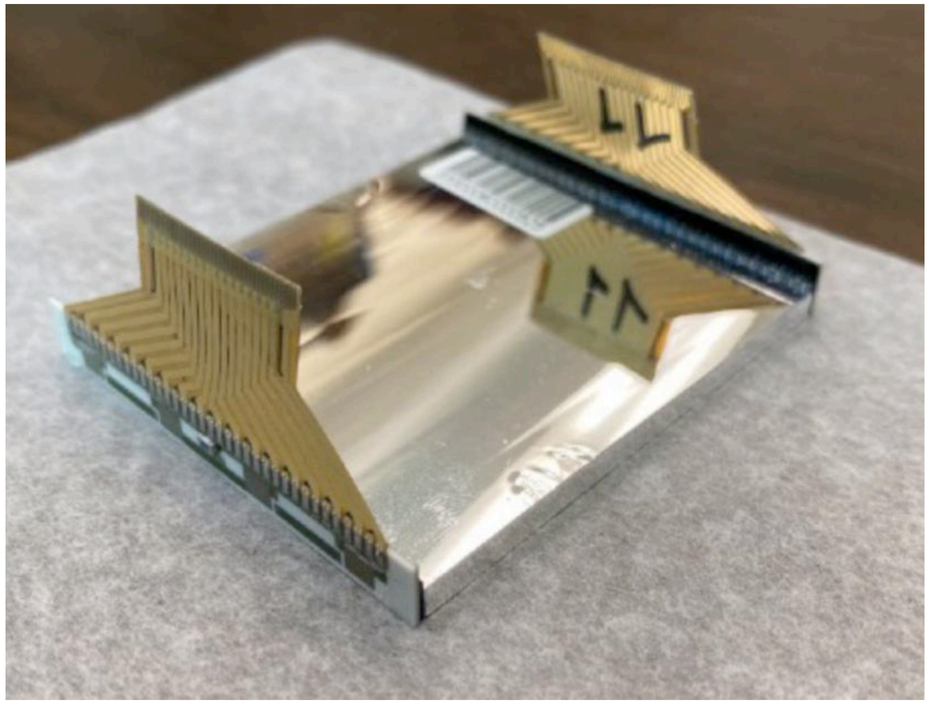

Early BTL module prototypes (2020)

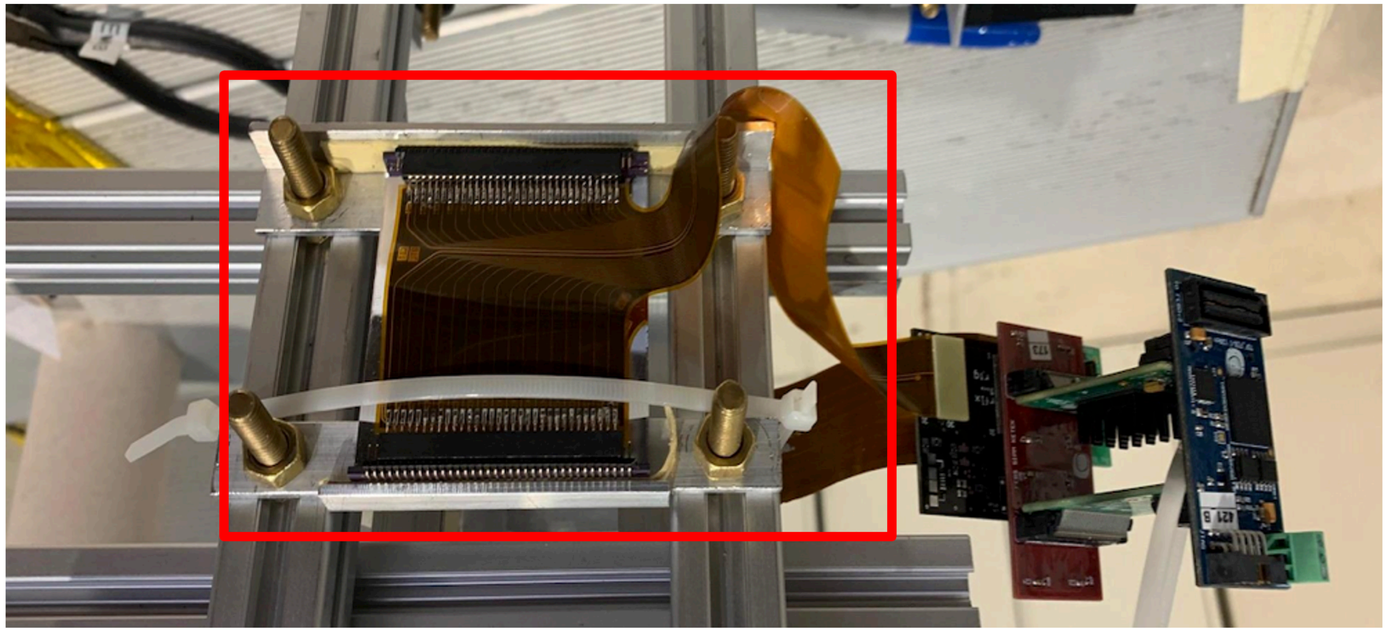

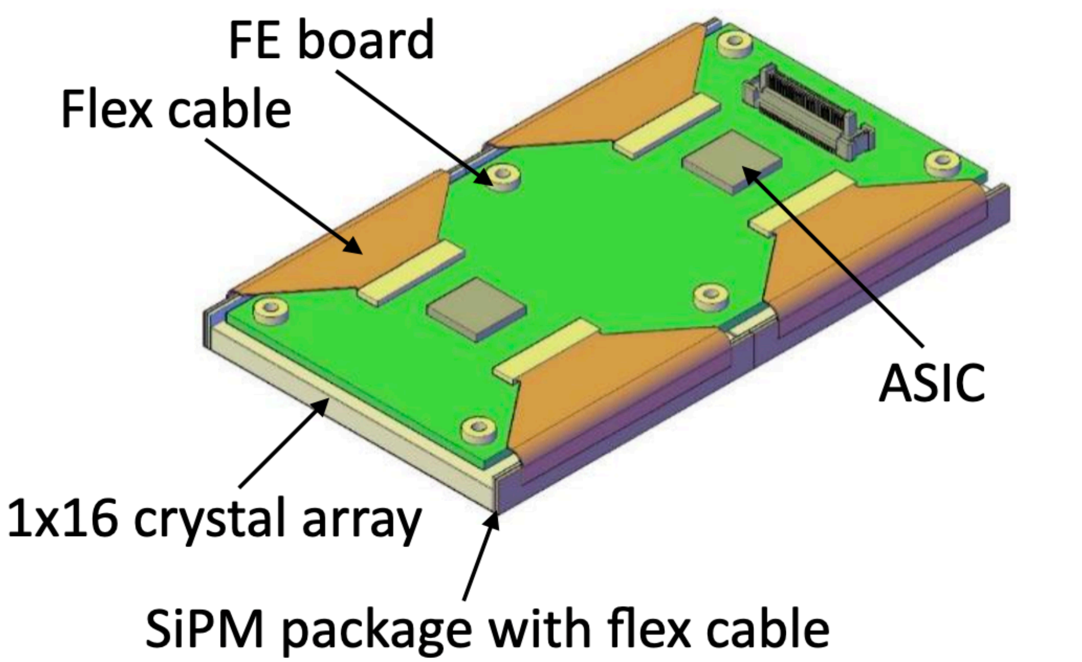

ETL Detector Layout

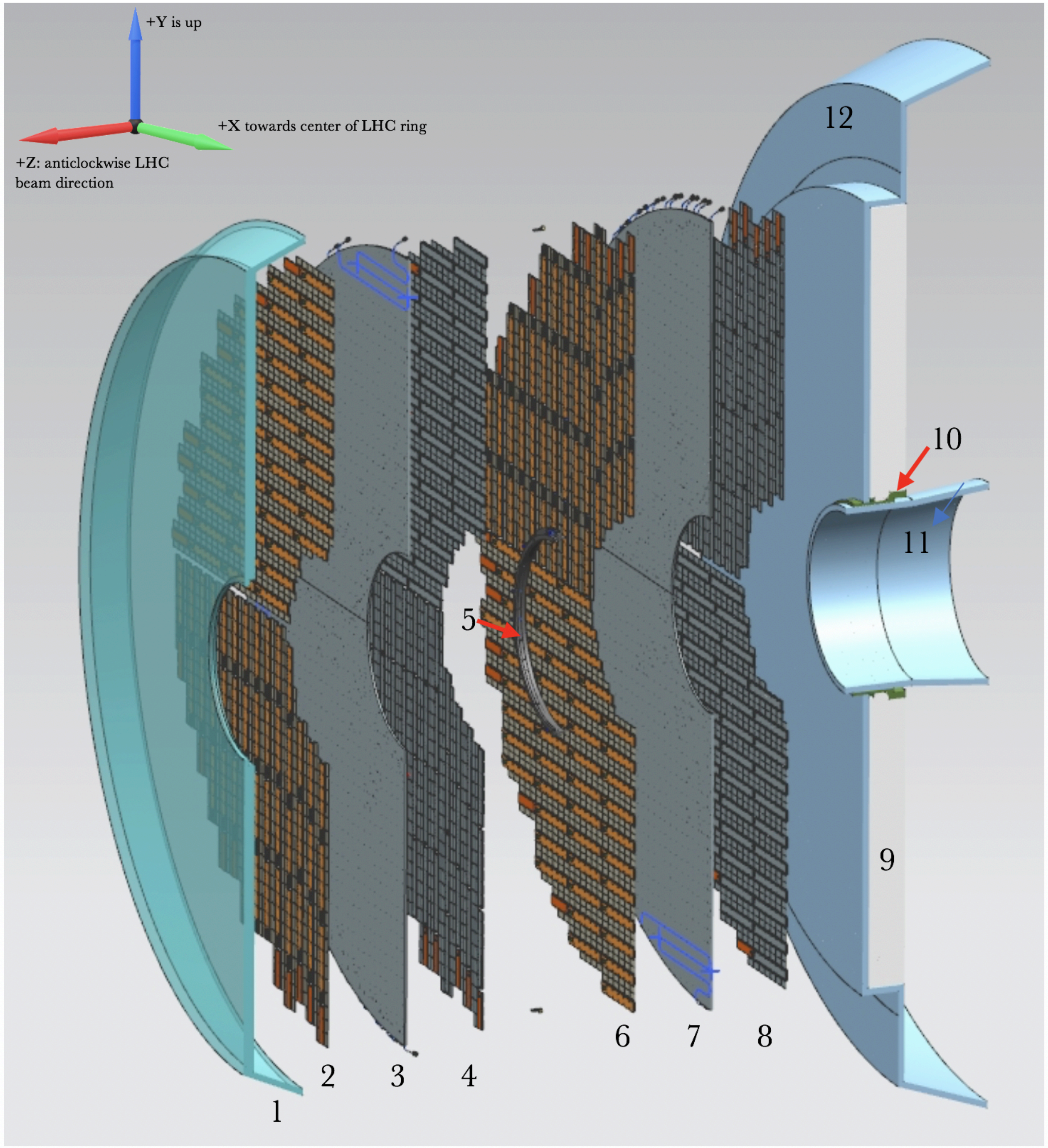

1: ETL Thermal Screen
2: Disk 1, Face 1
3: Disk 1 Support Plate
4: Disk 1, Face 2
5: ETL Mounting Bracket
6: Disk 2, Face 1
7: Disk 2 Support Plate
8: Disk 2, Face 2
9: HGCal Neutron Moderator
10: ETL Support Cone
11: Support cone insulation
12: HGCal Thermal Screen

Design target:
50 ps per hit, 35 ps per track

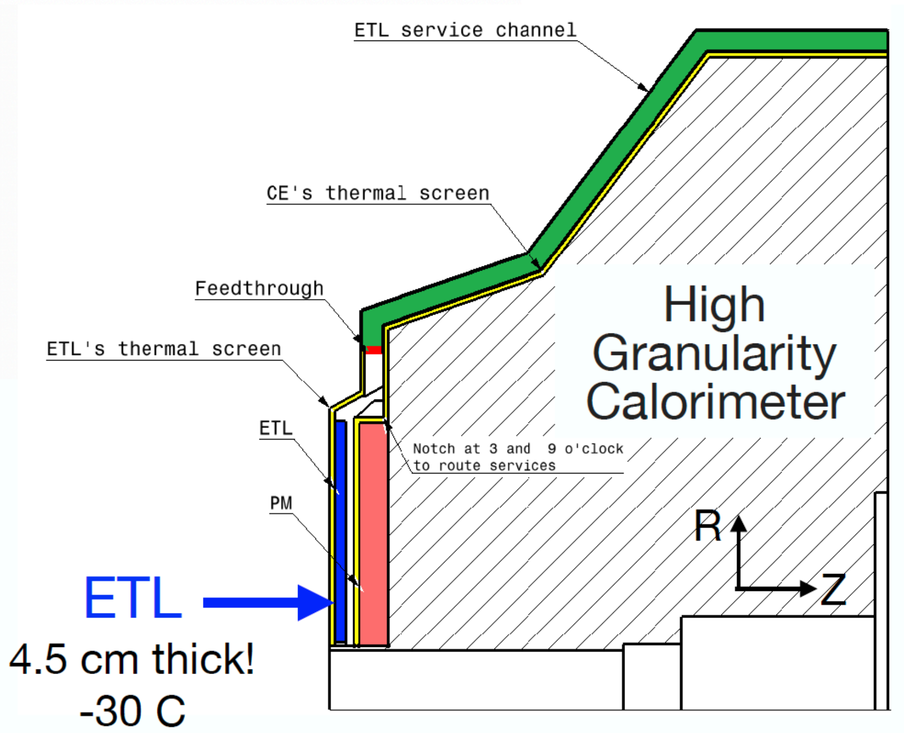

Low Gain Avalanche Detectors (LGADs)

- LGAD: ultra-fast silicon detectors with a highly doped p+ gain layer; moderate internal gain: 10-30
- Technology choice of ATLAS High-Granularity Timing Detector (HGTD) and CMS ETL

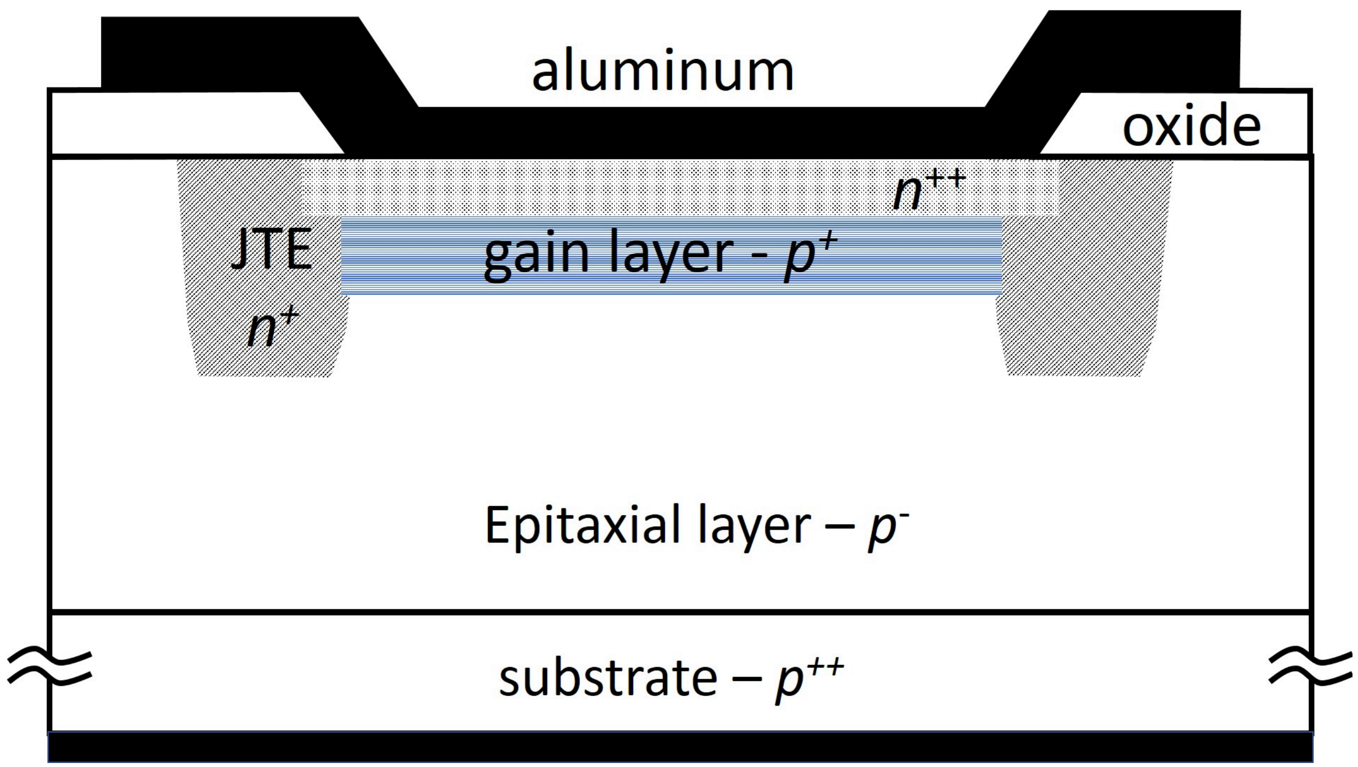

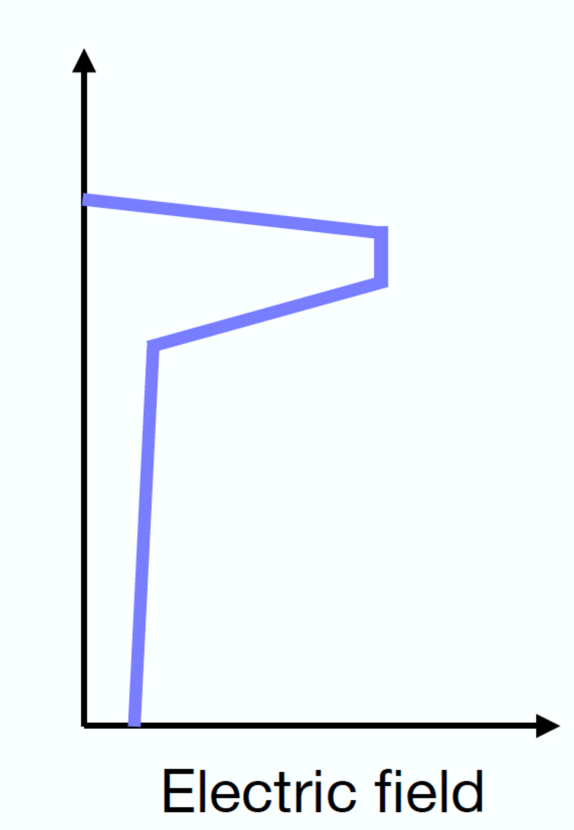

- ETL need 8.6 million channels, active area of 16 m^2
- Never been done in large areas before
- Need for next-generation fast ASIC electronics

ETL LGAD Design

Key sensor characteristics

Depletion region thickness	50 µm
Pad size	1.3x1.3 mm^2
Sensor size	16 x 16
Interpad gap	< 90 µm
Time res. after irradiation	< 40 ps

FBK UFSD3

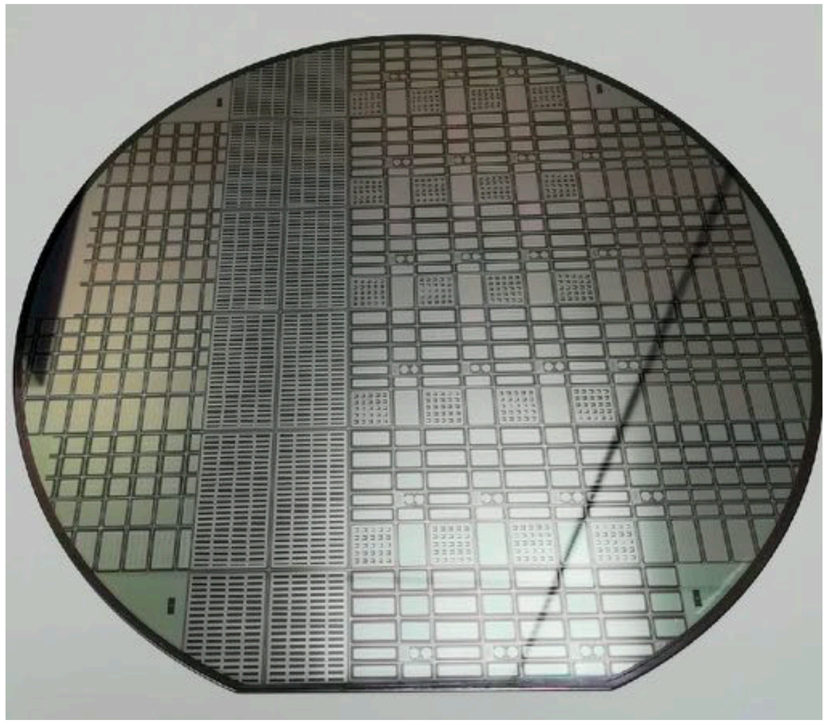

5x5 array from HPK

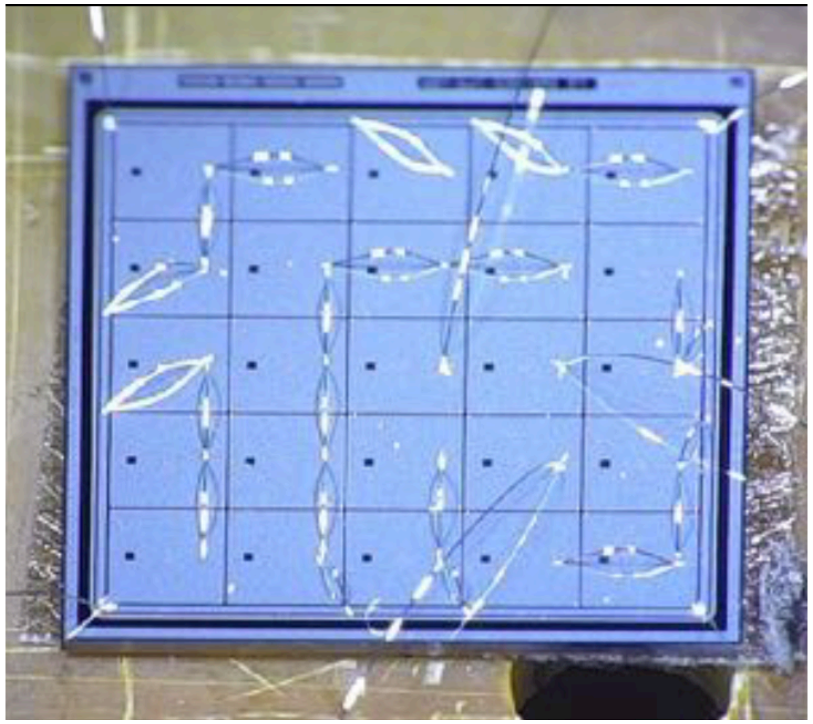

ETL test beam measurement

- First beam tests of prototype sensors and front-end ASIC
- For pre-rad sensors operating above 20 fC, time resolution of 40-50 ps with discriminator per sensor achieved
- Excellent first results - within design goal for final detector

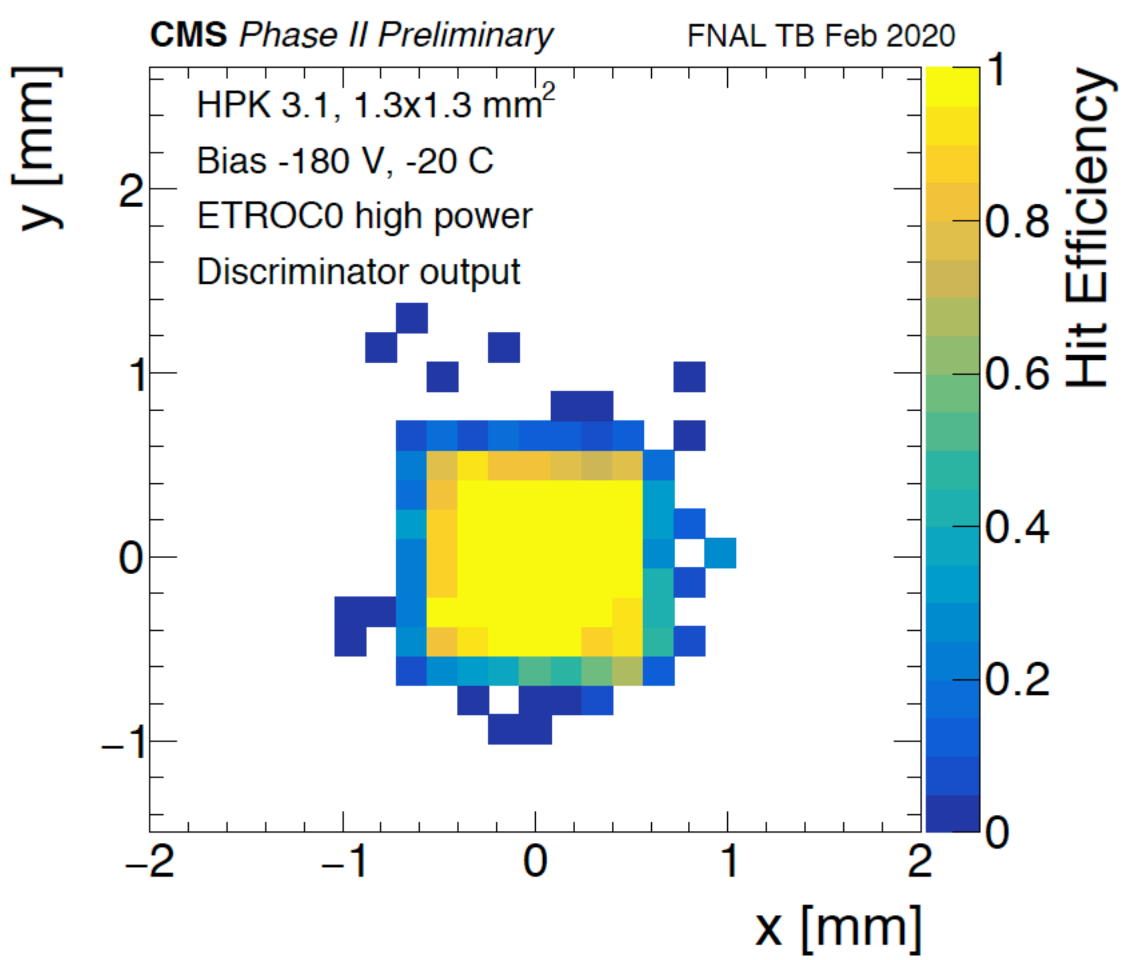

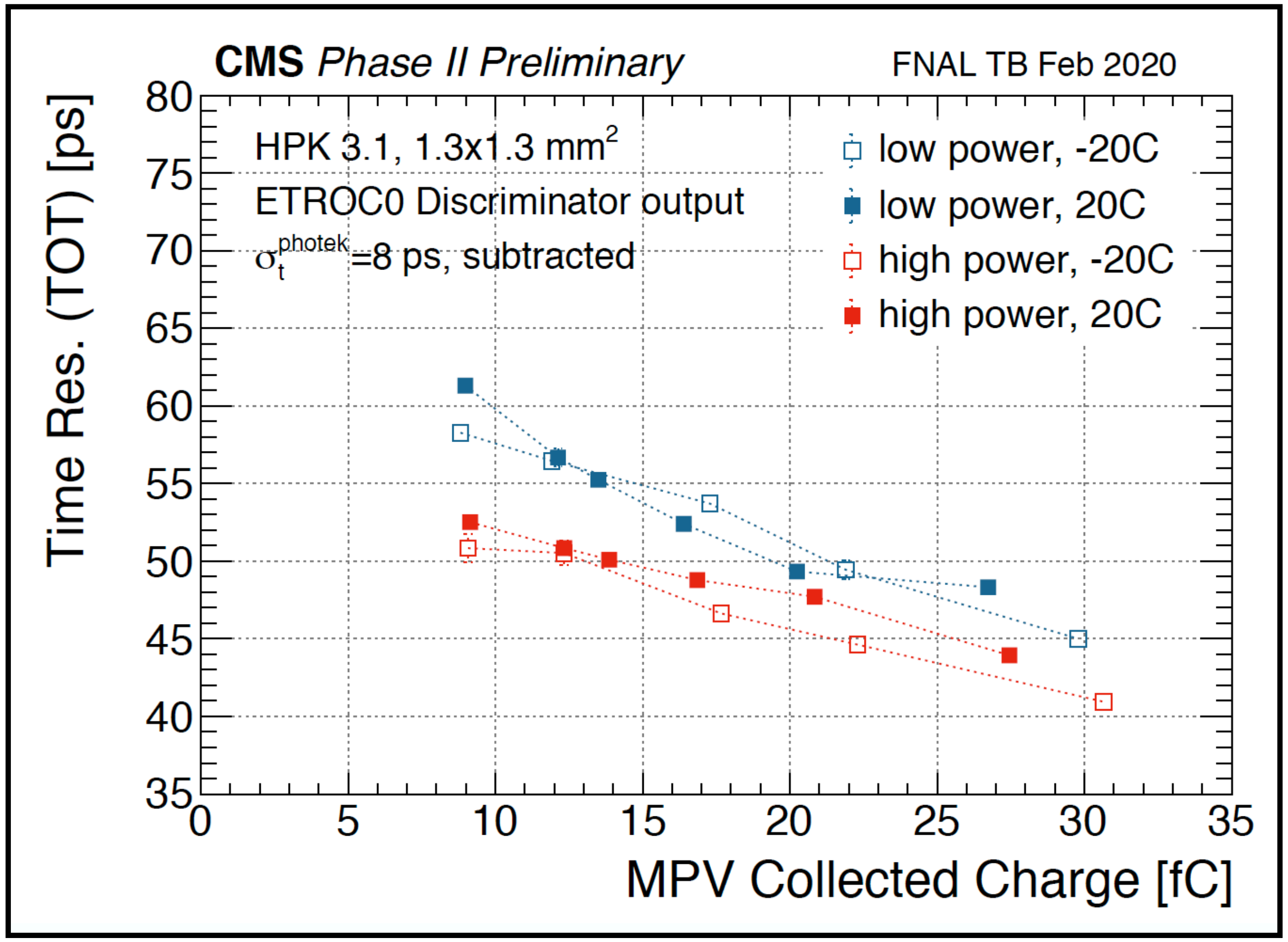

ETROC0 : single analog channel

Summary

- **CMS observed (expected) 3.0σ (2.5σ) experimental evidence for H→μμ decay using full Run 2 data:**
  - Higgs boson coupling measured with 19%, in agreement with Standard Model prediction $\kappa_\mu = 1.13^{+0.21}_{-0.22}$ at 68% CL
  - What's next: LHC data in Run 3 and HL-LHC will enable the observation and a precise measurement of κ_μ through H→μμ
- **CMS phase-2 upgrade will include a new MIP timing detector with a time resolution of 30-40 ps for MIPs**
  - Broad impact on HL-LHC physics potential
  - Sensor technology: LYSO:Ce crystals readout by SiPM for barrel, LGAD for endcap
  - Steady progress to prototyping and system test stage

Thank you!

backup slides

Where to look: Higgs boson mass

- The Higgs boson mass m_H is a free parameter in the SM. Once m_H is known, all Higgs boson couplings to Standard Model particles are fixed
- Most precise m_H measurement currently: **~0.11%** precision by CMS experiment

CMS **Phys. Lett. B 805 (2020) 135425**

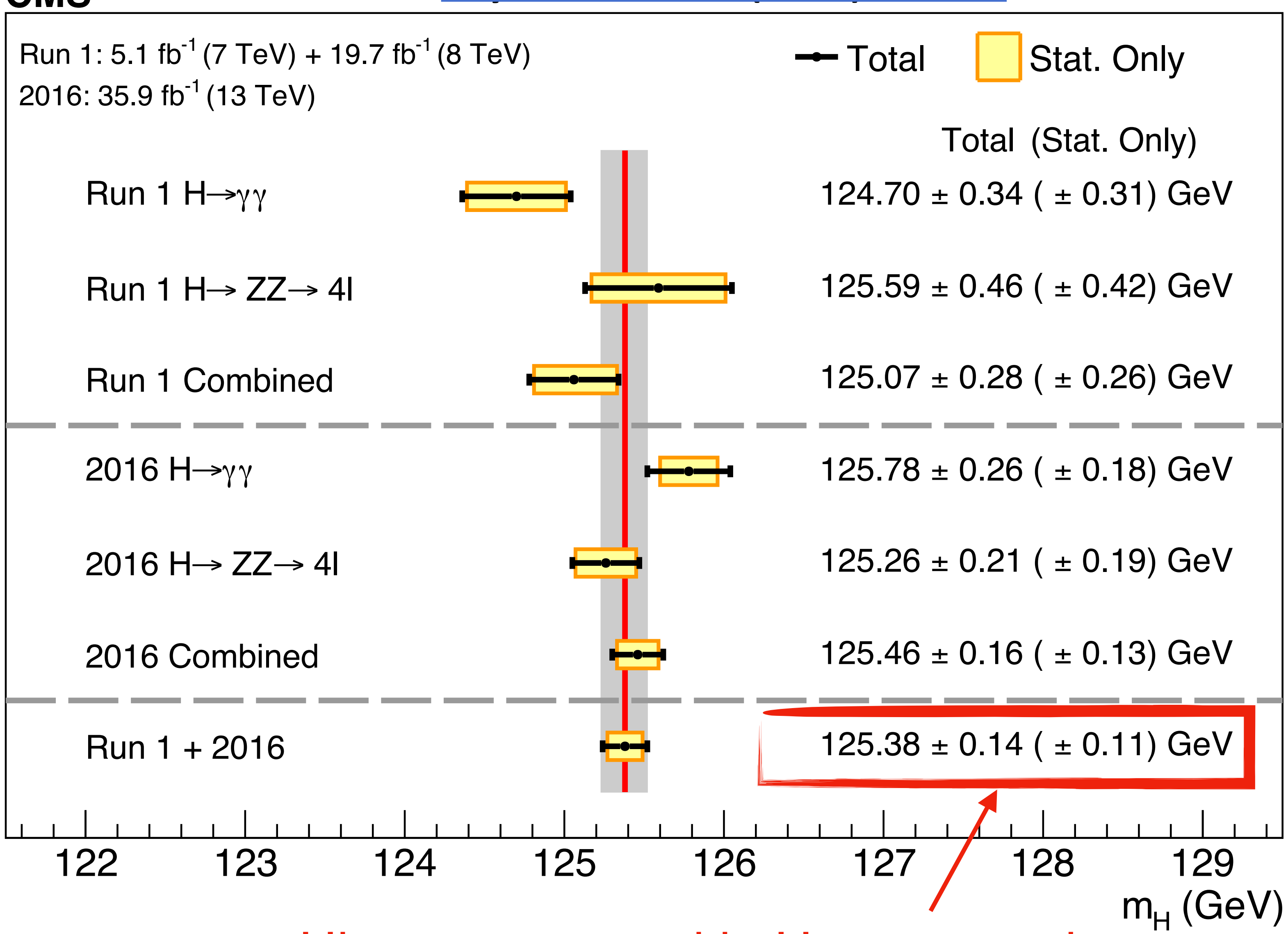

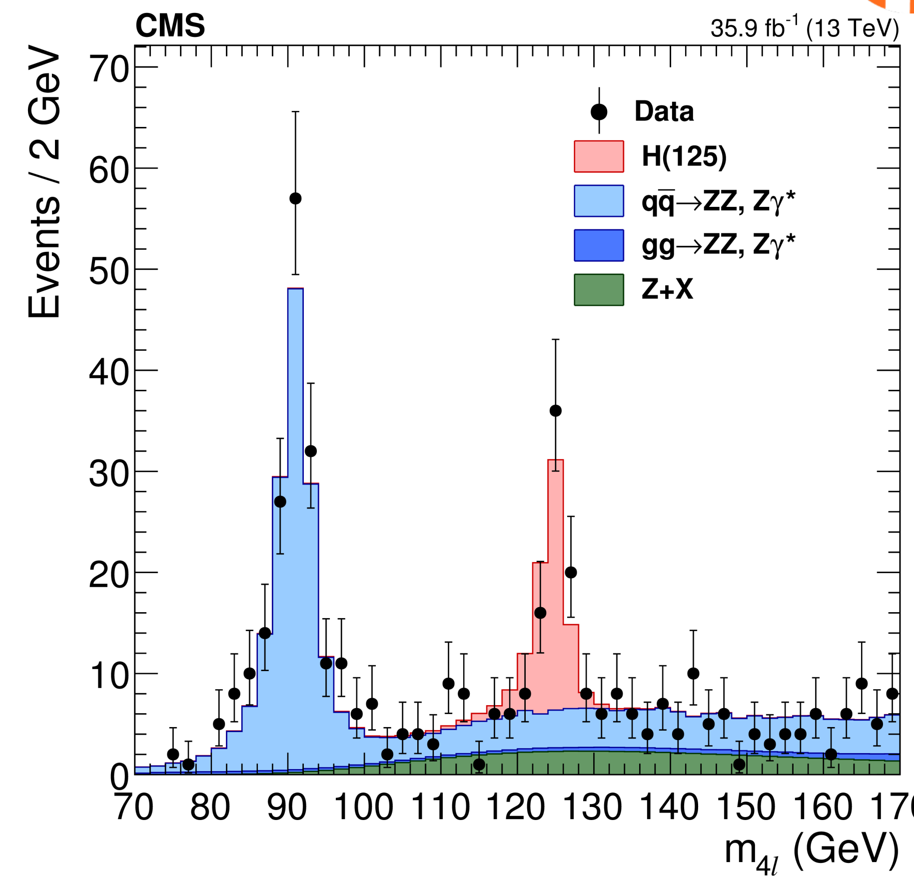

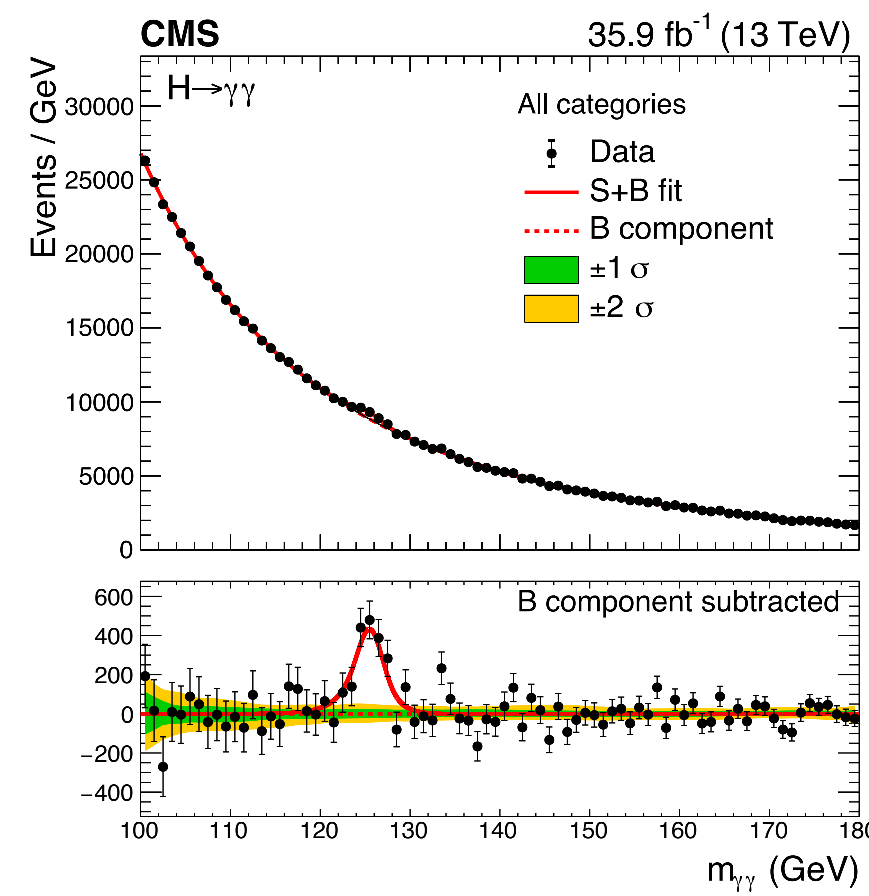

Higgs mass used in H→μμ search

Recap: CMS H→μμ search with 2016 data

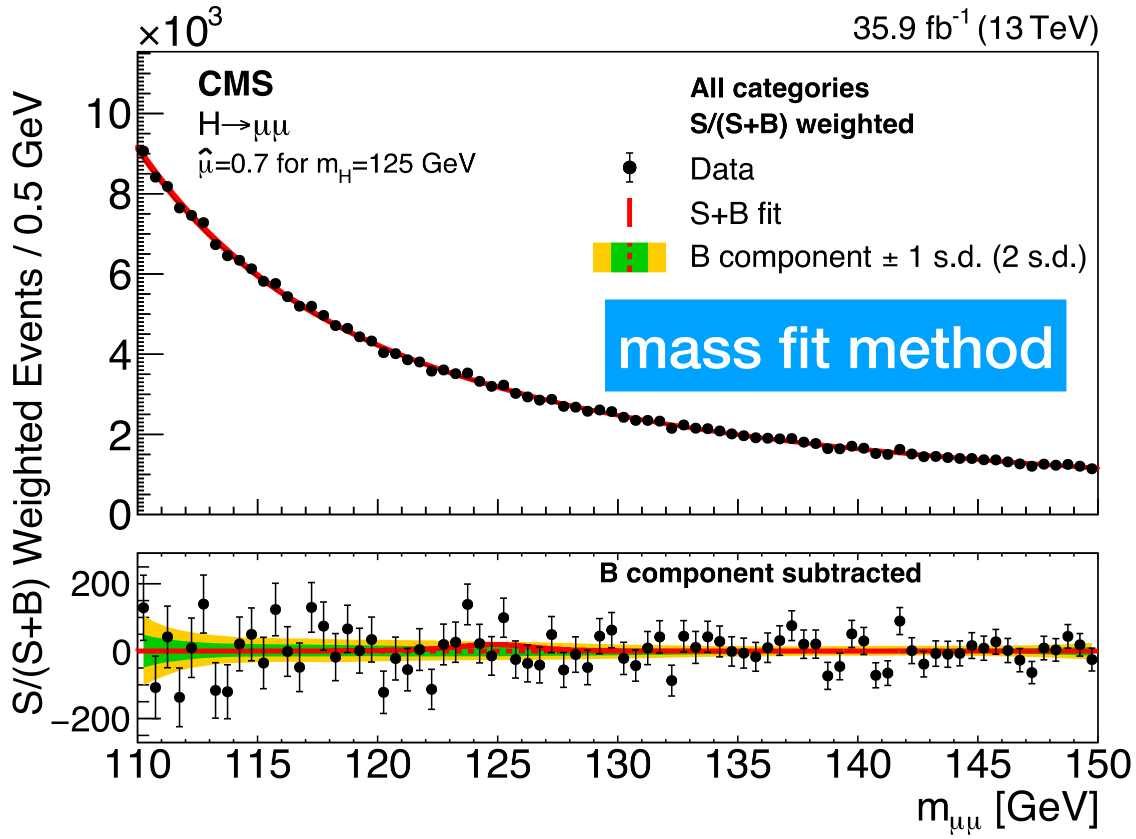

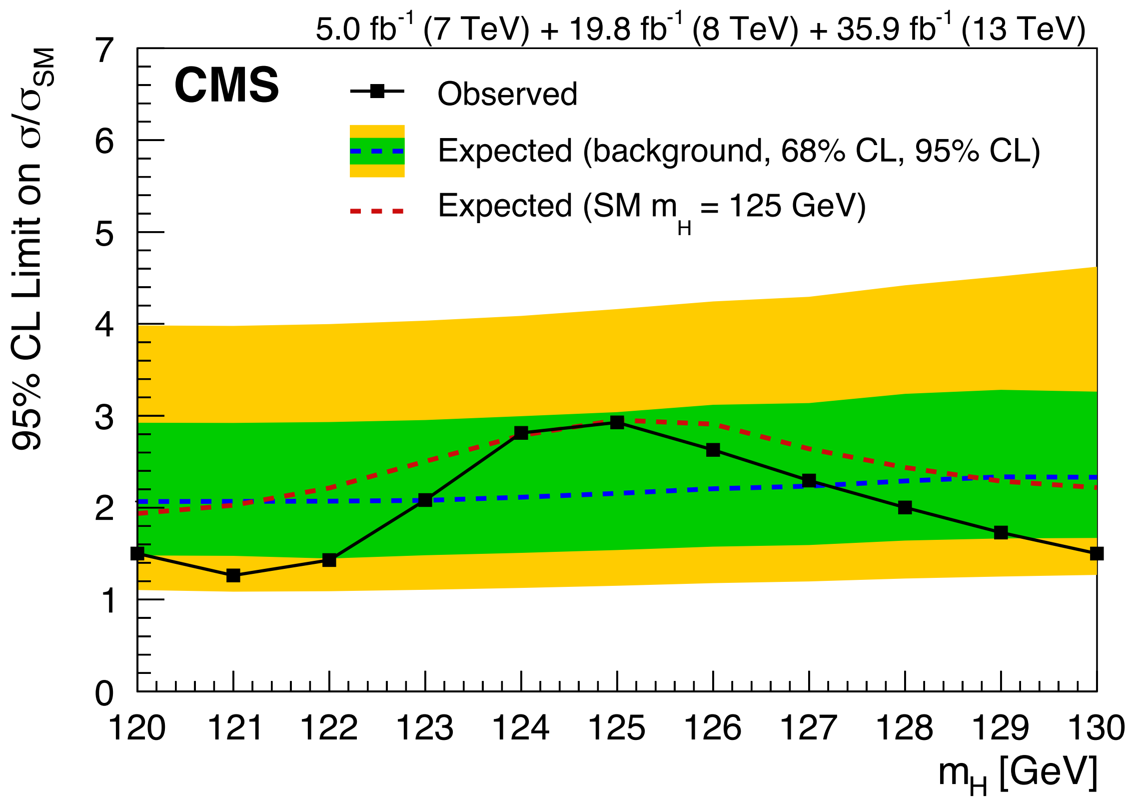

Observed (expected) significance 0.9σ (1.0σ)

Boosted Decision Tree (BDT) trained targeting ggH and VBF signals

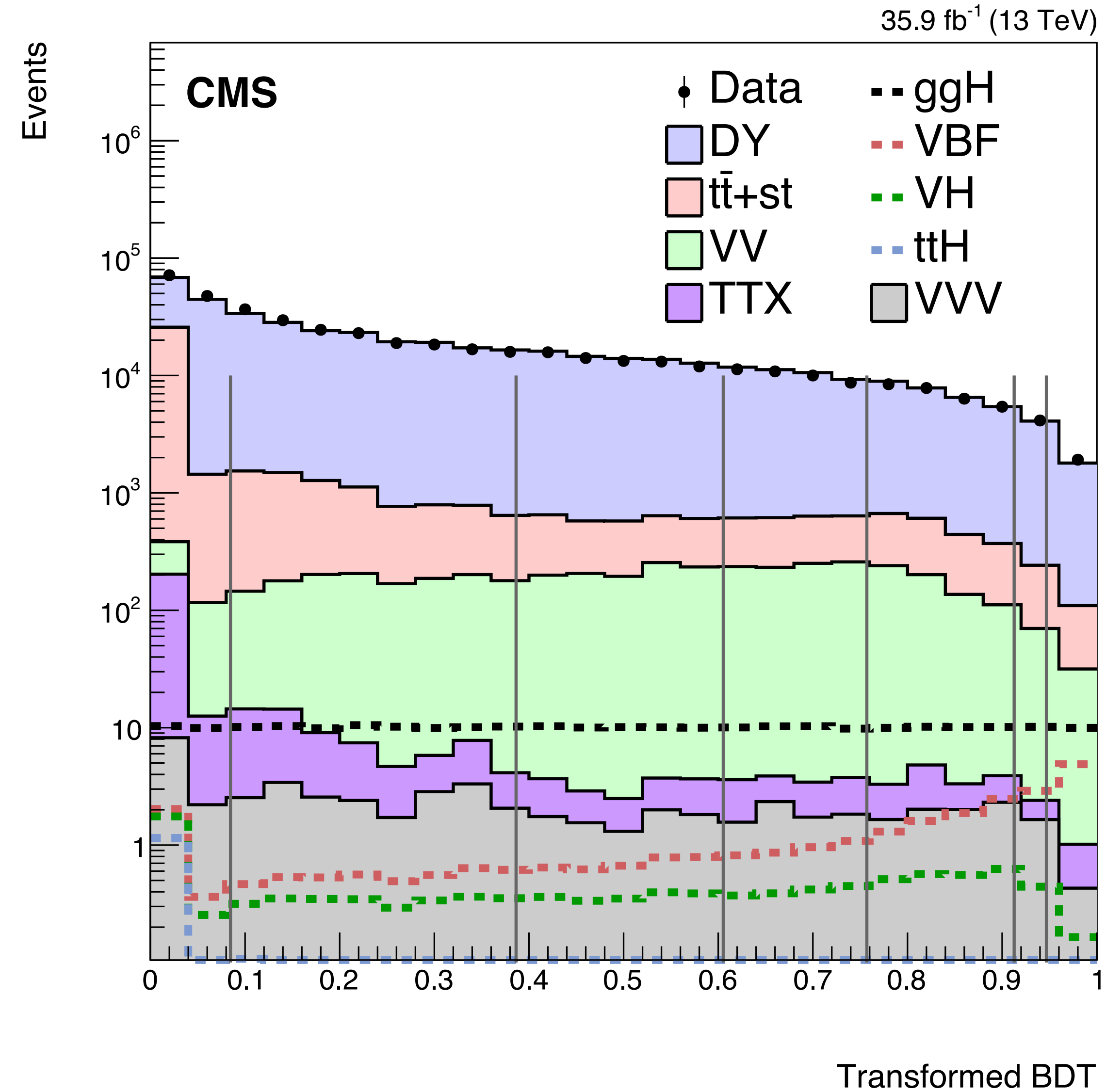

Categorization based on BDT output score and the maximum |η| of the two muons

Rev. Lett. 122 (2019) 021801

Physics Objection Selection

muons:

- $|\eta|<2.4$
- leading muon pT>26 (2016, 2018)/29 (2017)
- sub-leading muon pT>20 GeV
- loose isolation criteria
- medium muon ID
- global muon
- correction to the muon pT: final state photon recovery and geo-fit correction

Top tagging

- Only used in the ttH category
- MVA-based resolved hadronic top tag with 3 jets [PRL **122**, 011803 (2019)]

Jets:

- pT> 25 GeV, $|\eta| < 4.7$
- reject jets originate from pileup
  - MVA pile-up jet identification
- Calibration on jet energy

B-jet tagging

- pT> 25 GeV and $|\eta|< 2.5$ within tracker coverage
- DeepCSV b-tagging algorithm
  - Loose (85% efficiency, 10% mis-ID)
  - medium (70% efficiency, 1% mis-ID)

Event Simulation

Monte Carlo (MC) simulation samples:

signal

Process	Generator (Perturbative order)	Parton shower	Cross section	Additional corrections
ggH	MADGRAPH5_aMC@NLO (NLO QCD)	PYTHIA	N3LO QCD, NLO EW	$p_T(H)$ from NNLOPS
VBF	POWHEG (NLO QCD)	PYTHIA dipole shower	NNLO QCD, NLO EW	—
$qq \to VH$	POWHEG (NLO QCD)	PYTHIA	NNLO QCD, NLO EW	—
$gg \to ZH$	POWHEG (LO)	PYTHIA	NNLO QCD, NLO EW	—
$t\bar{t}H$	POWHEG (NLO QCD)	PYTHIA	NLO QCD, NLO EW	—
$b\bar{b}H$	POWHEG (NLO QCD)	PYTHIA	NLO QCD	—
tHq	MADGRAPH5_aMC@NLO (LO)	PYTHIA	NLO QCD	—
tHW	MADGRAPH5_aMC@NLO (LO)	PYTHIA	NLO QCD	—

bkg

Process	Generator (Perturbative order)	Parton shower	Cross section	Additional corrections
Drell–Yan	MADGRAPH5_aMC@NLO (NLO QCD)	PYTHIA	NNLO QCD, NLO EW	—
Zjj-EW	MADGRAPH5_aMC@NLO (LO)	HERWIG++/HERWIG 7	LO	—
$t\bar{t}$	POWHEG (NLO QCD)	PYTHIA	NNLO QCD	—
Single top quark	POWHEG/MADGRAPH5_aMC@NLO (NLO QCD)	PYTHIA	NLO QCD	—
Diboson (VV)	POWHEG/MADGRAPH5_aMC@NLO (NLO QCD)	PYTHIA	NLO QCD	NNLO/NLO K factors
$gg \to ZZ$	MCFM (LO)	PYTHIA	LO	NNLO/LO K factors
$t\bar{t}V$, $t\bar{t}VV$	MADGRAPH5_aMC@NLO (NLO QCD)	PYTHIA	NLO QCD	—
Triboson (VVV)	MADGRAPH5_aMC@NLO (NLO QCD)	PYTHIA	NLO QCD	—

ggH:

- Higgs pT distribution reweighted to match POWHEG NNLOPS predictions

Drell-Yan:

- Madgraph5_amc@NLO generator with up to two partons in the final state at the ME level
- Dedicated sample targeting the VBF phase-space created to reduce MC stats uncertainty

ttH Channel: Overview

- ttH leptonic: extra leptons (e or μ)
  - additional MVA identification for leptons *PRL 122, 132003 (2019)* to reduce background with non-prompt leptons from $t\bar{t}$ and DY
- ttH hadronic: N_{jets} >= 3, no extra lepton
  - hadronic top tagging *PRL 122, 011803 (2019)* used to increase signal purity

ttH signal

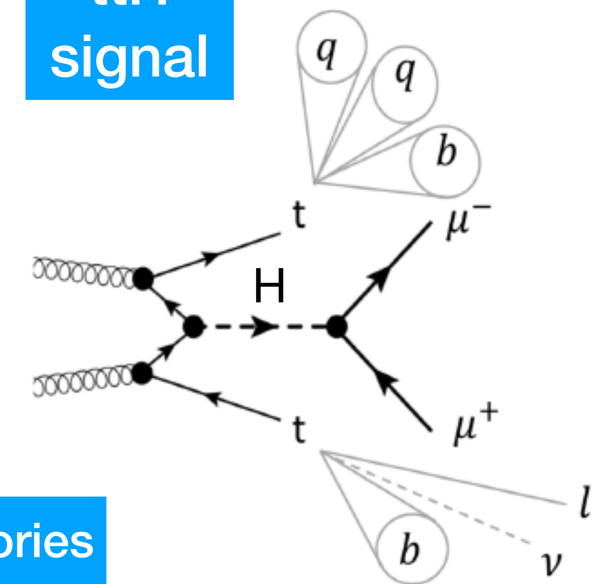

three ttH hadronic categories
main background: $t\bar{t}$

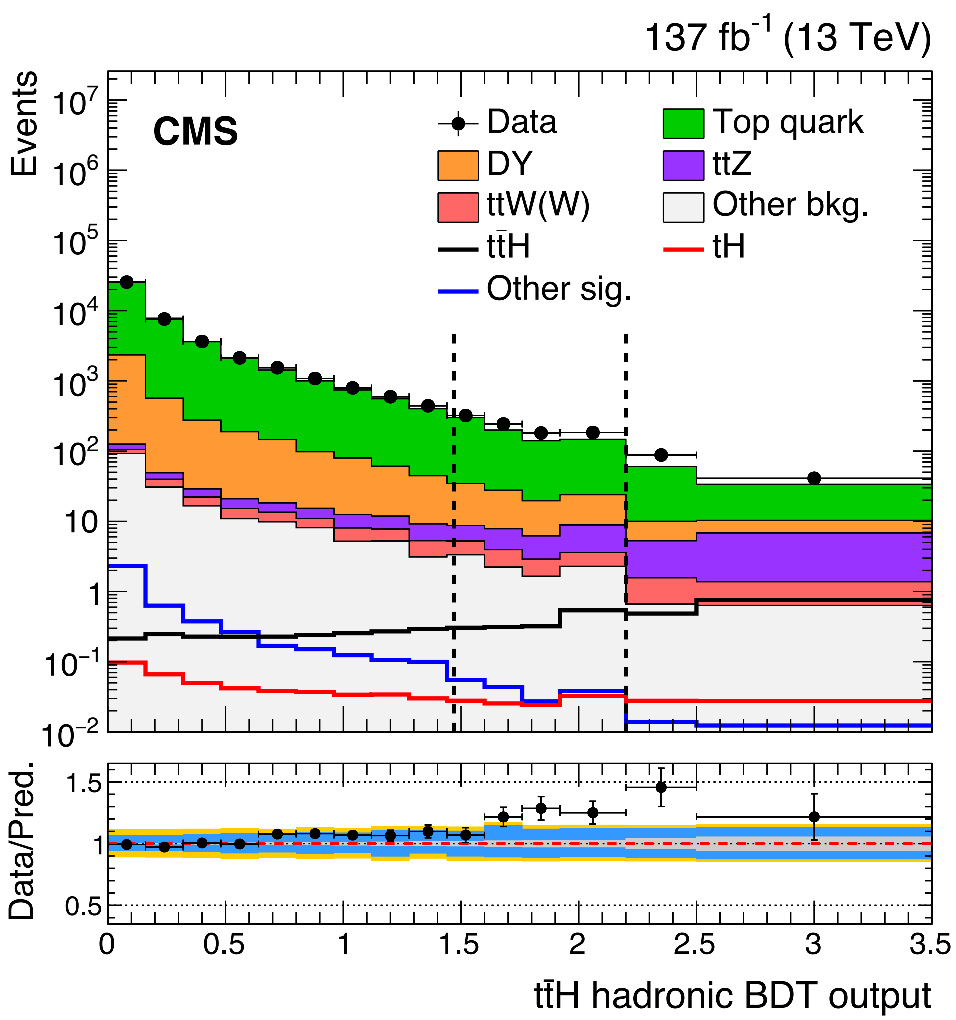

two ttH leptonic categories
main bkg: ttZ

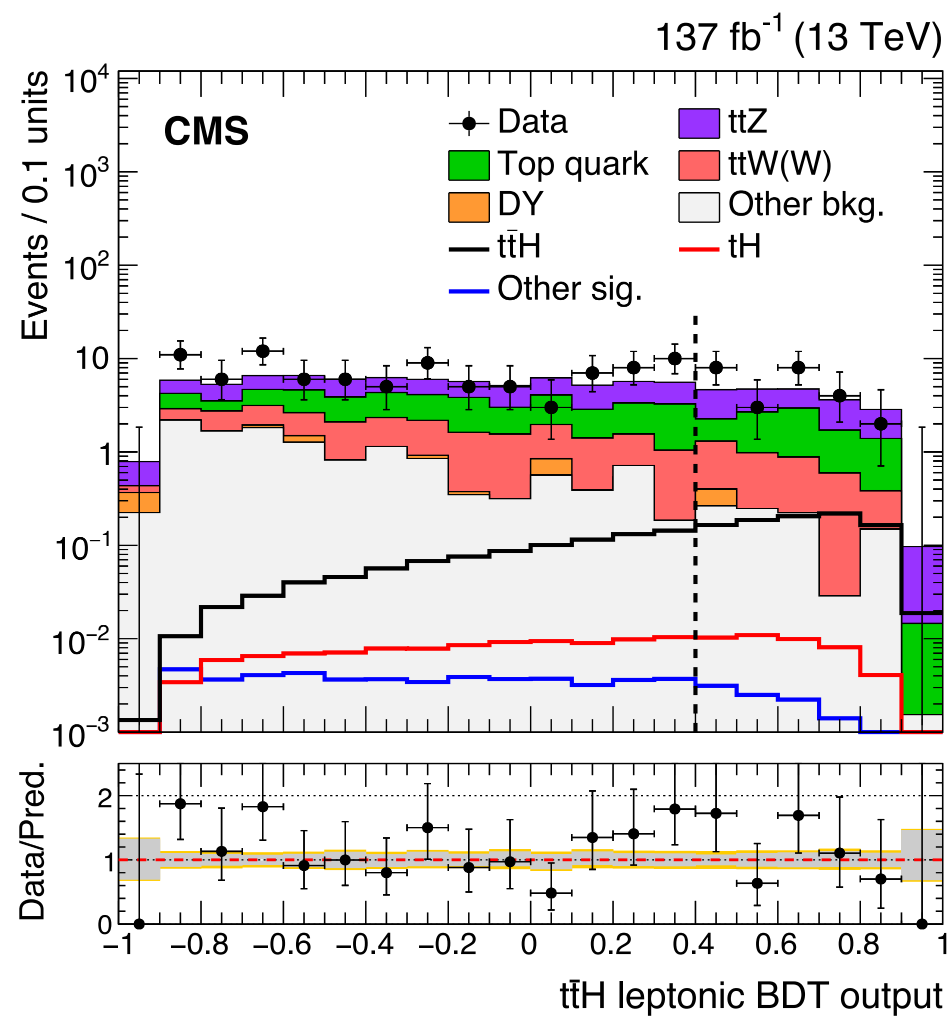

ttH Channel: Results

Fit strategy and signal modeling similar to ggH categories

- background functional form using agnostic functions:
  - second-order Bernstein polynomial for ttH-hadronic
  - exponential functions for ttH-leptonic

- observed (expected) significance: 1.20σ (0.54σ), m_H = 125.38 GeV

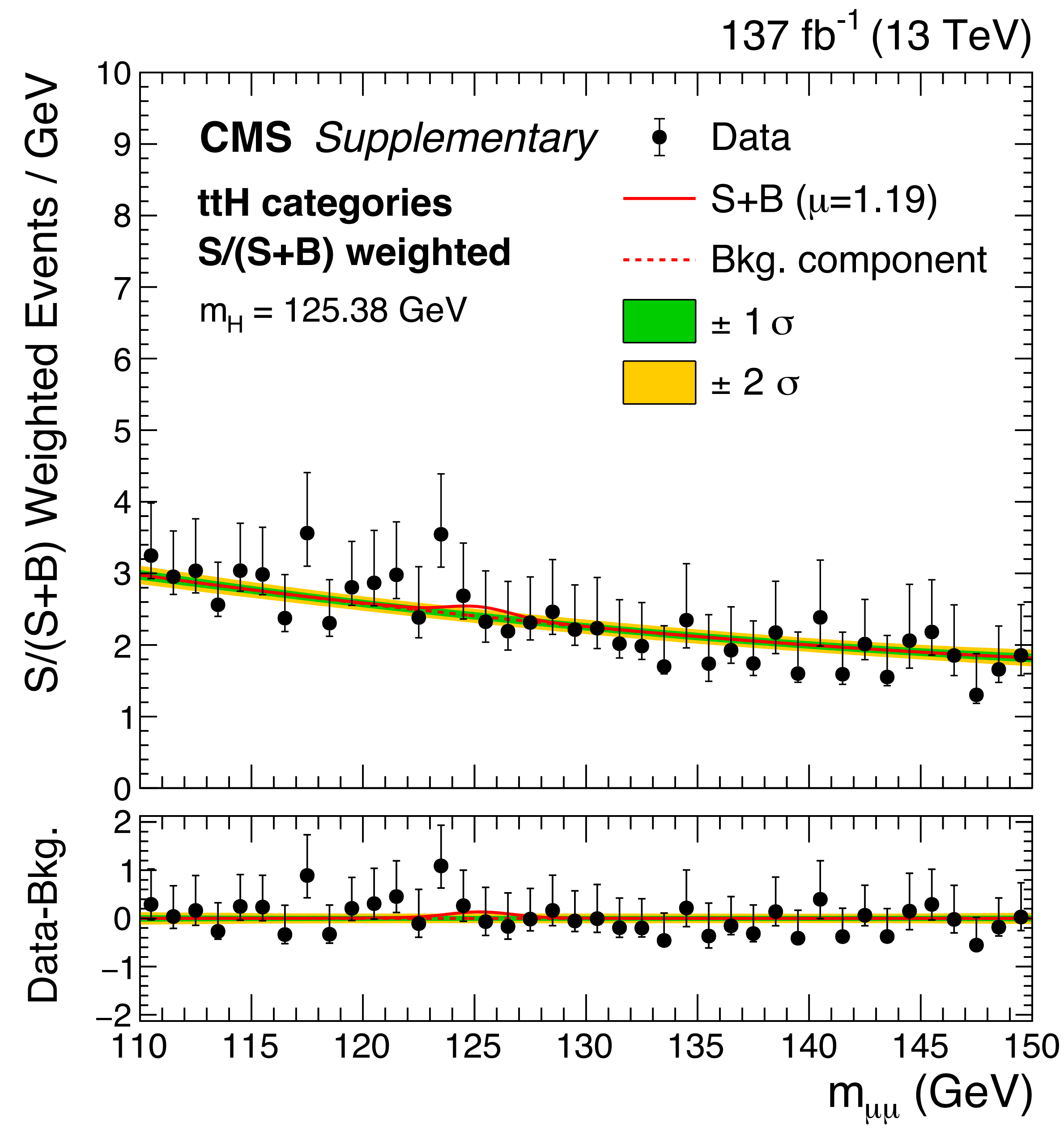

Event category	Total signal	$t\bar{t}$H (%)	ggH (%)	VH (%)	Other (%)	HWHM (GeV)	Bkg. fit function	Bkg. @HWHM	Data @HWHM	S/(S+B) (%) @HWHM	$S/\sqrt{B}$ @HWHM
$t\bar{t}$Hhad-cat1	6.87	32.3	40.3	17.2	10.2	1.85	Bern(2)	4298	4251	1.07	0.07
$t\bar{t}$Hhad-cat2	1.62	84.3	3.8	5.6	6.2	1.81	Bern(2)	82.0	89	1.32	0.12
$t\bar{t}$Hhad-cat3	1.33	94.0	0.3	1.3	4.4	1.80	S-Exp	12.3	12	6.87	0.26
$t\bar{t}$Hlep-cat1	1.06	85.8	—	4.7	9.5	1.92	Exp	9.00	13	7.09	0.22
$t\bar{t}$Hlep-cat2	0.99	94.7	—	1.0	4.3	1.75	Exp	2.08	4	24.5	0.47

VH Channel: Overview

- One extra lepton in WH category, additional same-flavor opposite-charge lepton pair for ZH category
- Additional MVA identification for leptons (as in ttH categories) to increase signal purity and reject non-prompt leptons coming from $t\bar{t}$ and DY
- Optimized lepton pairing forming the Higgs boson candidate

3 WH categories

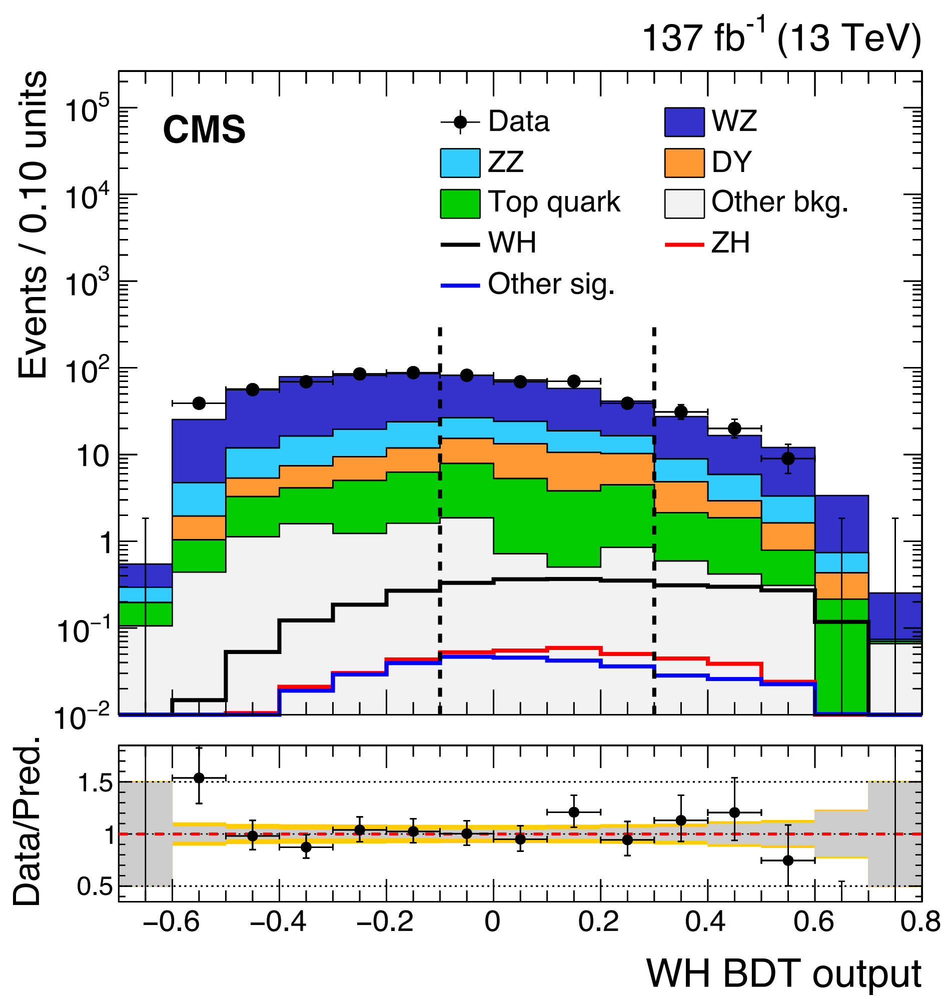

2 ZH categories

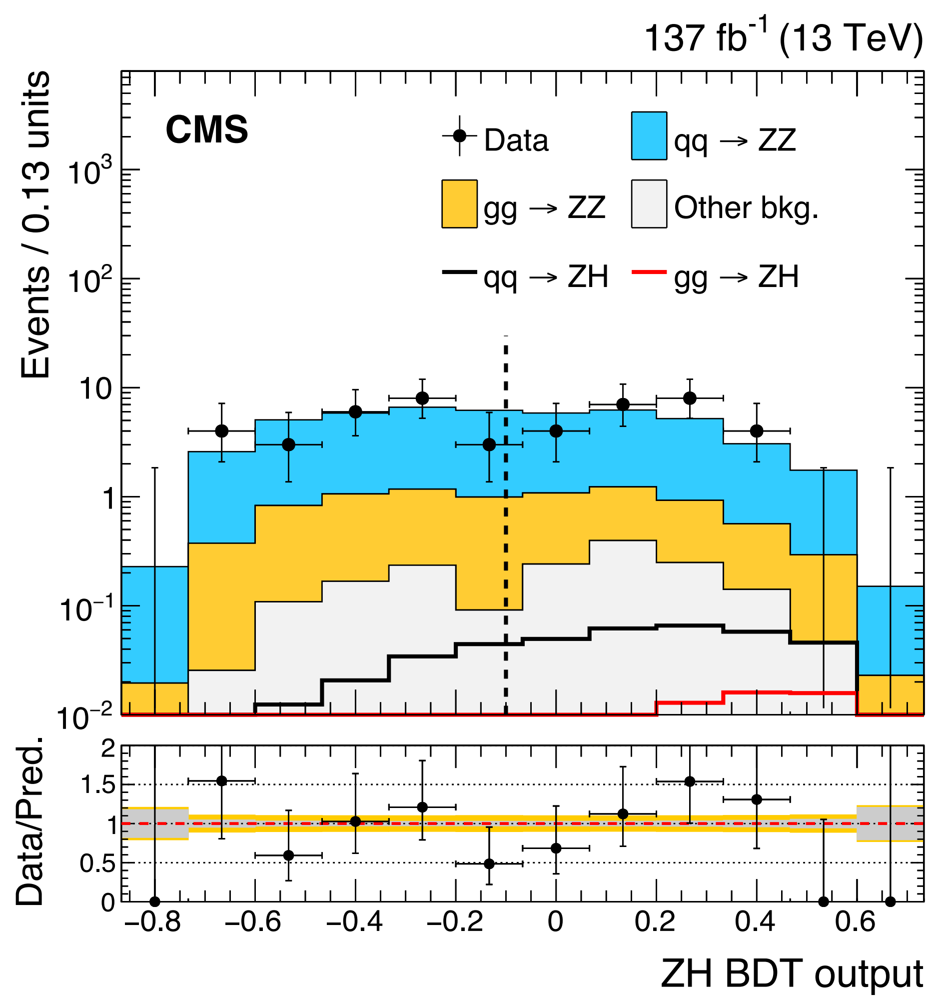

VH-leptonic Channel

Observable	WH leptonic		ZH leptonic	
	$\mu\mu\mu$	$\mu\mu$e	4μ	2μ2e
Number of loose (medium) b-tagged jets	$\leq$1 (0)	$\leq$1 (0)	$\leq$1 (0)	$\leq$1 (0)
Number of selected muons	=3	=2	=4	=2
Number of selected electrons	=0	=1	=0	=2
Lepton charge ($q(\ell)$)	$\sum q(\ell) = \pm 1$		$\sum q(\ell) = 0$	
Low-mass resonance veto	$m_{\ell\ell} > 12\,\text{GeV}$			
N($\mu^+\mu^-$) pairs with $110 < m_{\mu\mu} < 150\,\text{GeV}$	$\geq$1	=1	$\geq$1	=1
N($\mu^+\mu^-$) pairs with $\lvert m_{\mu\mu} - m_Z \rvert < 10\,\text{GeV}$	=0	=0	=1	=0
N(e^+e^-) pairs with $\lvert m_{ee} - m_Z \rvert < 20\,\text{GeV}$	=0	=0	=1	=1

Functional forms:

WH-cat1

$$\text{BWZGamma}(m_{\mu\mu}; a, f, m_Z, \Gamma_Z) = f \times \text{BWZ}(m_{\mu\mu}; a, m_Z, \Gamma_Z) + (1-f) \times \frac{e^{a m_{\mu\mu}}}{m_{\mu\mu}^2}$$

Other categories

$$\text{BWZ}(m_{\mu\mu}; a, m_Z, \Gamma_Z) = \frac{\Gamma_Z e^{a m_{\mu\mu}}}{(m_{\mu\mu} - m_Z)^2 + (\Gamma_Z/2)^2}$$

VH Channel: Results

Fit strategy and signal modeling similar to ggH categories

- Background functional form:
  - modified Breit-Wigner => due to background dominated by WZ and ZZ
- Observed (expected) significance: 2.02σ (0.42σ), m_H = 125.38 GeV

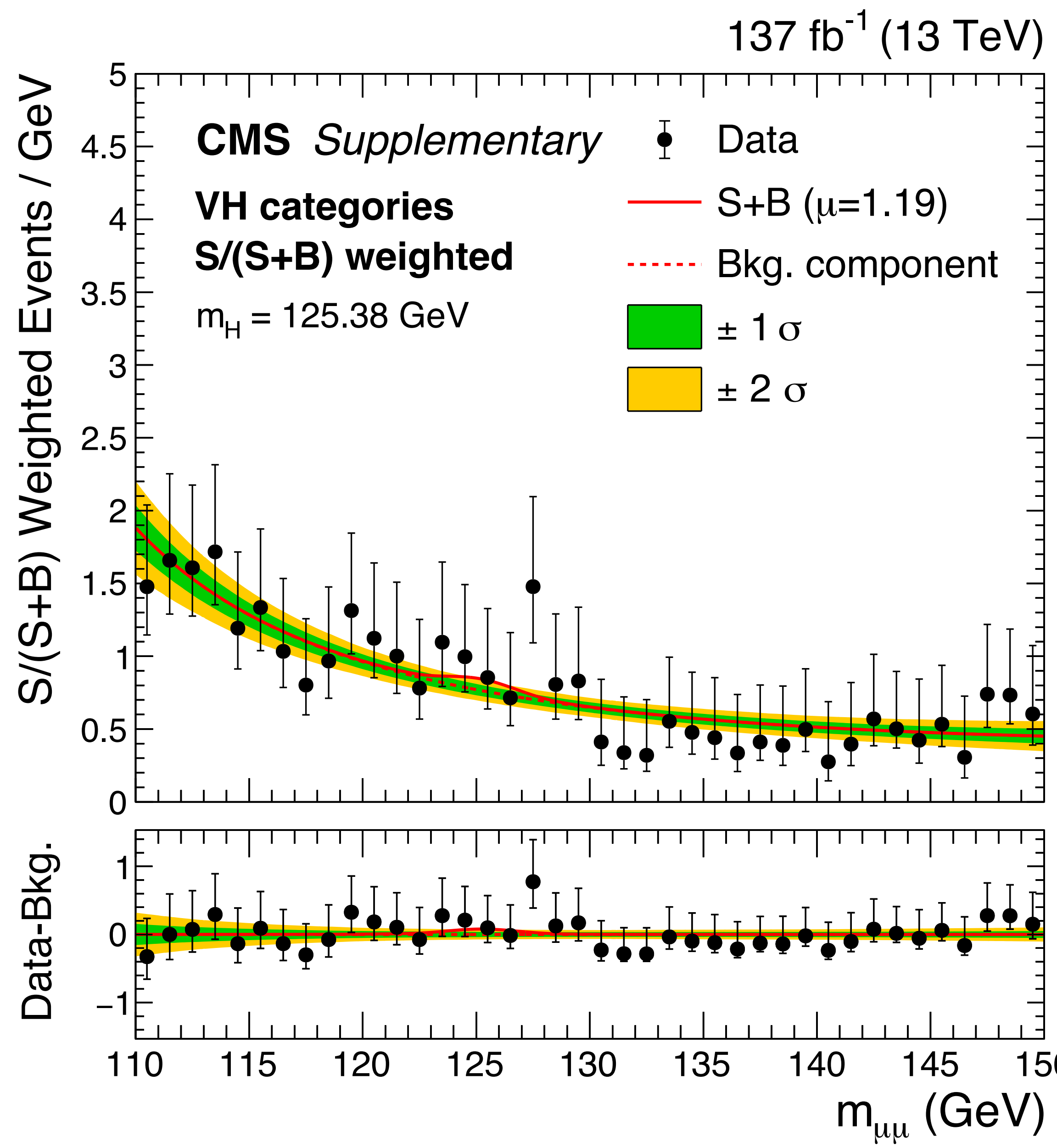

Event category	Total signal	WH (%)	qqZH (%)	ggZH (%)	$t\bar{t}$H+tH (%)	HWHM (GeV)	Bkg. fit function	Bkg. @HWHM	Data @HWHM	S/(S+B) (%) @HWHM	$S/\sqrt{B}$ @HWHM
WH-cat1	0.82	76.2	9.6	1.6	12.6	2.00	BWZγ	32.0	34	1.54	0.09
WH-cat2	1.72	80.1	9.1	1.5	9.3	1.80	BWZ	23.1	27	4.50	0.23
WH-cat3	1.14	85.7	6.7	1.8	4.8	1.90	BWZ	5.48	4	12.6	0.35
ZH-cat1	0.11	—	82.8	17.2	—	2.07	BWZ	2.05	4	3.29	0.05
ZH-cat2	0.31	—	79.6	20.4	—	1.80	BWZ	2.19	4	8.98	0.14

VBF Channel: Deep Neural Network

- DNN trained on kinematic information of the two muons and VBF signature (24 variables):
  - **Dimuon variables:** $m_{\mu\mu}$, $\sigma(m_{\mu\mu})$, $m_{\mu\mu}/\sigma(m_{\mu\mu})$, $p_{T\mu\mu}$, $\log(p_{T\mu\mu})$, $y_{\mu\mu}$, $\cos\theta^*$, ϕ^*
  - **Dijet variables:** pT, η, ϕ of jet_1, jet_2, $\log(m_{jj})$, m_{jj}, $\Delta\eta_{jj}$
  - **Soft track-jet variables:** $N_{\text{soft jet} > 5\text{ GeV}}$, $H_{T\text{ soft jet} > 2\text{ GeV}}$ (H_T: scalar sum of p_T):
    - jets reconstructed by charged tracks associated to the primary vertex
    - not associated with jet_1, jet_2 or the two muons
  - **Kinematic variable of the dimuon (μμ) and dijet system**
    - mim(Δη(μμ, jet_1), Δη(μμ, jet_2))
    - Zeppenfeld variable
    - pT balance ratio of μμ and jets $R(p_T) = \dfrac{|\vec{p_T}^{\mu\mu} + \vec{p_T}^{jj}|}{p_T^{\mu\mu} + p_T(j_1) + p_T(j_2)}$
  - **Quark/gluon likelihood:** jet_1, jet_2 (jets in DY process can originate from gluons)

most sensitive variable: $m_{\mu\mu}$

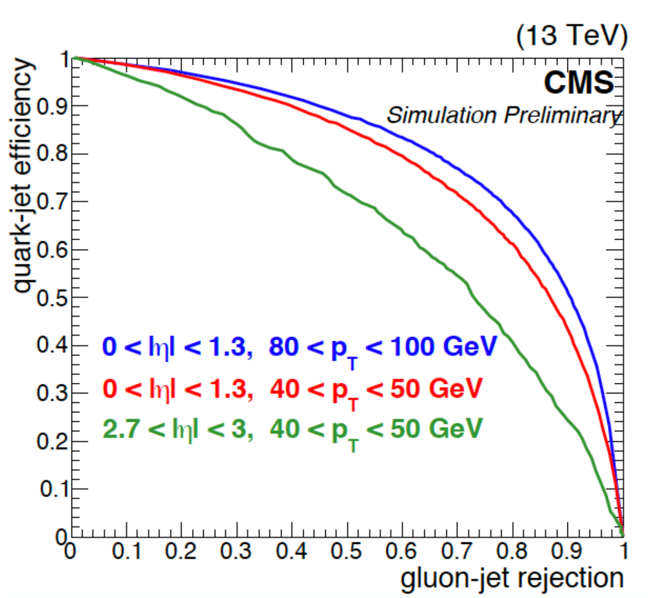

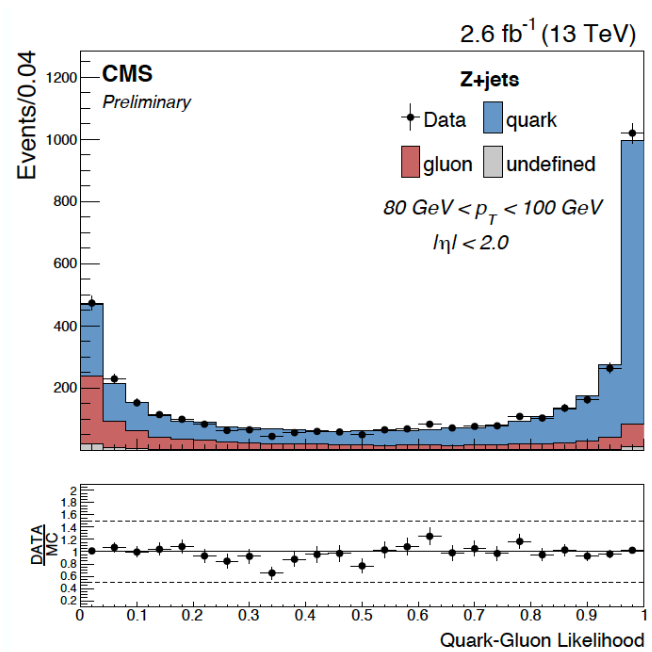

VBF: 2016 signal and sideband region

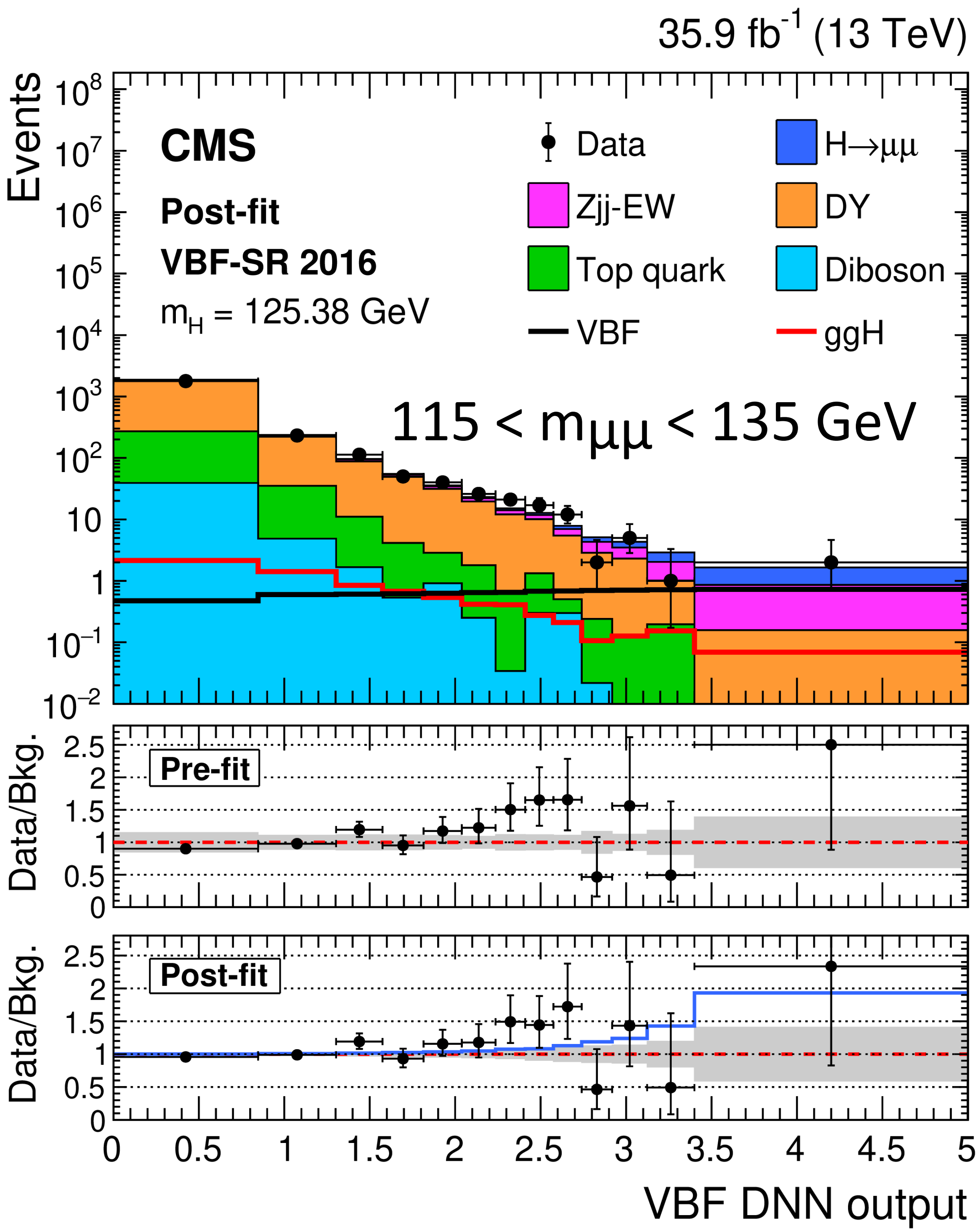

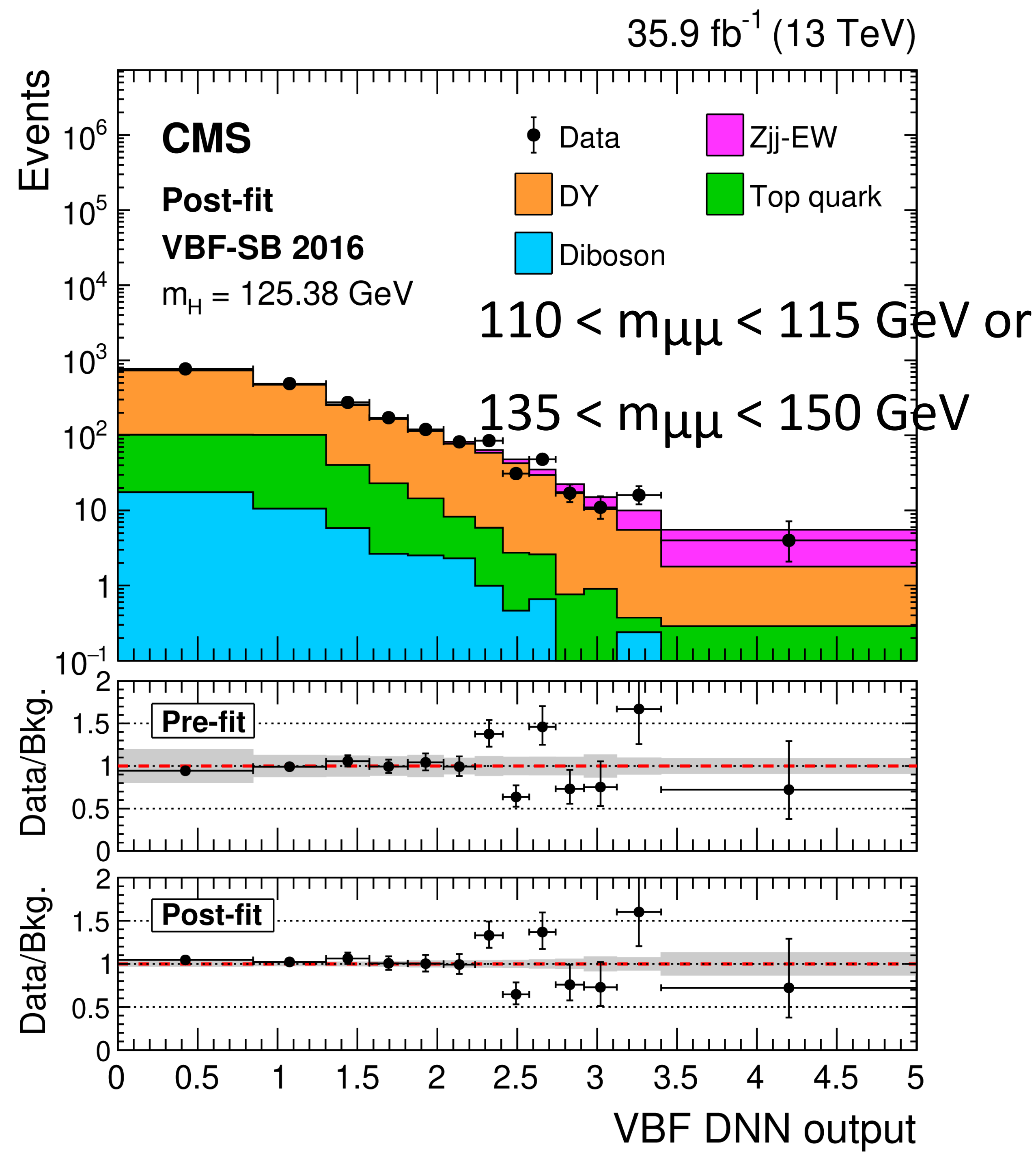

VBF: 2017 signal and sideband region

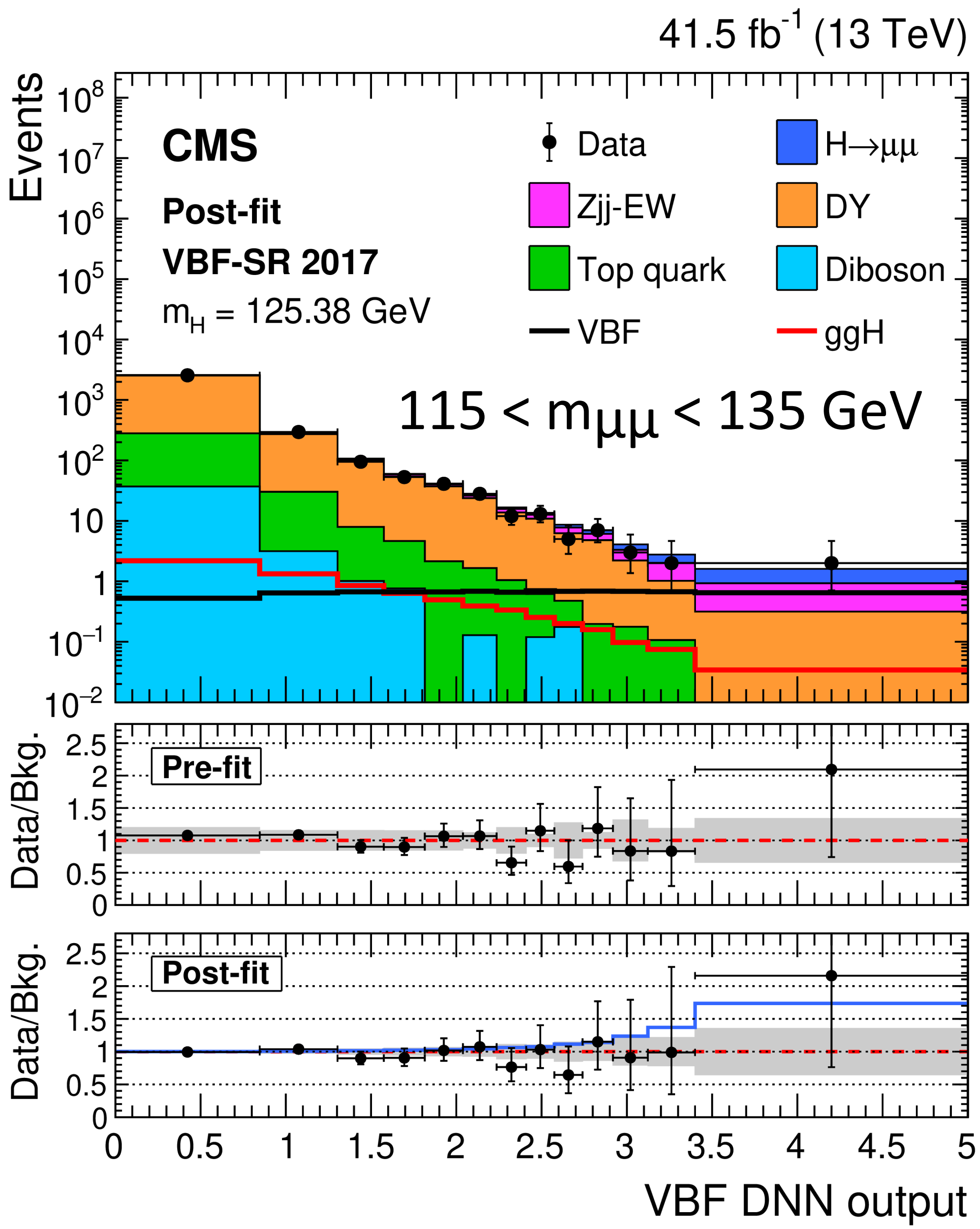

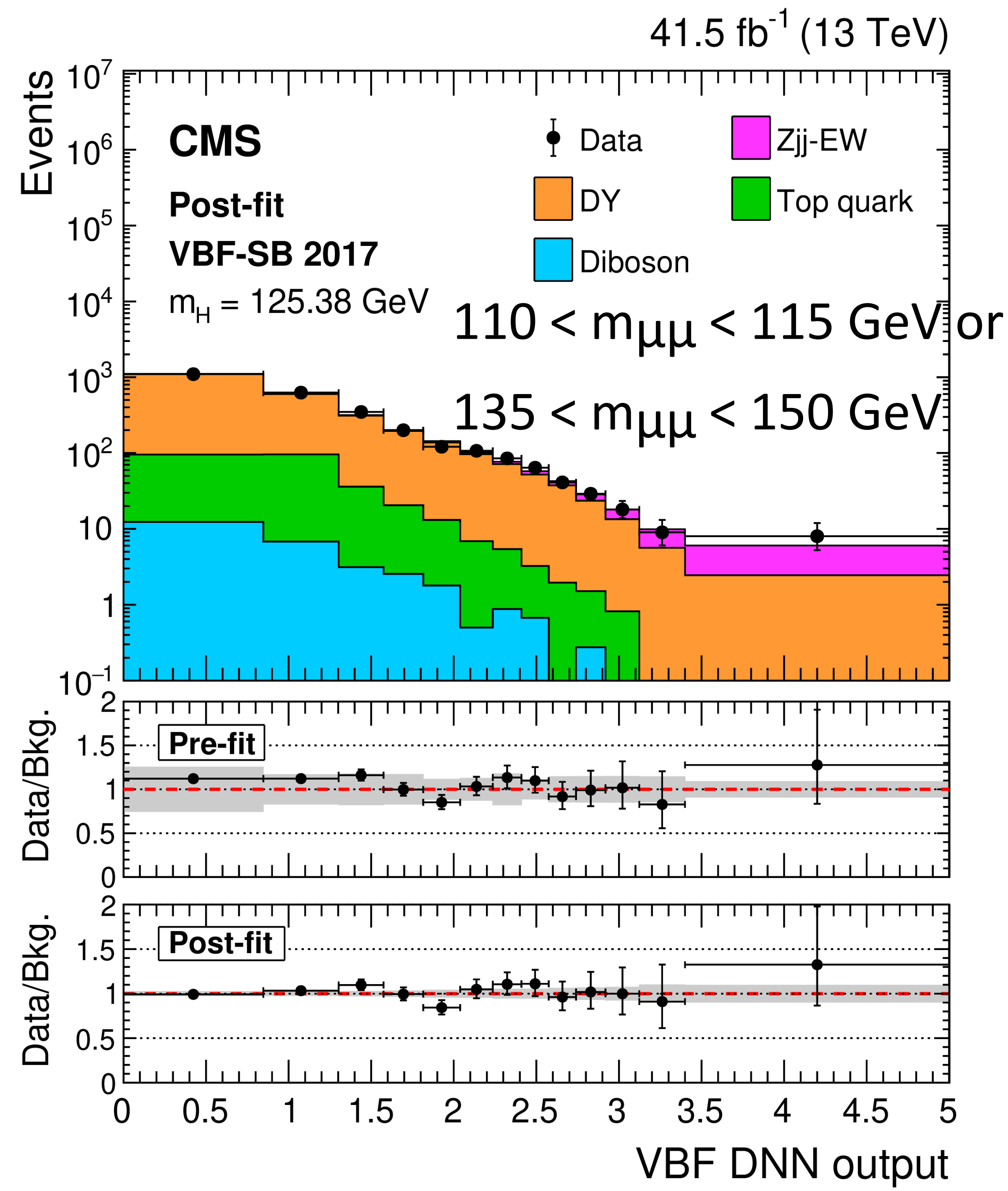

VBF: 2018 signal and sideband region

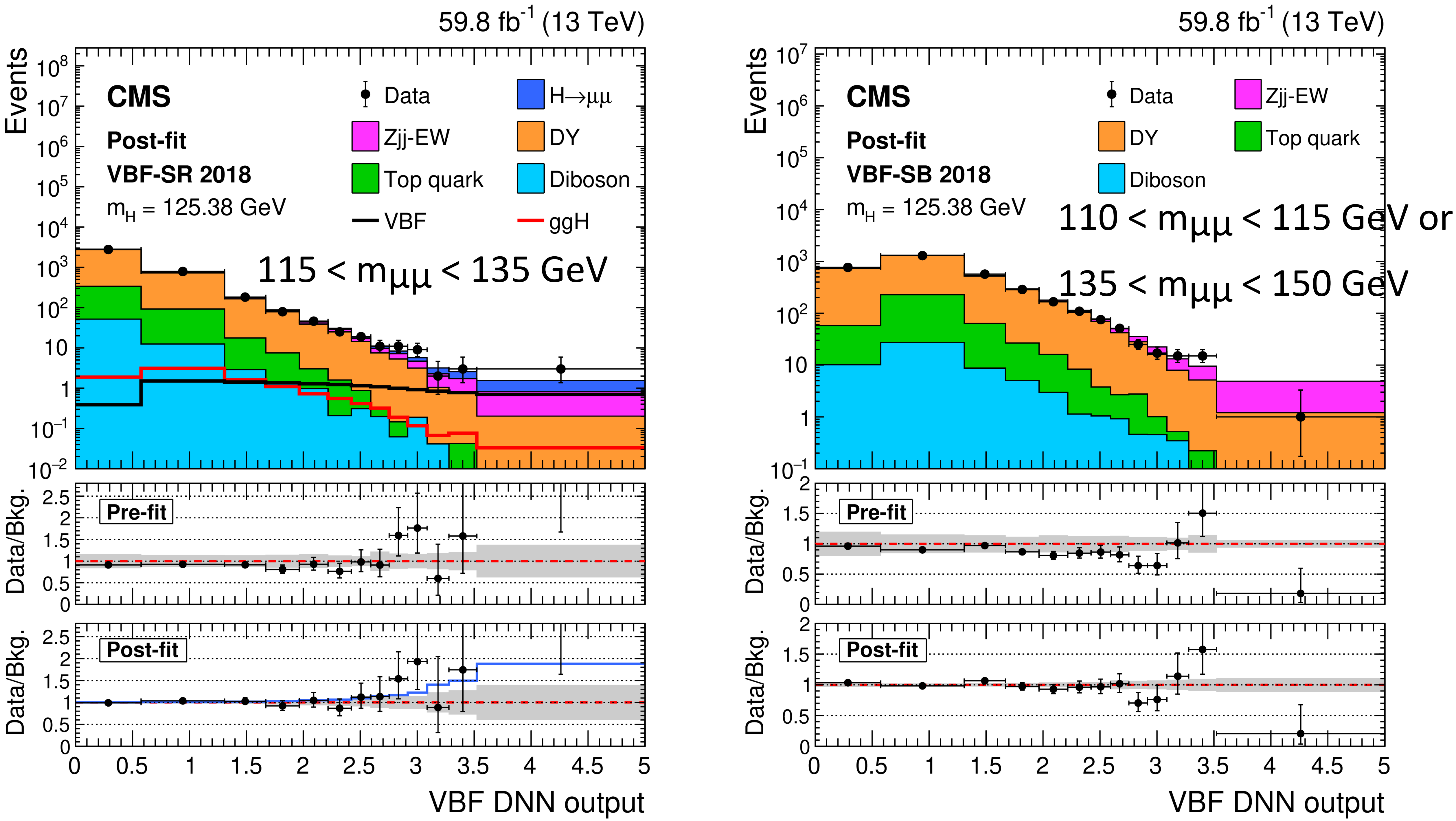

VBF channel: systematic uncertainties

Experimental uncertainties

- Jet energy scale and resolution uncertainties
- the rate of DY process with a jet not matched to a generator level jet, contained by the low DNN score events.
- MC stats uncertainty
- 2016 and 2017 a 20% uncertainty of the correction for the modeling of the inefficiency in the L1 trigger in region 2.4<eta<3
- luminosity uncertainty 2.5%
- modeling of the pileup conditions during data taking
- measurement of muon identification, isolation and trigger efficiencies
- muon energy scale and resolution
- quark/gluon likelihood reweighs

Theory uncertainties

- QCD scale, pdf, parton shower (PS) uncertainty for signal and background is included. In particular VBF and electroweak Zjj-EW PS uncertainty: difference between HERWIG (angular-ordered) and PYTHIA (dipole shower)

ggF channel: background modeling

- background modeled with analytical functions: core-pdf method

$$B_{cat}(m_{\mu\mu}, \vec{\alpha}, \vec{\beta}) = N_B \times \boxed{F_{core}(m_{\mu\mu}, \vec{\alpha})} \times T_{SMF}(m_{\mu\mu}, \vec{\beta})$$

Background shape: same core function in all categories

- discrete profiling method[1] choose one from three functional forms during the fit to the data
  - main background DY process physics motivated functions
    - (1) modified Breit–Wigner $\mathrm{mBW}(m_{\mu\mu}; m_Z, \Gamma_Z, a_1, a_2, a_3) = \frac{e^{a_2 m_{\mu\mu} + a_3 m_{\mu\mu}^2}}{(m_{\mu\mu} - m_Z)^{a_1} + (\Gamma_Z/2)^{a_1}}$
    - (2) shape derived from the FEWZ v3.1 generator (NNLO in QCD and NLO in EW) × a third-order Bernstein polynomial
  - agnostic functions
    - (3) a sum of two exponential functions

[1]: 2015_J._Inst._10_P04015

ggF channel: background modeling

- background model with analytical functions: core-pdf method

$$B_{cat}(m_{\mu\mu}, \overrightarrow{\alpha}, \overrightarrow{\beta}) = \boxed{N_B} \times F_{core}(m_{\mu\mu}, \overrightarrow{\alpha}) \times \boxed{T_{SMF}(m_{\mu\mu}, \overrightarrow{\beta})}$$

background yield:
uncorrelated across categories

- per-category shape modulation: account for shape variations in categories
  - 2nd or 3rd order Chebyshev polynomial
  - parameters uncorrelated across ggH categories

- Bias from background modeling has < 1% effect on measured signal rate, thus neglected
  - bias on signal extraction < 20% of post-fit uncertainty on the signal yield

Core-pdf method for background modeling brings 10% improvement in sensitivity compared to 2016 data analysis

Signal composition

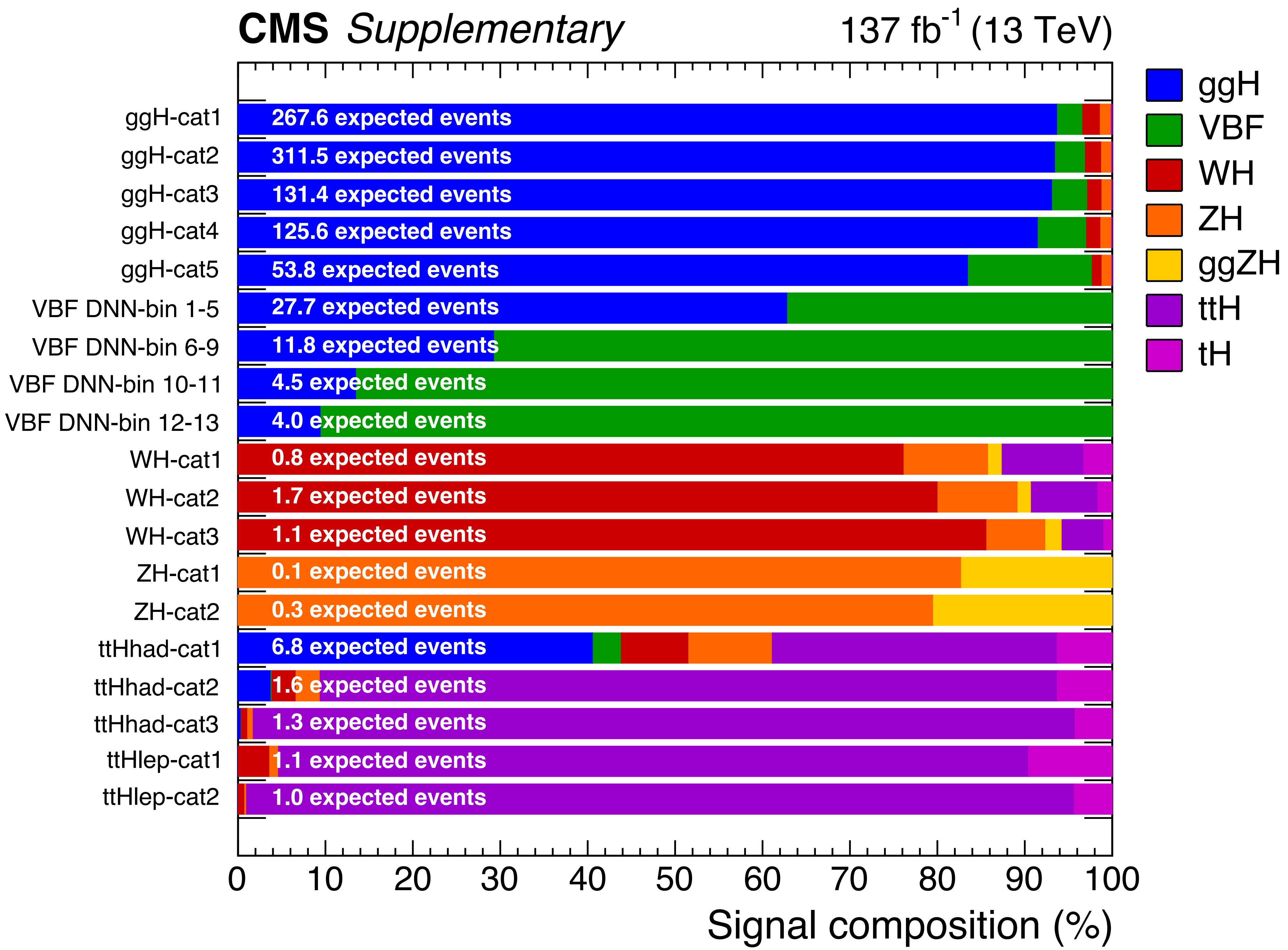

$H \to \mu\mu$: Higgs boson coupling to muon

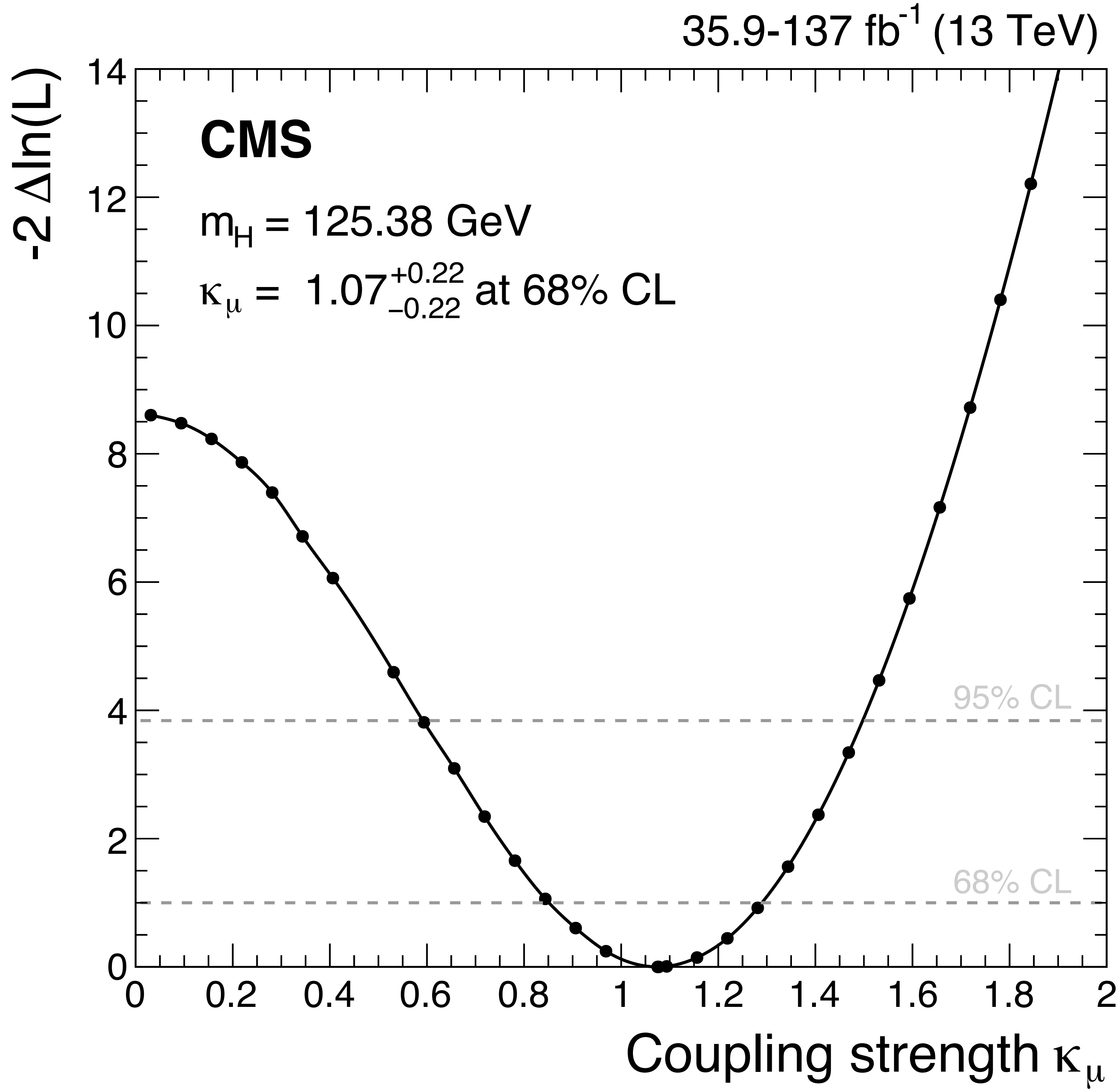

Ranking of systematic uncertainties

- Leading systematic uncertainty: VBF signal parton shower uncertainty
- No strong shifts from central values or constraint on the size of systematic uncertainty

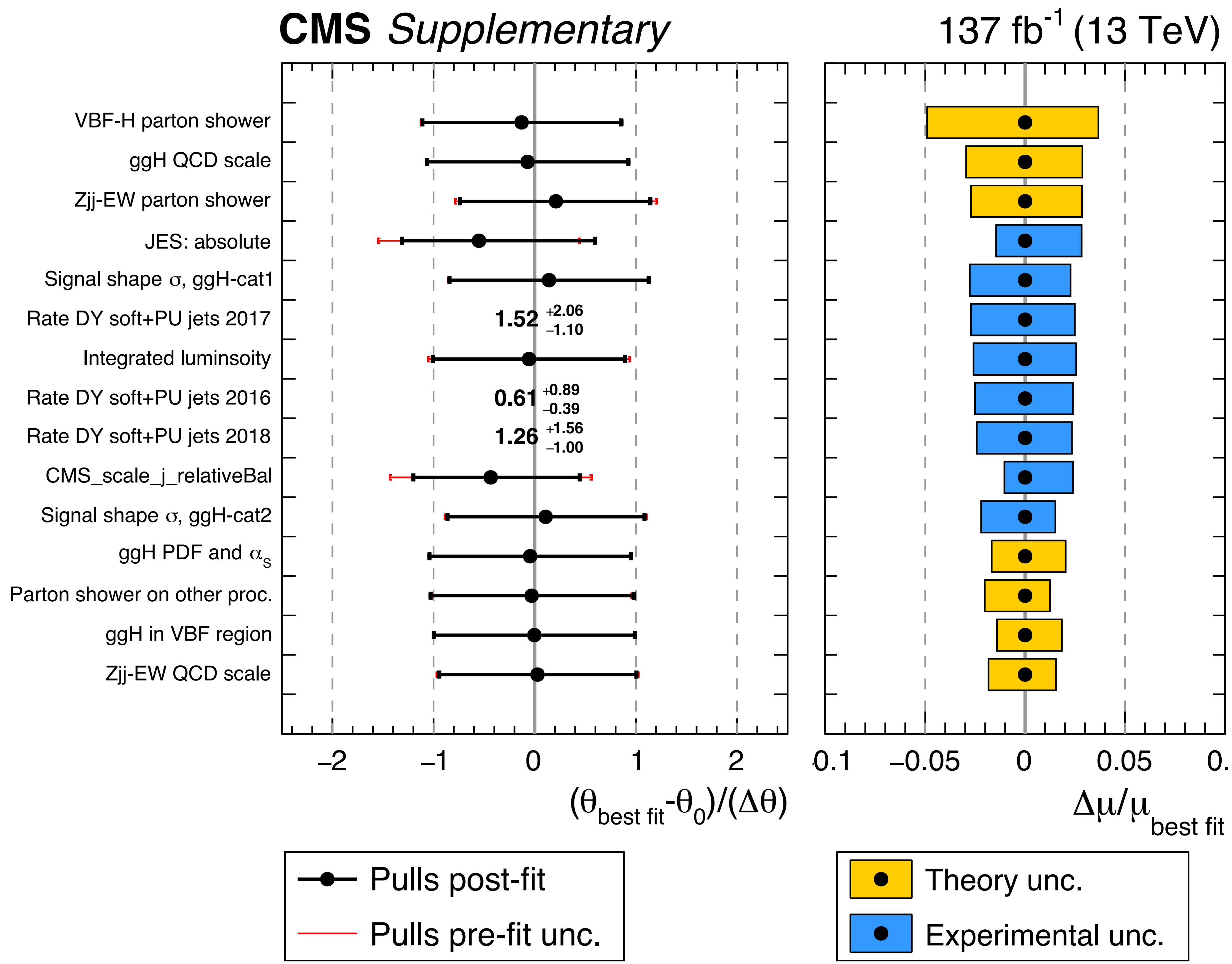

Signal Strength Measurement of H→μμ

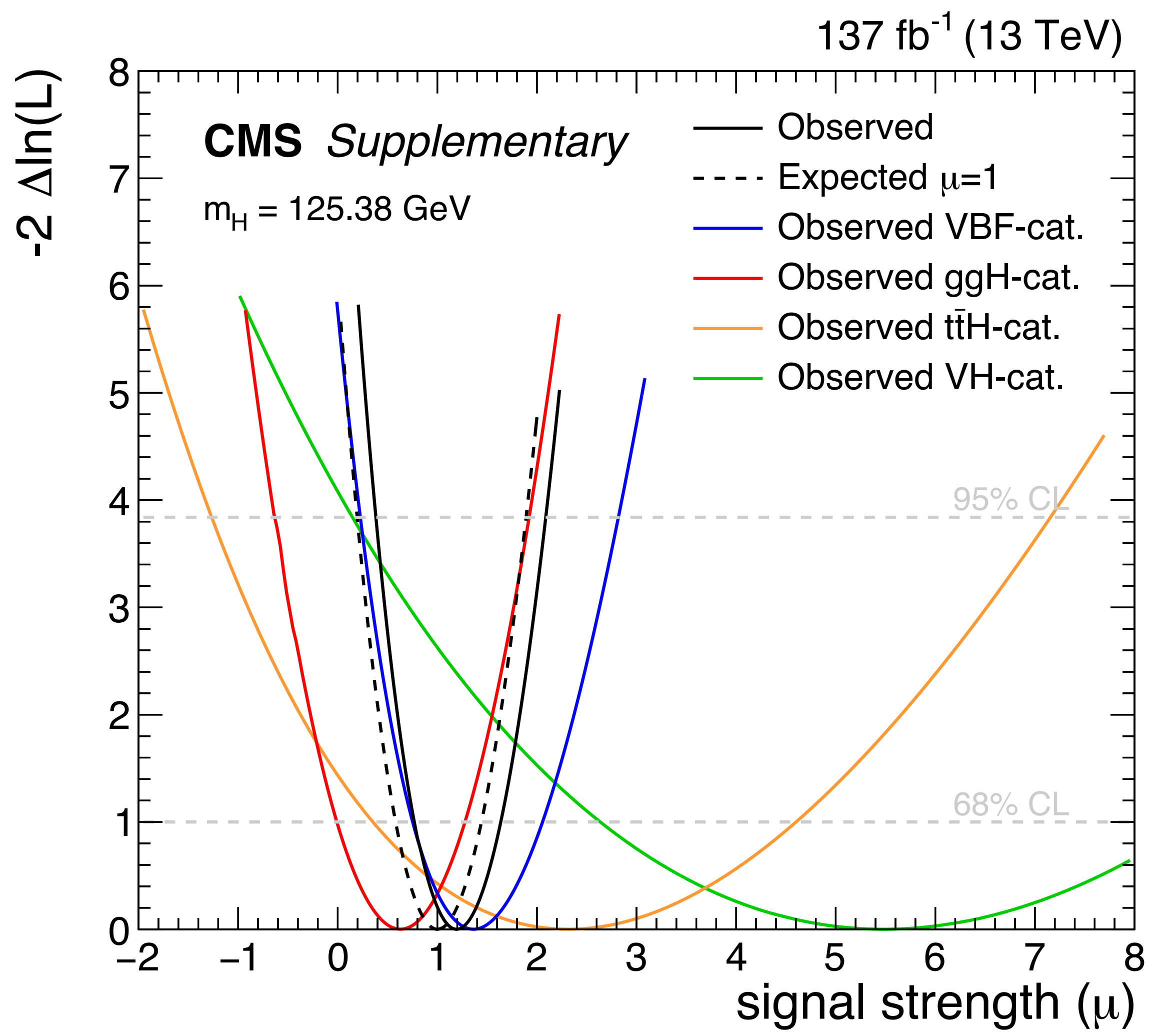

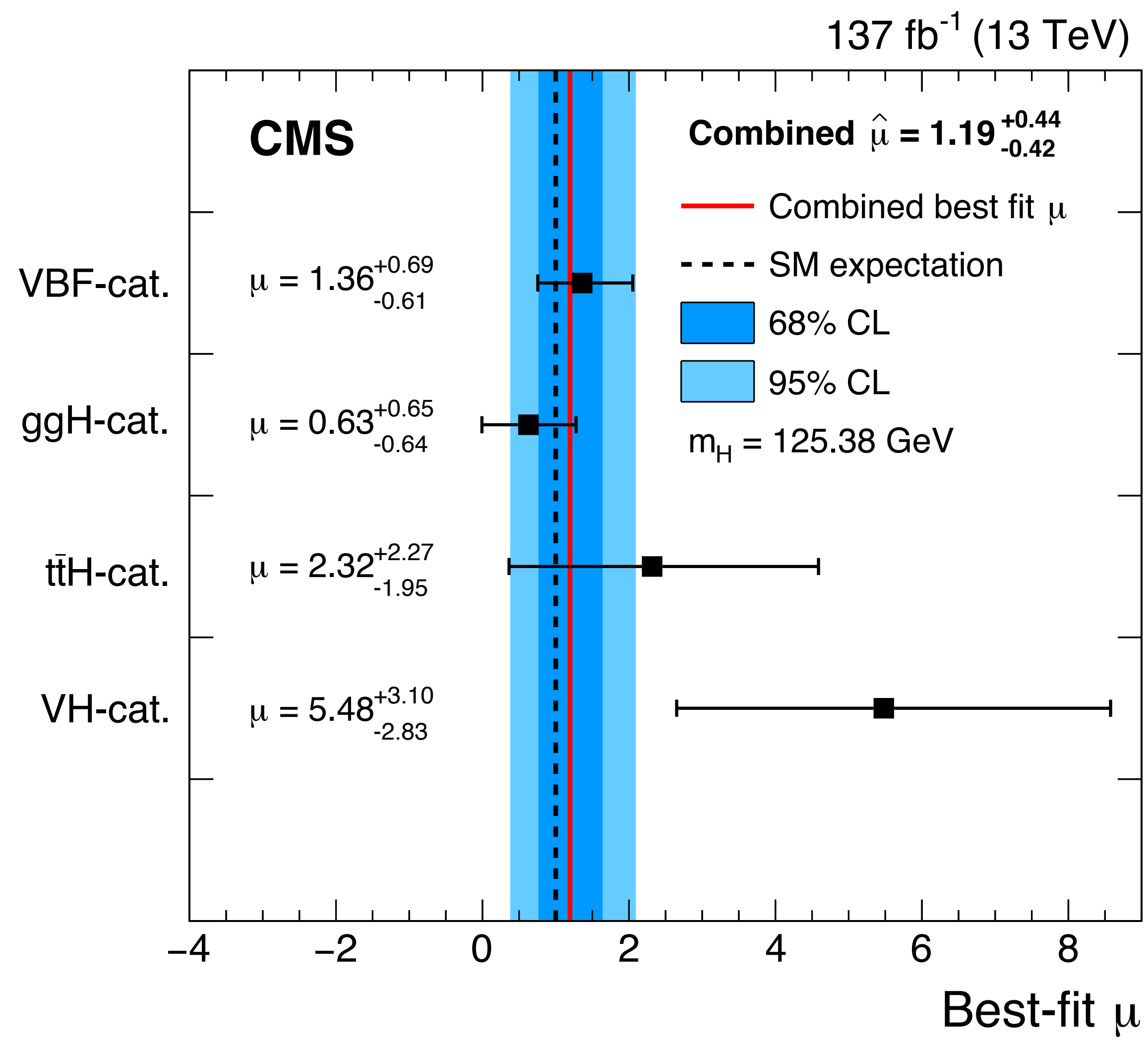

Combined signal strength of all channels : $\mu = \sigma B(H \rightarrow \mu\mu)_{obs} / \sigma B(H \rightarrow \mu\mu)_{SM}$

$$\mu = 1.19^{+0.44}_{-0.42} = 1.19^{+0.41}_{-0.40}(stats.)^{+0.10}_{-0.11}(theo.)^{+0.12}_{-0.11}(exp.)^{+0.07}_{-0.06}(MCstats.)$$

measurement dominated by statistical uncertainty in data

Muon momentum resolution

$\sigma/p_T \approx 1\%$ @ 50GeV to 10% @ 1TeV

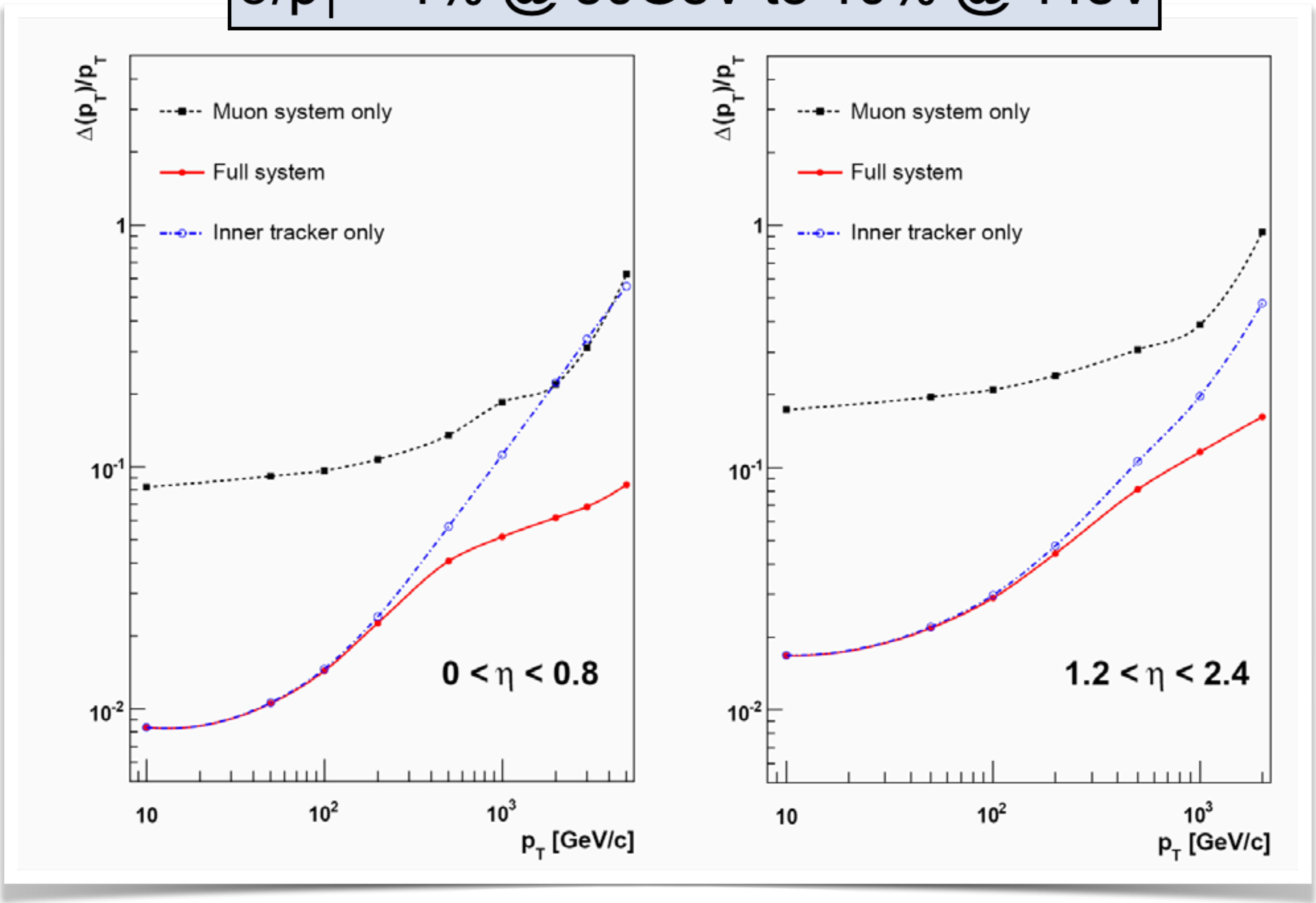

H→μμ events:

- typical p_T of muons: 50~60 GeV
- muon p_T resolution $\sigma(p_T)/p_T$ dominated by measurements by tracker

Comparison with ATLAS results

signal significance $\propto 1/\sqrt{\sigma(m_{\mu\mu})}$

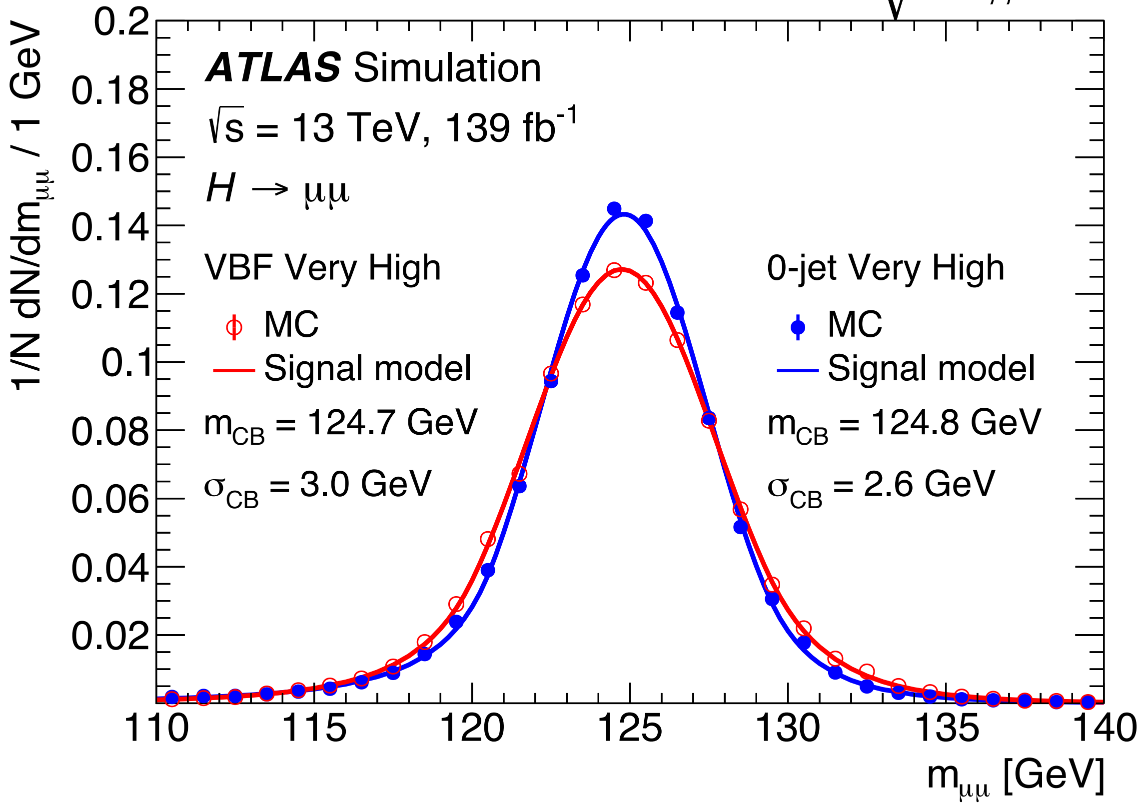

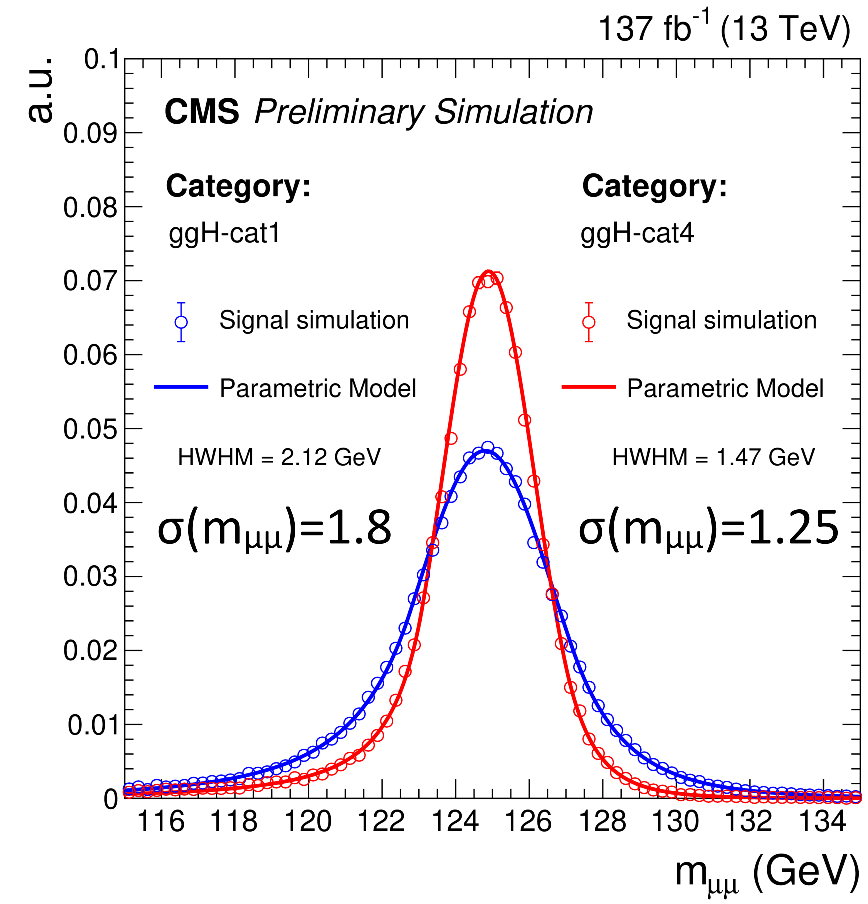

Phys. Lett. B 812 (2021) 135980

ATLAS:

- Expected significance 1.7σ, observed 2.0σ
- Signal strength: $\mu = 1.2 \pm 0.58(stats.)^{+0.13}_{-0.08}(theory)^{+0.07}_{-0.03}(exp.) \pm 0.10(spurious)$

CMS:

- Expected significance 2.5σ, observed 3.0σ
- Signal strength: $\mu = 1.19^{+0.41}_{-0.39}(stats.)^{+0.10}_{-0.11}(theory)^{+0.12}_{-0.10}(exp.)^{+0.07}_{-0.06}(MCstats.)$

Main difference in the result of two experiments: $\sigma_{CMS}(m_{\mu\mu})/\sigma_{ATLAS}(m_{\mu\mu})$ = 48~60%

Summary of improvements

- 2016 data analysis (Phys.Rev.Lett.122.021801):
  - bump hunt in m(μμ) spectrum targeting ggH and VBF signals
  - expected sensitivity with 2016 data of 36 fb^{-1}: 1.0σ
- Full Run 2 data analysis strategy has **35% improvement** wrt 2016 data analysis:
  - muon pT corrections: (1) final state radiation recovery (2) muon track momentum correction using interaction point position information
  - new analysis strategy for VBF channel: MC template fits to allow reaching unprecedented signal purity (42% in last DNN bin)
  - significantly improved analysis strategy for the ggH channel:
    - improved BDT, aware of the dimuon resolution
    - robust background modeling with less free parameters: core-pdf method
  - new categories for VH and ttH signals, less explored previously

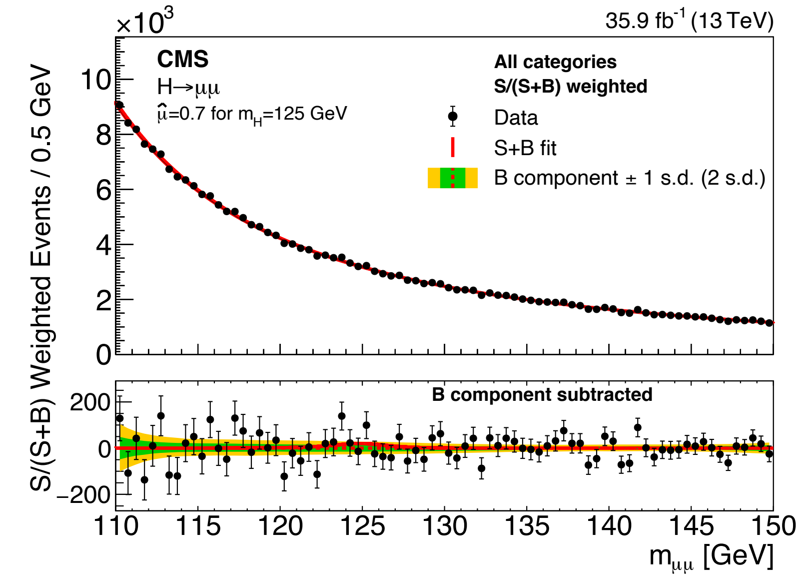

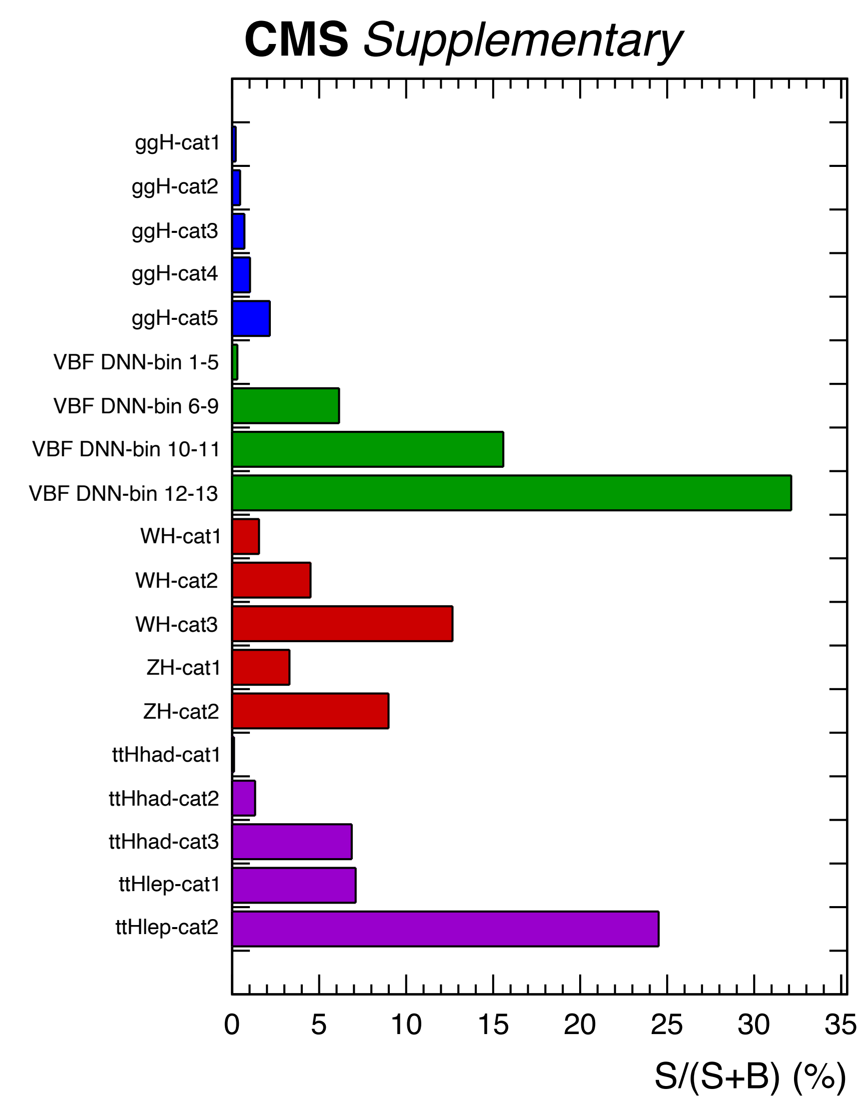

MTD Physics Potential

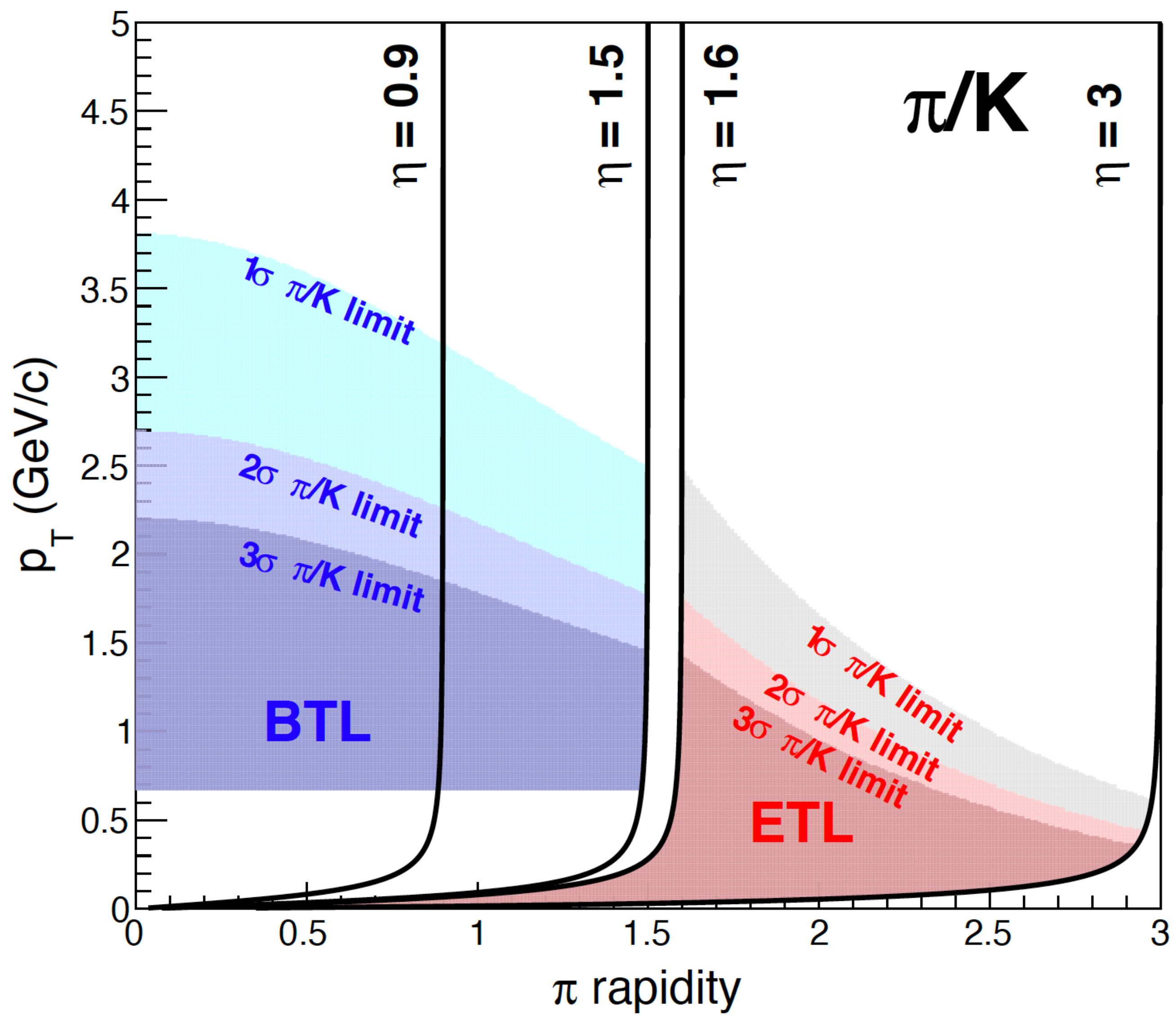

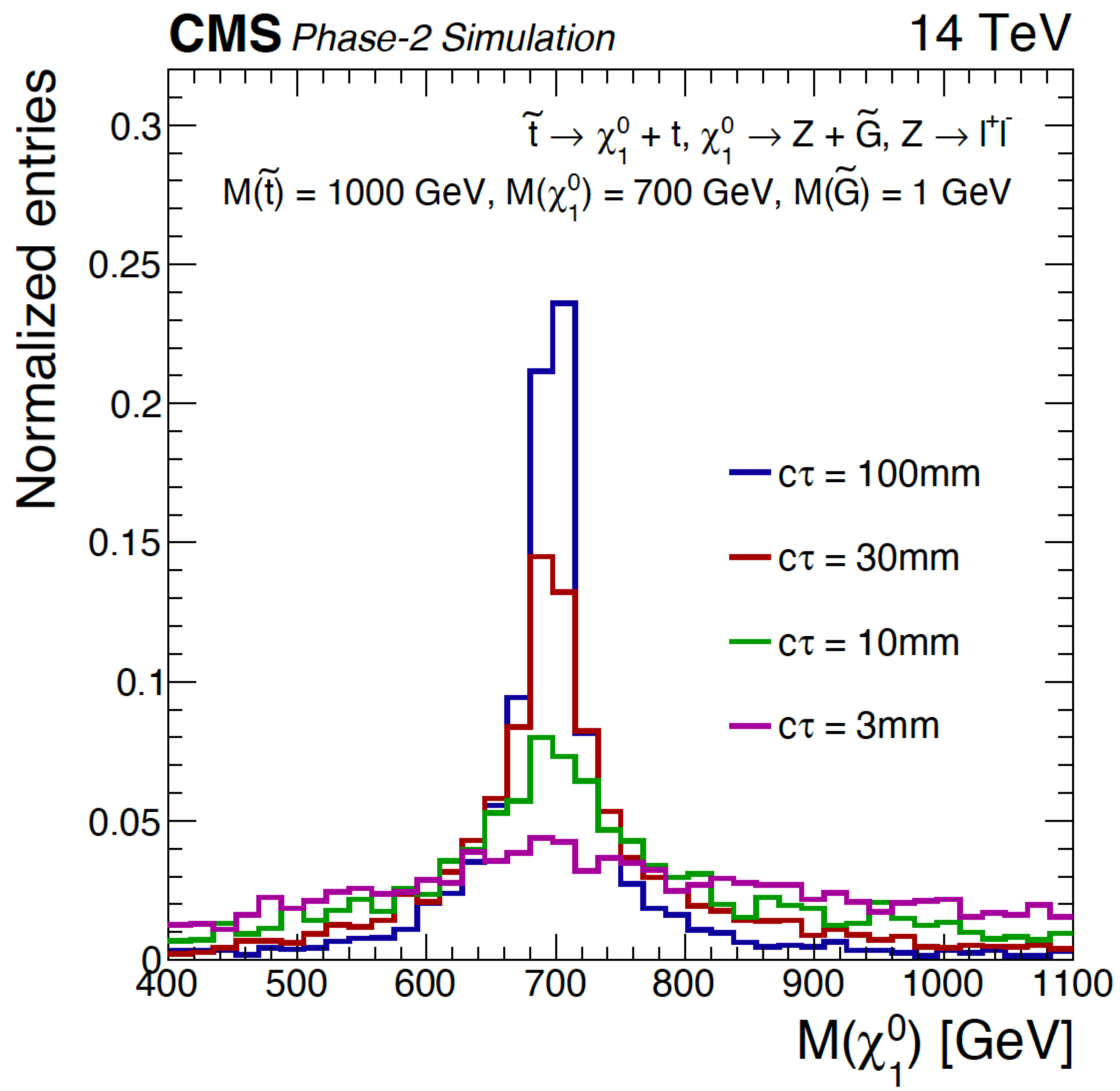

BTL Detector Layout

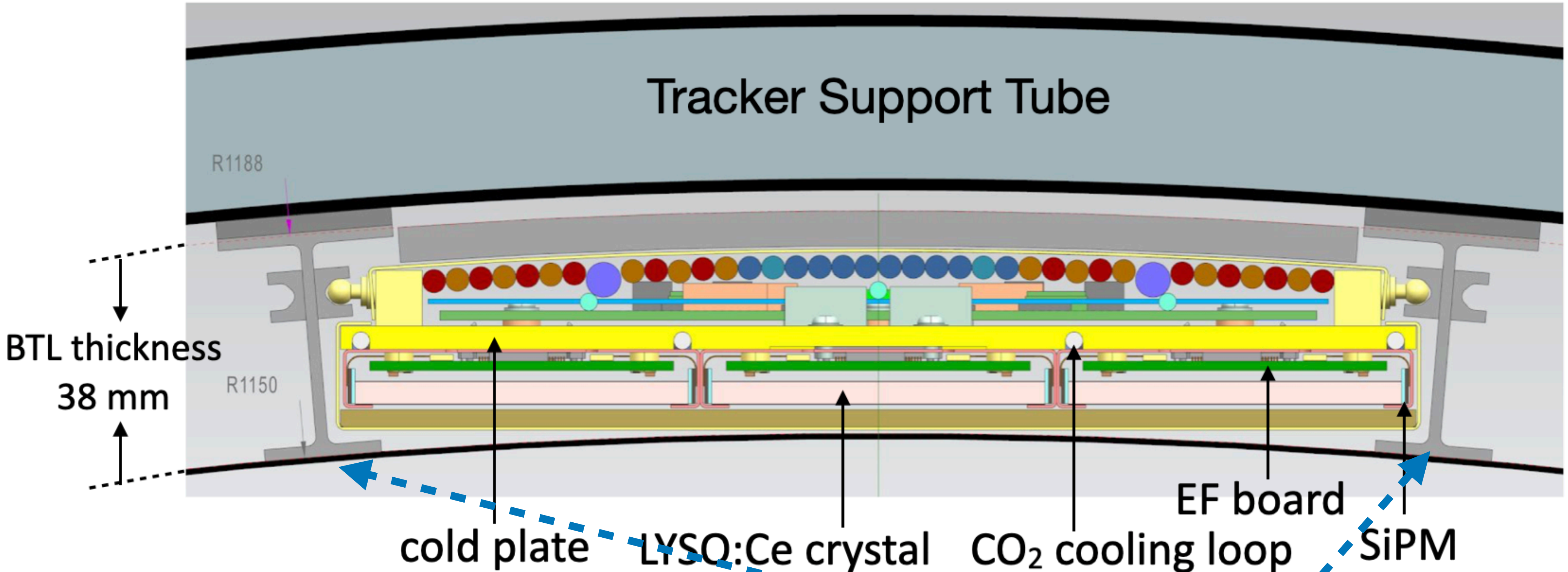

- Coverage: |η| < 1.45
- Surface ~38 m²
- 332k channels
- BTL detector mounted on inner surface of Tracker Support Tube

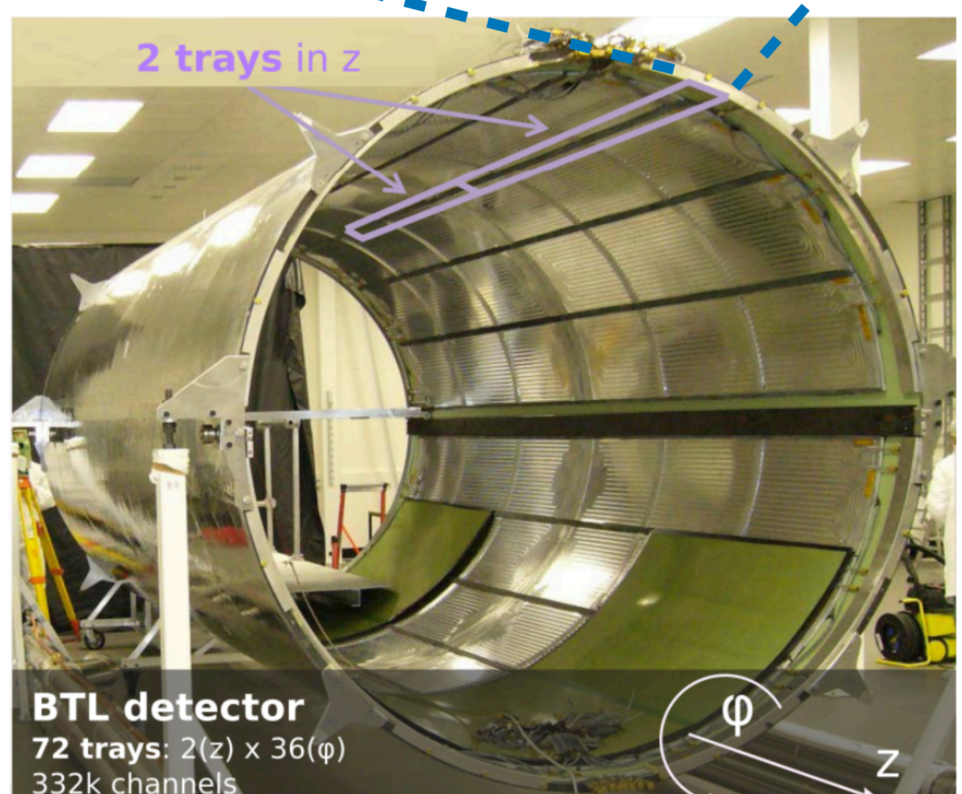

BTL Time Resolution Factors

- **Photostatistics** **and** **DCR noise** **contributions dominate timing resolution**

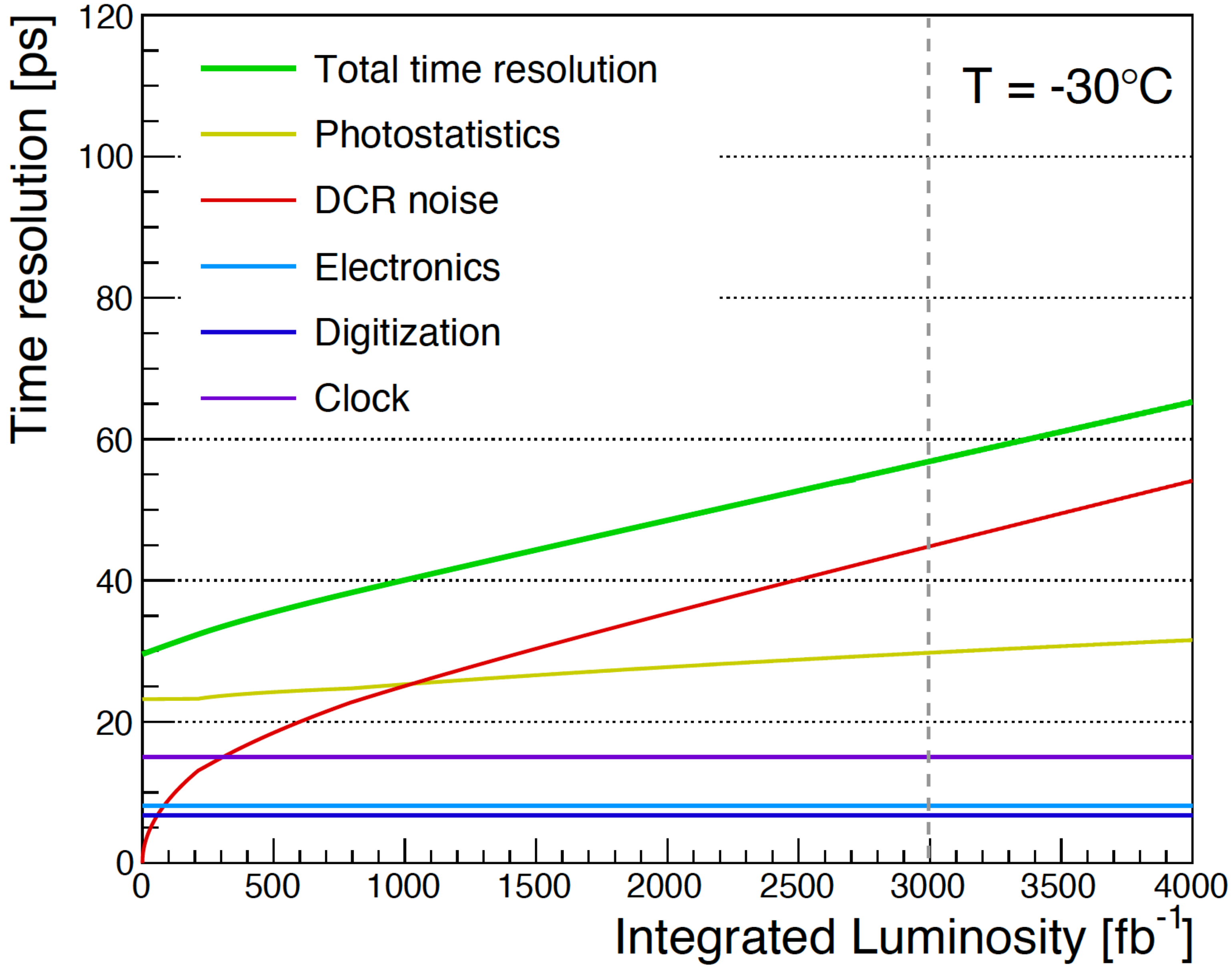

- Photostatistics: 25 - 35 ps, stochastic fluctuations in the time-of-arrival of photons detected at the SiPM
- DCR noise: < 60 ps after 3000 fb^{-1}
- Electronics: 7ps
- Digitization: 6 ps
- Clock distribution: 15 ps

ETL Front-end ASIC ETROC

Time resolution $\sigma_t^2 = \sigma^2_{Jitter} + \sigma^2_{Ionization} + \sigma^2_{Distortion} + \sigma^2_{TDC}$

- $\sigma^2_{Jitter} \quad \frac{e_n C_d}{Q_{in}}\sqrt{t_{rise}}$: jitter contribution subdominant at high gain
- $\sigma^2_{Ionization}$: fluctuations in Landau ionization. ~50 ps, dominates at high gain for 50 μm thick LGAD
- $\sigma^2_{Distortion}$: non-uniform weighting field and non-saturated drift velocity
- σ^2_{TDC}: effect of the TDC binning

ETL Time Resolution Factors

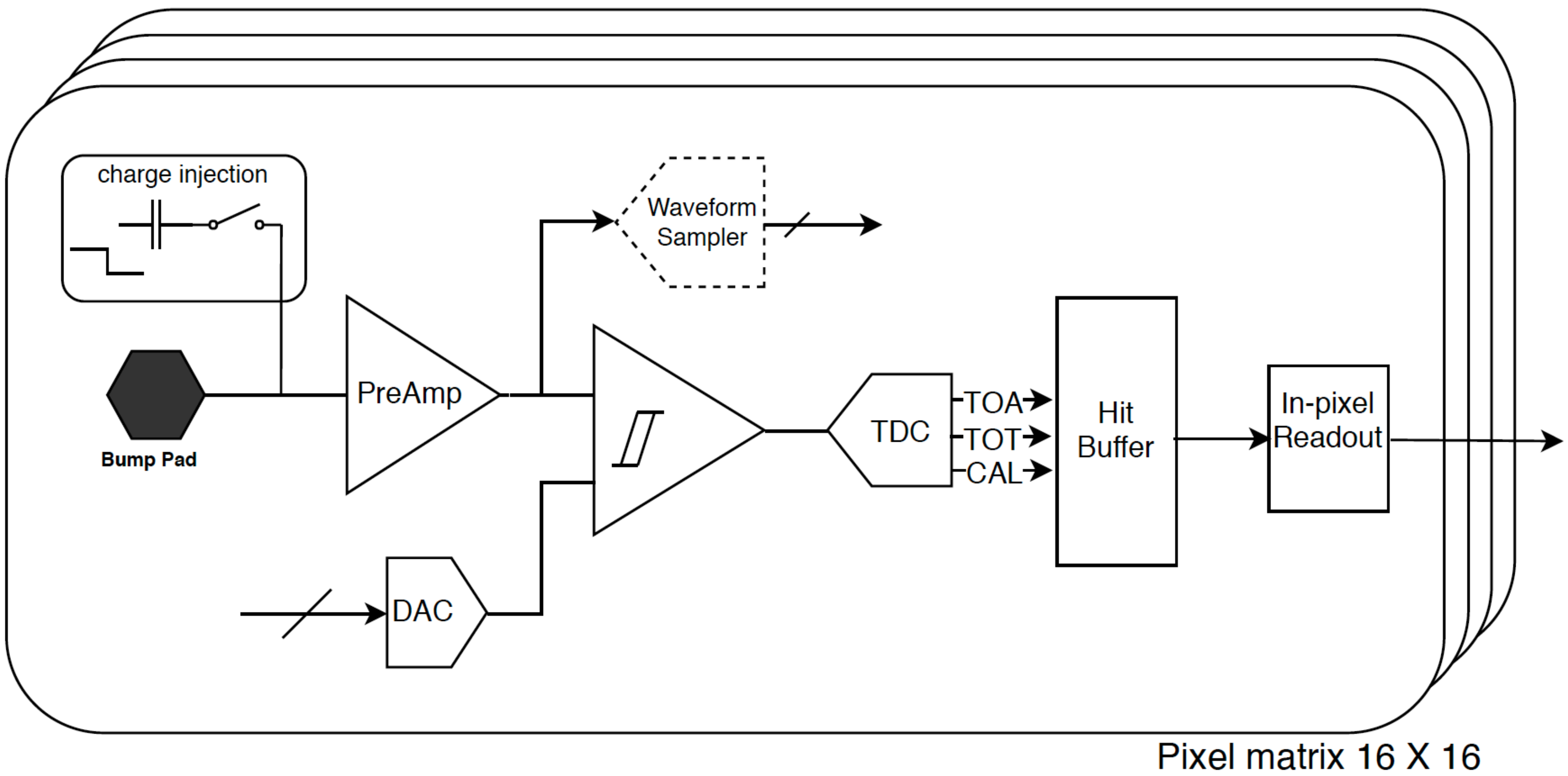

ETROC0 : single analog channel

ETROC1: with TDC and 4x4 clock tree

ETROC2: 8x8 full functionality

ETROC3: 16x16 full size chip